Deliverable n°8
Final report

CONTRACT N° : FIKW-CT-2000-00063

ACRONYM : MUSE

TITLE : The MUSE experiments for sub critical neutronics validation

PROJECT CO-ORDINATOR : F. MELLIER, C.E.A. Cadarache – DEN/DER/SPEX/LPE

CONTRACT PARTNERS

Belgian Nuclear Research Center (SCK/CEN Mol), Belgium
Université Joseph Fourier, Grenoble 1 (CNRS/IN2P3/ISN Grenoble), France
Forschungszentrum Karlsruhe GmbH (FZK), Germany
Forschungszentrum Jülich GmbH (FZJ), Germany
British Nuclear Fuels plc (BNFL), Great Britain
Ente per le Nuove tecnologie, l'Energia e l'Ambiente (ENEA), Italy
Nuclear Research consultancy Group (NRG, Petten), The Netherlands
Delft University of Technology (DUT), The Netherlands
Centro de Investigaciones Energeticas, Medio Ambiantales y Technologicas (CIEMAT, Madrid), Spain
Kungliga Tekniska Hogskolan (KTH, Stockholm), Sweden
Chalmers University of Technology AB (CTH Gothenburg), Sweden
University of Mining and Metallurgy (UMM Krakow), Poland

REPORTING PERIOD : From October 2000 to October 2004

PROJECT START DATE: 1st October 2000 **DURATION : 49 Months**

Date of issue of this report : June 2005

Project funded by the European Community under the '5th Euratom Framework' Programme (1998-2002)

Table of contents

Executive summary

Neutronic experiments and studies have largely been carried out in the past for fast critical reactors. The associated calculation tools developed for the predictions of such systems have been mainly based on integral experiments in critical reactor facilities. Experimental techniques have also been developed that are directly applied to power producing critical operating systems.

The same approach for studying neutronics of sub-critical systems driven by an external source is based on the decoupling of the validation of the sub-critical multiplying medium behaviour from that of the validation of the external source characteristics. Following this scheme, two major programmes have been carried out in the MUSE project from 2000 to 2004 : the MUSE-4 programme (Cadarache, F) and the PRE-SAD experiments (Dubna, RF).

The objectives of the MUSE-4 programme [1] were (1) to operate a fast subcritical core coupled to an external neutron source simulating the spallation source of an ADS without feedback effects, (2) to characterize such a system providing experimental input data for calculation tool validation and (3) to investigate techniques and analysis methods for sub-critical measurement and monitoring. With regard to the PRE-SAD experiments [2], the main objectives were (1) to determine experimentally the characteristics of hadron field around a bare spallation target bombarded by a high energy proton beam, (2) to measure the nuclides produced in the target and simulate these experiments using various codes and model option and (3) to examine the influence of core, reflector and shielding parameters of the SAD [3] core versions on its experimental properties and the possibilities to infer accurately the reactivity level.

The MUSE-4 experiments have been carried out at the MASURCA nuclear facility (CEA Cadarache, France). MASURCA facility is a mock-up which usually operates at delayed critical with a maximum power of 5 KW. Until the middle of the 90's, the programmes were devoted to the development of critical fast neutrons reactors. Since then, MASURCA has been used to test various reactor concepts for plutonium burning and for the transmutation of radioactive wastes.

Radial cut of the MUSE-4 configurations at core mid plane

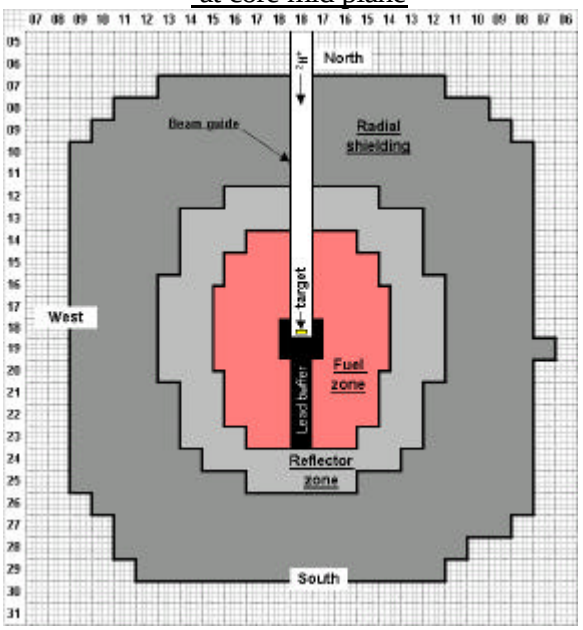

For the MUSE-4 experiments, all the configurations, representative of a fast burner reactor, were loaded with MOX fuel and sodium as a coolant. The core was surrounded, axially and radially, with a reflector composed of sodium and stainless steel. The simulation of the neutron source and the spallation target consisted of a 250 keV deuteron beam horizontally guided on a target located at the centre of the core and surrounded by a lead buffer. A reference critical core and several subcritical configurations with reactivity levels ranging from near-criticality to –14$ (~-4500 pcm) were investigated. In the very last phase of the programme, a configuration where sodium was replaced by lead in one third of the fuel zone was also studied.

Measurements have been realized in both critical and subcritical configurations. When the cores were subcritical, we used, by turns, the intrinsic source, a ^{252}Cf source as well as the 2.7

or 14 Mev neutron sources provided by the GENEPI neutron generator [4], as the driving source. Intensities of these sources varied from 1.4 10^8 n/s to 1.2 10^{10} n/s.

The experimental programme, in the first phase, consisted of a full characterization of the critical configuration. The goal was to have a reference measurement point allowing the determination of the initial calculation biases due to the presence of new heterogeneities. In this aim, a number of fission rate traverses (~70) and spectral indices (~150) have been performed in all zones of interest for a large range of fission chambers (Th, U, Np, Pu, Am and Cm). Measurements have also been achieved to study the influence of a ^{252}Cf source located at the center of the core. Then, irradiations of more than 300 activation foils (indium, iron, cobalt, nickel, etc.), principally near the lead/fuel, beam guide/fuel and fuel/reflector interfaces, allowed a deeper study of the spectral and spatial fluctuations of the neutron distribution. Finally, kinetics parameters (β_{eff}, Λ) and rod experiments have been performed on the critical configuration for the reactivity scale determination. In a second phase, the same kinds of measurements were reproduced for each subcritical level with a limited number of measurements. The impact of the source could be highlighted as well as different aspects such as the moderation in the central lead zone and the streaming effects in the beam guide. In a last phase, sodium was replaced by lead in twenty two sub-assemblies of the central zone. Since the total number of fuel subassemblies was not modified, the reactivity effect and the changes in the fission rate distributions and spectral index values were only related to the lead effect.

The investigation of different calculation routes for these parameters yielded some interesting conclusions. The C/E value for the determination of k-eff was found to be very satisfactory for both deterministic and Monte Carlo codes although the uncertainties on the experimental values, with a standard deviation in the range 6-8%, did not allow to draw more definite conclusions. The comparison between experiment and deterministic codes for the kinetic parameters measured in near-critical conditions was found to be very good. With regard to Monte Carlo methods, a new and fast technique was developed for the calculation of â$_{eff}$ which also yielded a very good C/E value in near-critical conditions although the interpretation of the mean neutron lifetime Ë is still an open issue with the Monte Carlo codes. Concerning fission rate distributions, an overall good agreement was found for measurements at delayed critical. In subcritical configurations, we also found a good agreement for ^{235}U, and which was less so for isotopes with threshold reactions. The ^{238}U flux traverses in the centre of the configuration were shown to be very sensitive to the exact level of subcriticality in the calculation. Spectral indices with fission chambers exhibited some problems that are still to be resolved where the foil activation technique lead to very interesting conclusions. Finally, the simulation of the experiments performed in the lead phase showed similar effects and at present did not shed light on any major problem due to this material. Nevertheless, further calculations, in particular Monte Carlo simulations, should be carried out to analyse more deeply these measurements.

In addition, a series of experiments was conducted at JINR (Dubna, Russia) and concentrated on the measurements with several bare lead targets exposed to the 660 MeV/3.2 µA proton beam provided by the Phasotron available at JINR. Several experimental set-up were used and a large number of measurements were achieved. First experiment was devoted to the measurement of neutron spectra around the target, activation measurements of angular and surface distributions of hadrons around the target, and measurement of specific activities of threshold activation detectors in front of and behind the target. Experiment 2 and 3 were aimed at determining the axial distributions of radionuclides activity in the target where as experiment 4 was proposed to measure the radial distributions of the activity induced in Bi samples irradiated in the target. Among all the experimental data obtained, the most spectacular result was the distributions of Bi isotopes (^{207}Bi, ^{206}Bi, ^{205}Bi), which can be produced from Pb in

proton induced reactions solely (e.g. (p,xn)). They revealed a characteristic sharp peak about 30 cm inside the target in the region where proton energy decreases to 30 – 80 MeV.

Analyses of experiments and calculations demonstrated that angular distribution of hadrons around the target shows an agreement within 6-15 % where as much larger discrepancies, at the worst within one order of magnitude, were observed for the axial distributions of activity. Almost always the C/E ratios were found to be between 3 and 1/3. It was concluded that one cannot point out a single code and/or nuclear reaction model yielding good results simultaneously for all examined nuclides. Yet, it was noticed that the model of Cugnon gave the best agreement with experimental values - about 70 % of results remain within 30 % difference.

Turning to the reactivity measurement aspect of the MUSE programme, there were five teams that were involved in this field of the physics of subcritical systems. We studied the traditional rod drop/MSM method, source-jerk methods, variations of the pulsed neutron source methods, and noise methods. We had some problems with the MSM method that lead to larger uncertainties than expected. We also had some difficulties with the standard source jerk method that demonstrated that this technique could only be used, in a real ADS, during start-up or loading/unloading phases. The source modulation technique gave better results but, today, it cannot be seriously envisaged for the reactivity monitoring of an industrial machine. A rapid variation of the pulse frequency from a high frequency to a low frequency seems indeed difficult to implement in a power reactor. We showed that traditional noise methods (driven by the intrinsic or Cf source) such as the CPSD, Rossi- and Feynman-á were can only be used in the case where the reactivity is close to critical. A Rossi type technique driven by the neutron generator seemed nevertheless promising but it appeared, in definitive, that some form of the PNS method will be the most useful. Since GENEPI operates in pulsed mode with a rate ranging from 10 Hz up to 4.7 kHz which is always smaller than the reactor break frequency, several PNS models based on the interpretation of the slope of the signal (2-region, 3-region, kp-method) could be investigated. Analyses based on the fitting of the prompt neutron population was shown to be very sensitive to the kinetics model and fitting parameters. On the contrary, the so-called kp-method demonstrated the advantage of a simple and robust interpretation algorithm but have the disadvantage to require extensive Monte Carlo simulations. In definitive, studies have demonstrated that the so-called PNS "area method" is quite forgiving in relation to other PNS models based on the study of the slope of the signal. It seems that this method could be set-up in a cold start-up configuration of an ADS. In general, the approach for the assessment of biases and uncertainties to apply to all these results need to be investigated with more details in order to consolidate the overall demonstration.

Finally, for the continuous monitoring, we concluded that some form of a proton current/power/reactivity relation could be used. In general, if all remains constant, the ratio of the flux and proton current are proportional to a simple function of the reactivity, and simple real time monitoring (as in a typical power reactor) will yield sufficient information for control in normal operations. The potential problem occurs if there is an unknown configuration change, leading to a change in the source importance or a change in local reactivity values. Simply monitoring the flux and current will not provide any information for such a change. Thus, some form of independent, periodic, absolute determination will be required that can yield an independent measure of the reactivity. At the present time, it is envisioned that some sort of beam chop will be used, but it was not possible to test such a technique in the MUSE project. This, together with the on-line monitoring will be a major task for the IP-Eurotrans Domain 2 (experiments on coupling).

In summary, the MUSE project has been a great success in providing a major contribution to the R&D in support of ADS systems. It allowed more especially to extend the experimental

database relating to coupled systems and to study the viability of various methods of reactivity monitoring. Numerous advances have been made in understanding the behaviour of sub-critical systems although it was also demonstrated that some aspects still need to be further studied. Last, but not least, the programme produced some of the best collaborations seen in recent years, certainly in the reactor physics community. It brought together some of the best experimental reactor physicists in Europe, produced eight Ph.D. theses since the year 2000, and numerous publications in conferences and journals.

References

[1] Neutronic Studies in Support to ADS: The Muse Experiments in the MASURCA Facility
R. Soule & al
Nuclear Science and Engineering, Vol. 148 (2004) 124-152

[2] Experimental Assessment of Radionuclide Production in Materials Near to the Spallation Target,
J. Janczyszyn, W.Pohorecki, S. Taczanowski, G. Domañska V.N. Shvetsov, G. Gerbish
Proceedings of International Conference on Accelerator Applications/Accelerator Driven Transmutation Technology and Applications (AccApp/ADTTA'01), Reno, November 12-15, 2001, CD-ROM, ISBN: 0-89448-666-7, 2002

[3] ADS's based on the 660 Mev proton Phasotron of JINR for research on utilization of Plutonium
V.S Barashenkov, I.V. Puzynin, A. Polanski
Proceedings of the 10th International Conference on Emerging Nuclear Energy Systems (ICENES), Petten, 24-28 September 2000, p. 429

[4] The GENEPI accelerator operation feedback at the MASURCA reactor facility
C. Destouches & al
Submitted to AccApp'05 - International Topical Meeting on Nuclear Applications of Accelerator Technology - Venise,/Italy – 28 August/1 September 2005

Glossary

ADS : Accelerator Driven System

APSD : Auto Power Spectral Density

ASM : Approached Source Method/Multiplication

CPSD : Cross Power Spectral Density

E/W : East/West

FC : Fission Chamber

GENEPI : GEnérateur de NEutrons Pulsés Intense

MASURCA : MAquette de SURgénérateur à CAdarache

MSM : Modified Source Method/Multiplication

MUSE : Multiplication par Source Externe

N/S : North/South

PNS : Pulse Neutron Source

PR : Pilot Rod

PRU : Pilot Rod Up (in high position – Level 200 mm)

PRD : Pilot Rod Down (in low position – Level 1200 mm)

SAD : Sub-Assembly in Dubna

SC : SubCritical

SR : Safety Rods

1 Preamble

The MUSE project has been conducted within the frame of a large international collaboration composed of :

- partners involved in the project by the way of the contract with the European Community (Contract n°FIKW-CT-2000-00063 of the Fifth EURATOM Framework Programme),

Commissariat à l'énergie atomique (**CEA**/DEN/DER, Cadarache), France
Belgian Nuclear Research Center (**SCK**/CEN Mol), Belgium
Université Joseph Fourier, Grenoble 1 (**CNRS**/IN2P3/LPSC Grenoble) France
Forschungszentrum Karlsruhe GmbH (**FZK**), Germany
Forschungszentrum Jülich GmbH (**FZJ**), Germany
British Nuclear Fuels plc (**BNFL**), Great Britain
Ente per le Nuove tecnologie, l'Energia e l'Ambiente (**ENEA**), Italy
Nuclear Research consultancy Group (**NRG**, Petten), The Netherlands
Delft University of Technology (**DUT**), The Netherlands
Centro de Investigaciones Energeticas, Medio Ambiantales y Technologicas (**CIEMAT**, Madrid), Spain
Kungliga Tekniska Hogskolan (**KTH**, Stockholm), Sweden
Chalmers University of Technology AB (**CTH** Gothenburg), Sweden
Akademia Gomiczo Hutnicza/University of Science and Techonology - former University of Mining and Metallurgy - (**AGH**/UST, Crakow), Poland

- organisms who signed specific collaboration agreement with one of the above institutions,

Paul Scherrer Institute (**PSI**, Villigen), Switzerland (collaboration agreement with CEA)
Argonne National Laboratory (**ANL**) , USA (collaboration agreement with CEA)
Politecnico di Torino (**POLITO**), Italy (collaboration agreement with ENEA)
Japan Atomic Energy Research Institute (**JAERI**), Japan (collaboration agreement with CEA)

All these organisms, depending on their area of expertise, contributed :

- to the preparation of the MUSE experiments (Work-package (WP) n°1 of the project funded by the EC),
- to the performing of the experimental programme in the MASURCA facility (WP n°2)
- to the analysis and the interpretation of the results obtained (WP n°3).

A number of activities in support to the SAD project (ISTC project n°2207), because of the complementarity of this project with the MUSE programme, have been grouped in a specific work-package (WP n°4). These studies have been conducted by AGH/UST Krakow with the active participation of collaborators from :

Joint Institute for Nuclear Research (**JINR**, Dubna), Russia
Institute of Nuclear Physics (**INP**, Cracow), Poland

All the above institutions have contributed to this report.

2 Introduction

Especially due to its operating mode, a fast sub-critical reactor coupled to a particle accelerator, the so-called Accelerator Driven Sub-critical System (ADS) constitutes an attractive nuclear reactor concept which could allow to transmute waste with a good efficiency. Compared to a critical reactor, core sub-criticality should permit to load higher quantities of minor actinides without damaging its characteristics in terms of safety. But this potential and the real resistance of the core to severe transients or accidents has to be demonstrated, in comparison to conventional critical cores.

Beyond all the demonstrations needed before the commissioning of such a ADS system, it has been decided that a qualification, component-by-component, must be first achieved. Following this strategy, various projects have been launched in Europe in the field of accelerators, spallation targets, innovative fuels and materials, nuclear data and reactor physics. Among all these topics, the need for validating the calculation tools used for the core design studies lead to propose experimental programmes with a view to contributing to the extension of the experimental database and also to improve the understanding of the neutronic behaviour of these new reactor core concepts. The accomplishment of the MUSE-4 experimental programme in the MASURCA facility [2.1] and the PRE-SAD measurements in Dubna [2.2] aimed to contribute to these objectives. These two "zero-power experiments" constituted the first step before conducting experiments that will be more representative of a future ADS device.

3 Presentation of the programme

Neutronic experiment and studies have largely been achieved in the past for fast critical systems. The associated calculation tools (including recommended nuclear data and calculation routes) and bias factors developed for the predictions of such systems have been mainly based on integral experiments in critical facilities. Experimental techniques have also been developed, that are directly applied to power critical operating systems.

The same approach for studying neutronics of sub-critical systems driven by an external source is based on the decoupling of the validation of the sub-critical multiplying medium behaviour from the validation of the external source characteristics.

The above first item can be accomplished using well characterised neutron external sources and well known cores. From 1995, the MUSE programme at the MASURCA facility (CEA Cadarache, France) was aimed to propose such a contribution. First, the MUSE-1 [3.1] and then the MUSE-2 experiments [3.2], performed with a ^{252}Cf source located at the centre of the MASURCA core, lead to demonstrate that experimental measurement techniques used for critical cores could also be used for sub-critical configurations. Later, in 1998, the MUSE-3 experiments [3.3] constituted the first important parametric study with the loading of several configurations with increasing sub-criticality levels. Based on the use of a commercial neutron generator these experiments helped to optimize the design of the MUSE-4 programme and to specify the characteristics of a neutron source, that is more intense and more suitable to the envisaged measurements. This fourth phase (MUSE-4) has been conducted from 2000 to 2004. Mainspring of the MUSE-4 experiments, the GENEPI (Générateur de Neutrons Pulsés Intenses) neutron generator rested on usual (D,D) and (D,T) reactions producing two different well-known neutron sources in terms of intensity and neutron energy [3.4].

The main topics of the MUSE-4 programme were to:

- define sub-critical experimental configurations of interest (in terms of fuel, geometric arrangement, external source type and operating modes).

- develop new specific experimental techniques mainly in support to the operation of sub-critical systems, but also for standard integral parameters to obtain a wide range of experimental results to define accurate experimental uncertainties.

- experimentally characterize these configurations (in terms of reactivity level and neutron spectra) by integral experiments using standard or new experimental techniques.

- analyze these experimental results by use of different nuclear data files and calculation methods (deterministic and Monte-Carlo tools) with the objective to evaluate the performances of current neutronic code systems and to contribute to the definition of reference calculation routes (including nuclear data and calculation tools) for the neutronic predictions of an ADS.

- propose new strategies allowing the determination of the reactivity level of sub-critical configurations without the need of a critical configuration.

On the other hand, complementary experiments that were conducted in the frame of the SAD project (project of a Sub-critical Assembly in combination with the existing proton accelerator in Dubna [3.5]) were aimed to validate the simulation of physics phenomenon in heavy materials bombarded by a high energy proton beam. They have been performed using different Pb targets and taking advantage of the 660 Mev proton beam supplied by the accelerator available at Dubna. The main goals of these experiments were to:

- determine experimentally the integral and differential characteristics of hadron field around a bare spallation target,

- measure the nuclides produced by the spallation process using samples of elements of the main elements composing the spallation target and surrounding construction materials,

- simulate these experiments using various codes and model option in order to contribute to the definition of a reference calculation route,

Since various experimental programmes will be performed in the future SAD facility, the relevance of neutronic experiment and more especially dynamics experiments have to be evaluated. These studies constitute a natural complement to the MUSE-4 programme. The main objectives are:

- to examine the influence of core, reflector and shielding parameters of the SAD core versions on its experimental properties,

- to study the possibilities to infer accurately the reactivity level.

4 Contribution to programme objectives

4.1 Overview of the activities conducted during the project

A large number of activities have been conducted all along the duration of the project (Fig. 4.1). Since the experiments at the MASURCA facility and at Dubna were at the centre of the project [4.1, 4.2], several activities of interest in the field of reactor physics have been carried out to improve the analyses of the measurements and to help to the understanding of the results and the discrepancies observed.

Fig. 4.1: Activities conducted within the project

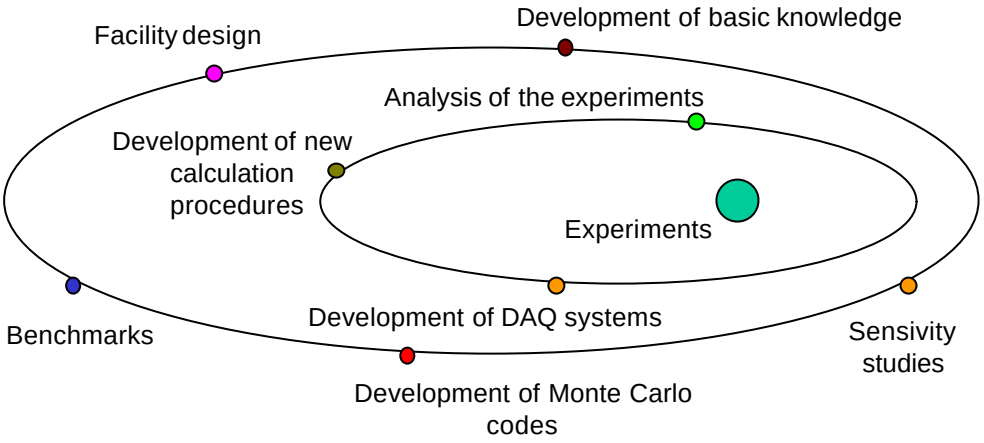

First, in view of the MUSE-4 experiments, new acquisition systems have been developed by the teams involved in the experimental programme [4.1]. Most of these systems have been designed with the objective to replay experiments off-line using various analysis techniques. For that purpose, a timing of any event detected, such as counts outgoing from detectors operating in pulse mode, is achieved. These systems have been successfully used all along the measurement campaigns.

The simulation and the analysis of the experiments performed in subcritical configurations focused the effort of most of the partners involved in the MUSE experiments [4.3]. Numerous calculations have been performed to understand the experimental results and more especially those concerning the key issue of the subcriticality measurement. First, the simulation of these experiments confirmed the experimental data obtained in the detectors located in the core. Then, these calculations allowed us to explain why the detectors located in the reflector and the shielding had not the same behaviour. Last, following new calculation procedures defined and tested within the frame of the project, these discrepancies among the detectors can be now corrected [4.4]. A simplified benchmark [4.5] as well as a computational benchmark initiated in the frame of the MUSE project and then managed by the OECD/NEA [4.6] gave also interesting trends and conclusions about the possible origin of some discrepancies.

Since the reactivity level expressed in dollars constitutes the parameter of interest from a safety point of view, the knowledge of the value of the delayed neutron fraction is of a prime importance. Nevertheless, this parameter can not be measured precisely (i.e. with a reasonable uncertainty) and most of the time it must be calculated. Untill now, few neutronic code systems and none stochastic tool allowed to calculate this parameter following the adjoint formulation. The major development performed during the MUSE project lead to propose a true Monte Carlo estimator, for the effective delayed neutron fraction assessment, in a single k_{eff} calculation [4.7].

This method was tested and it has been shown that it was faster and more accurate than all the others formulations.

The features of Monte Carlo codes make these tools very interesting especially in the case of complex geometries. These codes are thus often used as a reference to validate the results obtained with deterministic codes. However, their major problem is the time needed to obtain enough statistics for the parameter of interest. The simulation of time dependent experiments, more especially in detectors far from the core, is thus very difficult and very time consuming. The simulation of noise measurement in deep subcritical configurations is still much more hazardous and does not allow to perform parametric studies. In this context, the development of the semi-analog Monte Carlo method to simulate pulse-counting experiments with variance reduction methods is of a great interest [4.8]. Although this work is not yet fully completed, much work has been already accomplished.

Considering that code systems can not easily address certain problems (for instance, simulation of noise measurement in subcritical configuration), the development of simplified models is of great interest and allows one to have at our disposal tools easy to use. So, within the frame of the project, the derivation of the Rossi-alpha-function [4.9], the Feynman-alpha-function [4.10] and the CPSD-function [4.11] considering a pulsed neutron source has been achieved. Mathematical formulations for the Feynman-alpha-function have been established for both deterministically and randomly pulsed sources. The advantages and disadvantages of the different methods could be thus analyzed. The conclusions drawn from these studies can help to define future experiments.

Before turning to new projects and programmes, it is interesting to recall the representativity of the MUSE configurations on the basis of emerging concepts of eXperimental Accelerator-Driven Systems (XADSs). In this aim, specific investigations, via data sensitivity/uncertainty analyses in which the external neutron source has been considered, have been conducted to assess this aspect of the MUSE-4 programme [4.12].

To conclude this overview, it is obvious that the diversity of the activities briefly presented above do not allow that all these investigations and studies are described in detail in this report. On the other hand, they have been published in various scientific journals and also presented in numerous international conferences, meetings and workshops. A list of publications, oral presentations and posters related to the activities carried out during the contract period is thus given in annex 1. Last but not least, several PhD thesis directly connected with the MUSE-4 experiments have been completed from 2000 to 2004. The contributions of these young researchers were essential in the success of the MUSE project. These theses are listed in annex 2.

4.2 The MUSE-4 programme

The MUSE-4 programme has been established taking into account the availability of sodium and lead at MASURCA on one hand, and the important constraints caused by the eventual loading of a 100% lead core on the other hand. Thus, it was decided that :

- the first four configurations would use sodium coolant (MUSE-4 Sodium experiments),
- the fifth configuration would contain an optimised number of subassemblies loaded with lead instead of sodium. Due to the necessity of cladding the lead bars initially available at MASURCA, this sodium and lead cooled configuration was performed at the end of the programme .

As concerns the sodium cooled configurations:

- one reference critical state has been carried out for the reactivity scale determination by standard reactivity calibration measurement, and for core characterization in terms of neutron flux level and neutron spectra determination.
- then, three sub-critical states were studied with the GENEPI generator out and in operation. First, a slightly subcritical configuration (named SC0), then two states where subcriticality levels will be more representative of those considered for the standard operation of an ADS (SC2 with a k-effective close to 0.97 and SC3 with a k_{eff} equal 0.956). Static measurements using the « pseudo-continuous » mode of GENEPI have been performed to characterize the sub-critical media driven by well known external sources by way of different experimental techniques proposed by the different partners of the consortium.

As concerns the partial lead cooled configuration, only one configuration has been carried out in order to avoid long loading periods.

The well-known external neutron sources issued from the GENEPI accelerator by (D,D) or (D,T) reactions, have been successively used in « pseudo-continuous » mode for all the static measurements and in the pulsed mode with different frequencies (from 50 to 5000 Hz) for the dynamic measurements. However, owing to the subcriticality level and the low counting rates obtained, only the tritium target has been used for the two last configurations (SC3 Na and SC3 Na/Pb).

Using the pulse mode of GENEPI (with various frequencies) dynamic measurements have been performed and different experimental techniques allowing the sub-critical states determination of the different multiplying media have been investigated. These measurements were performed in the frame of an experimental benchmark among the different partners.

These experimental data sets have been then analysed by several partners with their own calculation tools (various nuclear data and calculation methods using both deterministic and Monte-Carlo codes). Inter-comparison of the analysis results have been made and lead to shed on light trends on methods and data. Finally, taking advantage of the large amount of experimental data and analysis results available, recommendations for the measurement of the subcriticality in a power ADS are proposed.

4.3 The SAD project and the PRE-SAD measurements

The idea of an experiment proposed in the Joint Institute for Nuclear Research (JINR) in Dubna and realised as the project SAD (Subcritical Assembly in Dubna) is a valuable response to the needs and a natural completion to the project MUSE. The applied spallation neutron source is of typical proton energy for real ADS (660 MeV). Also the power generated in the core (up to ~20 kW) makes it a good tool for precise measurements of heat generation.

The SAD core and its proton beam line are still in the phase of designing. So, the activities carried on during the period 2000-2004 concentrated on :

- calculations for examining the influence of core, reflector and shielding parameters of the SAD versions on its exploitation and experimental properties,

- measurements aiming at the verification of codes and data bases applied in modelling of integral and differential characteristics of hadron field around a spallation target bombarded by a high energy (660 Mev) proton beam,
- neutron shielding efficiency measurements, with a special attention to a « forward » direction (behind the target area, in the direction of the primary proton beam)
- measurements of radioactivity generated in the spallation target (and its surroundings),
- developing of the methodology for neutron spectrum and dose rate measurements for the energy range above 20 MeV.
- post-mortem analysis of the spallation target and special samples (transuranic isotopes) including radiochemical analysis,

will be performed and analysed for the validation of neutron shielding calculations of ADS.

4.4 Brief description of the experimental set-up

4.4.1 The MASURCA facility and the MUSE-4 cores

The MASURCA facility (Fig. 4.2 and 4.3) is one of the critical mock-up operated by CEA at the Cadarache Study Center in the department of "Les Bouches du Rhône". This nuclear facility is dedicated to the neutronic studies of fast lattices. It is an airflow cooled fast reactor operating at a maximum power of 5 kW and a flux level up to 10^{11} n/cm^2/s. The materials of the core are contained in cylinder rodlets, along with in square platelets. These rodlets or platelets are put into wrapper tubes having a square section (4 x 4 inches) and about 3 meters in height. The reactivity control is fulfilled by absorber rods in varying number depending of core types and sizes. These safety rods (SR) are composed of fuel material in their lower part, so that the homogeneity of the core is kept when the rods are withdrawn. A "Pilot Rod (PR)", with a reactivity worth less than half a dollar, allows the fine tuning of the reactivity. The core is cooled by air. Cores of various dimensions (1000 tubes maximum) can be simulated.

MASURCA had its criticality in 1966. Till the middle of the 90's, programme s were devoted to the studies conducted in support of the PHENIX, SUPERPHENIX and EFR (European Fast Reactor) projects. Since, it has been operated to test various reactor concepts that could be used for plutonium burner cores (CIRANO programme) and for the transmutation of radioactive wastes. In particular, from 1998 to 1999, the COSMO programme aimed to study the Physics of the irradiation of LLFP targets in moderated sub-assembly at the periphery of fast reactors. The effects of various moderators, $^{11}B_4C$, CaH, , ZrH_2, have been investigated. This programme helped in particular to the preparation of the ECRIX experiments that have been loaded in the PHENIX.

The MUSE-4 cores (2001-2004) are based on a basic fuel cell, composed of two Mox rodlets for two sodium rodlets, representative of a fast Pu burner core (Pu enrichment of » 25% with » 18% content of ^{240}Pu) with sodium coolant. This pattern is reproduced sixteen times in each fuel subassembly (Fig. 4.4). The fuel zone is radially and axially reflected by a stainless steel/sodium (75 %/25 %) shielding. The GENEPI deuteron guide was horizontally introduced at the core mid-plane and the deuterium or tritium target will be located at the core centre (see Fig. 4.5). To compensate the spatial effect due to the presence of the GENEPI guide in the north

part of the loading, the south symmetrical part was loaded with pure lead (99.99% of Pb) simulating the Pb circulation of the target. To simulate the physical presence of a Pb spallation source, a pure square (10 cm thick) lead zone is placed around the GENEPI target. Full details of these configurations and the materials used are reported in [4.13].

Fig. 4.2: Bottom view of MASURCA core

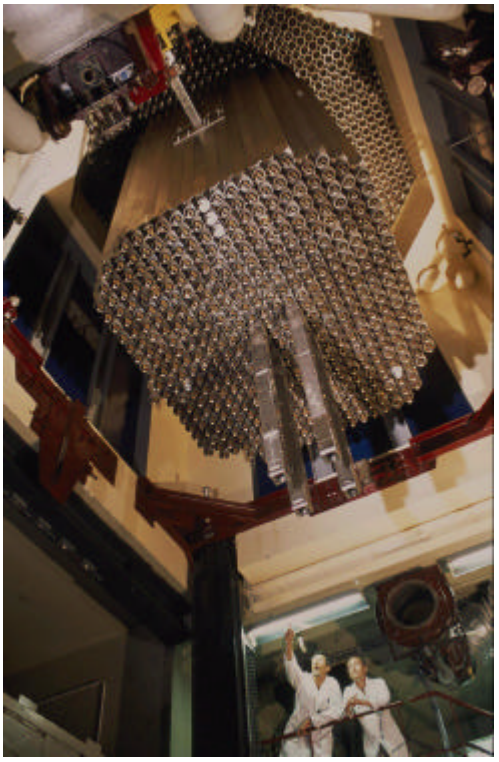

Fig. 4.3 : Top view of MASURCA core

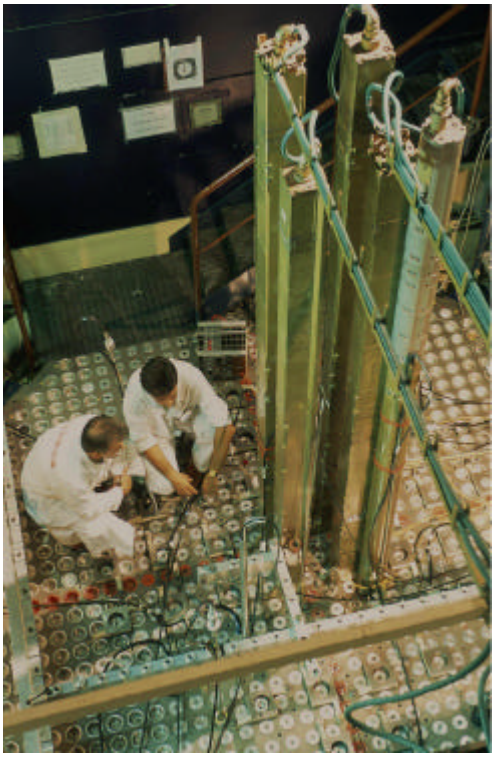

Fig. 4.4: Radial cuts of a fuel assembly and a reflector assembly

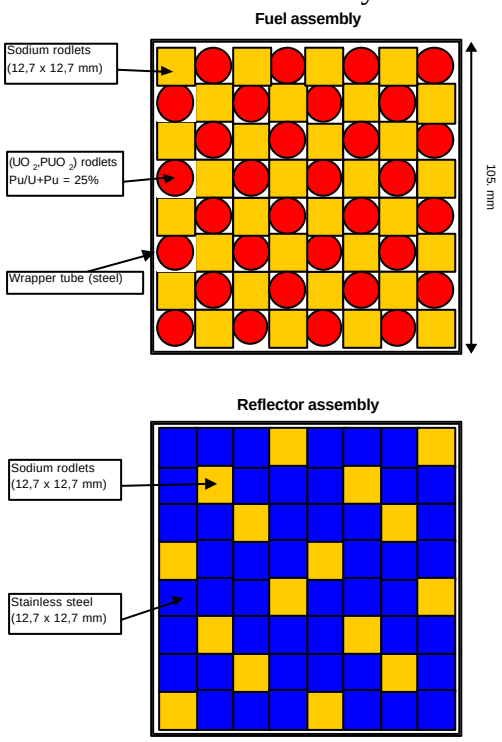

Fig. 4.5: Radial cut of the MUSE-4 critical configuration with 1115 fuel cells

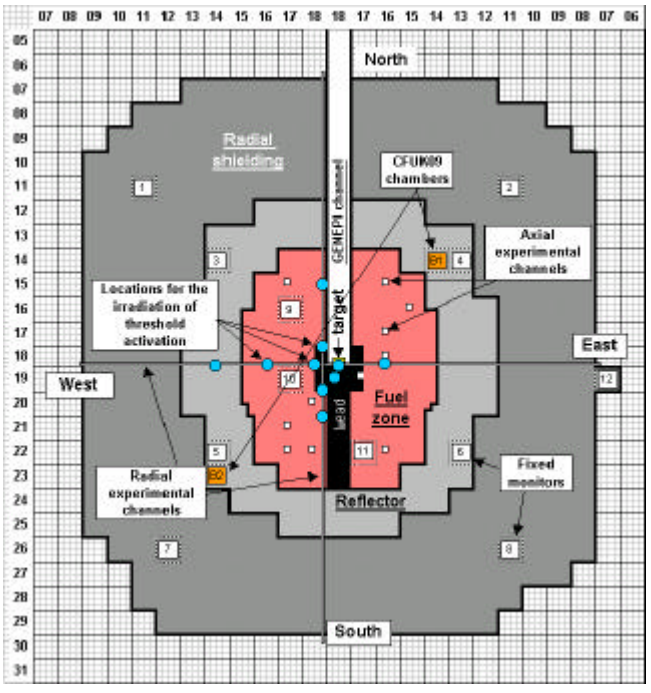

To perform the measurements, various devices are used :

- twelve fixed monitors, most of them with ^{235}U deposit (from 10 mg to 1g), were used in the pulse mode mainly for the subcriticality measurements. Their location changed several times all along the programme to optimise their use (to decrease the dead time or to increase the counting rate.

- two CFUK09 high efficiency fission chambers (^{235}U deposit is about 4.5g) located in E14-14 (B1) and W23-14 (B2) positions (reflector zone) have been used in current mode for noise measurements.

- last, special channels have been opened throughout the MASURCA tubes : two horizontal channels at 90° around the mid-plane (radial channels) and thirteen axial channels. They allowed to introduce and eventually move different devices such as miniature fission chambers, foils and also ^{252}Cf sources.

4.4.2 The GENEPI neutron generator

The carrying out of the MUSE-4 experiments needed the use of an intense variable external neutron source simulating the spallation source supposed to be used in an "ADS". Benefiting from the feedback and the experience gained during the MUSE-3 experiments, the ISN team designed and realized a specific pulsed deuteron accelerator, GENEPI (GEnérateur de NEutrons Pulsés Intense), which produces neutrons by the $D(d,n)^3He$ (deuteron-tritium) or $T(d,n)^4He$ (deuteron-deuterium) nuclear fusion reactions on the GENEPI target. The simulation of the spallation source is approached by the lead medium surrounding the GENEPI target, where (n,2n) reactions occur.

The accelerator is described in details in the reference [4.14] but a schematic description is given below and Fig. 4.6 presents the GENEPI implantation in the MASURCA facility. In the 250 kV High Voltage Head, the deuterium atoms are ionised by an arc discharge using a hot filament and form a plasma into the "duoplasmatron" source. The discharge is triggered by an auxiliary electrode at a rate ranging from 10 Hz up to 4,7 kHz and its duration is determined by an LC delay line. The ions are then extracted and focused creating a deuterons (D^+) beam. This beam is accelerated up to 250 kV maximum (3) and deviated by a 45° magnet (5) in order to select the D^+ ions (and remove the molecular D_2^+). This deviation is also necessary for first allowing GENEPI to enter in the MASURCA accelerator room and second for the withdrawal of the thimble of GENEPI introduced into the core. Indeed, the thimble is movable and is inserted into a channel dug along the North-South direction inside MASURCA core tubes.

The deuteron beam is transported over the 5 m beam line and focused by magnetic and electrostatic quadrupoles all along its trajectory. Magnetic and electrostatic Steerers associated to diagnostics finely adjust the beam position down to the copper target (49 mm diameter) supporting a TiT or TiD deposit (30 mm diameter). The mass of Tritium or Deuterium deposit is about 1.2 mg/cm^2, which corresponds to about a 12 Curies tritium activity.

A FARADAY cage surrounds the GENEPI design in order to avoid the electromagnetic interferences in case of sparking.

Local and remote control of the accelerator is provided through a dedicated software, "LABWINDOWS", and specific embedded PC cards.

Fig. 4.6: GENEPI implantation in the MASURCA facility.

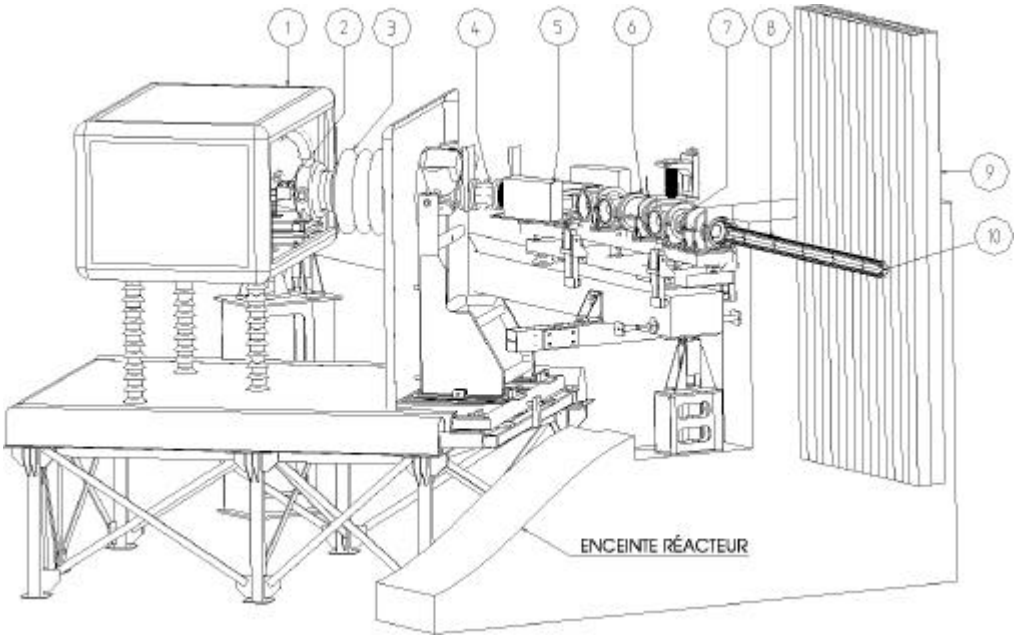

The GENEPI device performances are summed up in the Tab. 4.1. They are very close to the initials specifications [4.14].

Tab. 4.1: GENEPI beam characteristics

Beam energy (keV)	140 to 240
Peak current (mA)	50 to 60mA
Repetition rate (Hz)	10 to 4700
Minimum pulse duration (10^{-9} s) (at mid height signal) – for the target current signal	500 to 700
Minimum pulse duration (10^{-9} s) (at mid height signal) – for the neutrons pulse signal (α detector)	400 to 500
Mean beam current (μA)) (to be divided by 1.6 for an effective value)	150 (for a duty cycle of 4700 Hz)
Spot size diameter(mm)	≈ 25 mm
Pulses reproducibility	Fluctuations at 1% level

The GENEPI accelerator was designed and constructed by the ISN (now LPSC) team at the IN2P3 GRENOBLE site from September 1996 (first studies and calculations) to December 1998 (End of building of the A track). The physical studies and qualification were performed during the year 1999. The removal took place in February 2000 in order to make the implantation in the MASURCA facility. The set up of the accelerator was completed at the end of June 2000 and the first D+ beam was delivered to an inert target in August 2000.

The TiD target was mounted in November and the first neutrons were produced in the beginning of March 2001. The safety tests (compatibility with the functioning of MASURCA) were realized in the same period.

The first coupling of GENEPI TiD target with MASURCA all rods up in a slight sub-critical level (SC0 1086 cells+ISN tube) was performed on the 27th of November 2001.

The first coupling of GENEPI – TiT target with MASURCA all rods up in a slight sub-critical level (SC0 1108 cells) was performed at the end of November 2002.

4.4.3 The Phasotron at the JINR

The existing JINR proton accelerator called Phasotron (see Fig. 4.7) is the basic and unchanging element of all proposed versions of SAD. Its most important parameters from the point of view of the present experiment are the following:

- the maximum beam power: 2.1 kW
- the maximum proton energy: 659 ± 0.6 MeV
- the proton energy dispersion: 3.1 ± 0.8 MeV
- the pulse duration (subject to shortening efforts): 30 μs
- pulse repetition frequency 250 Hz

Fig. 4.7: The Phasotron in its hall

All the described below experiments were conducted on the same experimental stand placed in the room adjacent to the accelerator hall (Fig. 4.8) The principal destination of the stand is the research in the field of nuclear medicine. For this goal a low current beam is sufficient (~ 10^{10} p/s obtained from the nominal intensity ~ 10^{13} p/s by reduction with a narrow carbon collimator) and only such beam could be used in our measurements.

Fig. 4.8: Position of the experimental stand – cabin No 7; ML – magnetic lenses

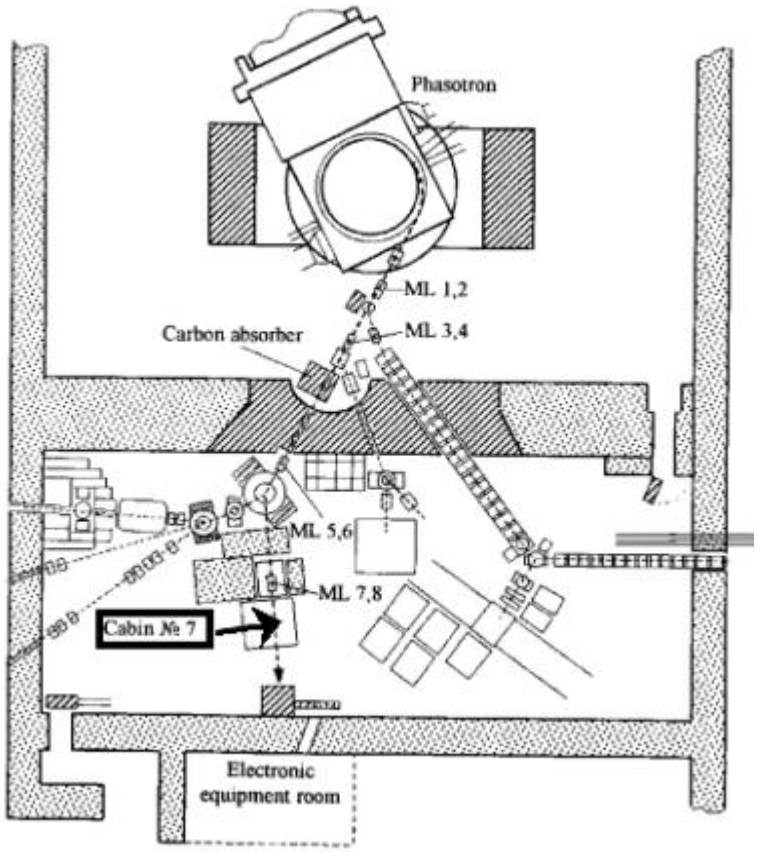

Values of the parameters applied in the presented experiments were :

- proton energy: 650 ± 4 MeV (nominally 660 MeV)
- max. proton yield: $I_{p,max} = 3 \cdot 10^{10}$ p/s,
- irradiation time: t_i = 10 m - 10 h,
- decay time: t_d = 2 h - 2 y.

For each experiment the beam was focused and the lead target longitudinal axis was positioned along it (Fig. 4.9). From a practical point of view, short-lived isotopes were measured at JINR when long-lived ones were analysed at UMM Cracow.

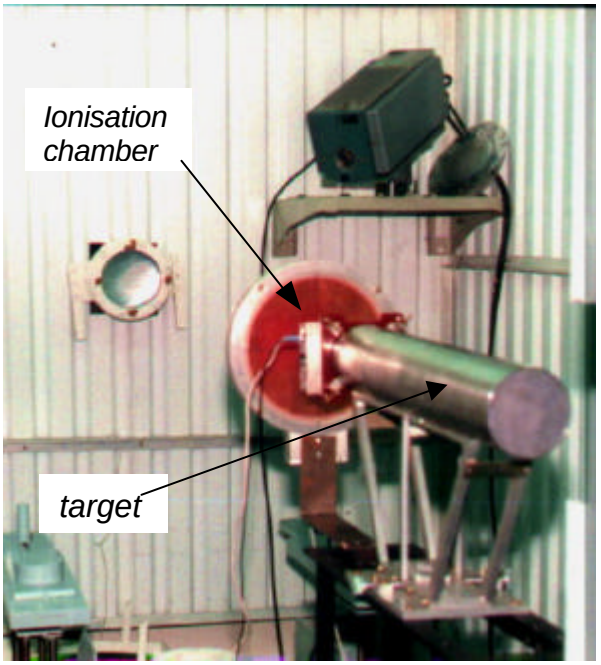

Fig. 4.9: View of the experimental stand with one of the applied targets (Pb/steel, f =85 mm, L = 500mm) assembled of four cylinders.

5 Characterization of the cores with and without neutron external source

5.1 Development of the MUSE-4 experiments – Main events

The loading of a core and the realization of experimental programme s at MASURCA is submitted to numerous rules and, in particular, to authorizations delivered by the safety authorities (at local, departmental or national level). In this aim, one (several) experiment safety report(s) describing the programme and its impact in terms of safety is (are) prepared in support of the request to carry out the experiments. These reports are examined and analysed by the safety authorities.

The specificity and the uniqueness of the MUSE-4 programme probably disrupt usual questionings of people generally in charge of analysing critical experiments In this context, long negotiations, numerous technical demonstrations, new procedures and specific tests had to be achieved to answer to the Safety Authority requests. In the same time, the set-up of GENEPI also needed to make several adds to the safety report of the facility. These requirements created an important extra work. As a consequence, the authorization to perform the experimental programme on subcritical configurations was delivered about one year later than planned. Very quickly the need to modify the initial work programme became evident and lead to prepare a first contract amendment including a reduction of the number of experiments and an extension of the duration till December 2003. This first amendment was signed by both parties on September 2003.

Since the subcriticality of the cores was adjusted by changing the number of fuel sub-assemblies rather than tuning the axial position of the control rods, much time is necessary to move and replace the subassemblies and in definitive to move on from one configuration to another one. All these activities have been underestimated and lead to increase the drift compared to the initial time schedule. On the other hand, the optimisation of the experiments, more especially subcritical experiments, lead to numerous small changes of core configurations and monitor locations. These efforts to improve the experimental conditions however amplified the delay. Last, maintenance problems with GENEPI and some operating constraints at MASURCA did not allow to reduce it. As a consequence, a second then a third amendment were signed on December 2003 and April 2004. Finally, the contract extended till 31 October 2004.

The progress of the MUSE-4 experiments is presented in annex 3. The main milestones and events were as follows :

22 September 2000	: Kick-off Meeting
1st October 2000	: Start-up of the contract
9 January 2001	: First criticality of the MUSE-4 reference core (configuration with 1112 fuel cells)
28 May 2001	: Authorisation to perform the experimental programme in the reference critical configuration
19 September 2001	: Authorisation to couple MASURCA and GENEPI with all the safety rods up
13 November 2001	: Authorisation to perform experimental programme in the three successive MUSE-4 subcritical configurations

27 November 2001	: First coupling of the accelerator with the reactor with all safety rods up. The reactivity level was close to –1.8$ (~-600 pcm)
January 2002	: Short experimental campaign with a reactivity level close to –2$.
March-September 2002	: Full characterisation of the reference critical configuration
October 2002-November 2003	: Study of the subcritical sodium cooled configurations
19 February 2004	: Authorisation to perform experimental programme on the subcritical partial lead cooled configuration
May-July 2004	: Measurement campaign on the partial lead cooled configuration
2 August 2004	: End of the experimental programme

5.2 Configurations studied

After a preparation phase that lasted from November 2001 to March 2002, the full characterization of the reference critical configuration was completed from April to June 2002. This long campaign was conducted in order to have a well-established reference measurement point. In particular, rod-drop experiments and measurements of kinetic parameters have been achieved with the objective of determining reference reactivity levels.

The study of subcritical states began again (a very brief campaign was conducted in January 2002) at the beginning of October 2002 with the investigation of the SC0 clean core configuration using neutron external sources provided by GENEPI. After this measurement phase ended on March 2003, configurations with reactivity levels more representative of an industrial ADS have been studied : SC2 configuration (k_{eff} around 0.97) was from April to July 2003 and the SC3 configuration with a k_{eff} around 0.956 was studied from September to November 2003. A very last configuration with a central zone loaded with lead rodlets instead of the current sodium rodlets was conducted from May to July 2004.

Main features of these five main configurations are presented in Tab. 5.1, Fig. 5.1 and 5.2. In fact, a total of thirteen different configurations have been loaded. For more details about these sub-configurations we refer to the three experimental reports [4.1].

Tab. 5.1: Characteristics of the main configurations studied

	Configuration						
	Reference	SC0		SC2		SC3	SC3 Na/Pb
Number of equivalent fuel cells	1125	1108		1006		972	972
Position of the 4 SR	Up	Up		Up		Up	Up
Position of the PR	Down	Down		Down		Down	Down
Reactivity* : - in dollars - in pcm (date)	-0.26 ± 0.01 -86 ± 4 (01/09/2001)	-1.86 ± 0.1 -622 ± 37 (10/21/2002)		-8.72 ± 0.59 -2911 ± 207 (03/26/2003)		-13.58 ± 0.92 -4534 ± 322 (08/27/2003)	-11.06 ± 0.86 -3695 ± 299 (05/26/2004)
Target	-	D	T	T	D	T	T
Period	03/09 2002	11/12 2002	01/03 2003	04/06 2003	07 2003	09/11 2003	05/07 2004
Maximum power with GENEPI ON	-	<10 W	<50 W	<10 W	<2W	<5 W	<5 W

* : the reactivities were determined using the Modified Source Method (MSM). The uncertainties correspond to one standard deviation. The beta effective value used to express the reactivity in pcm is 334 pcm [4.1].

Fig. 5.1: Radial cuts of the four main sodium cooled configurations

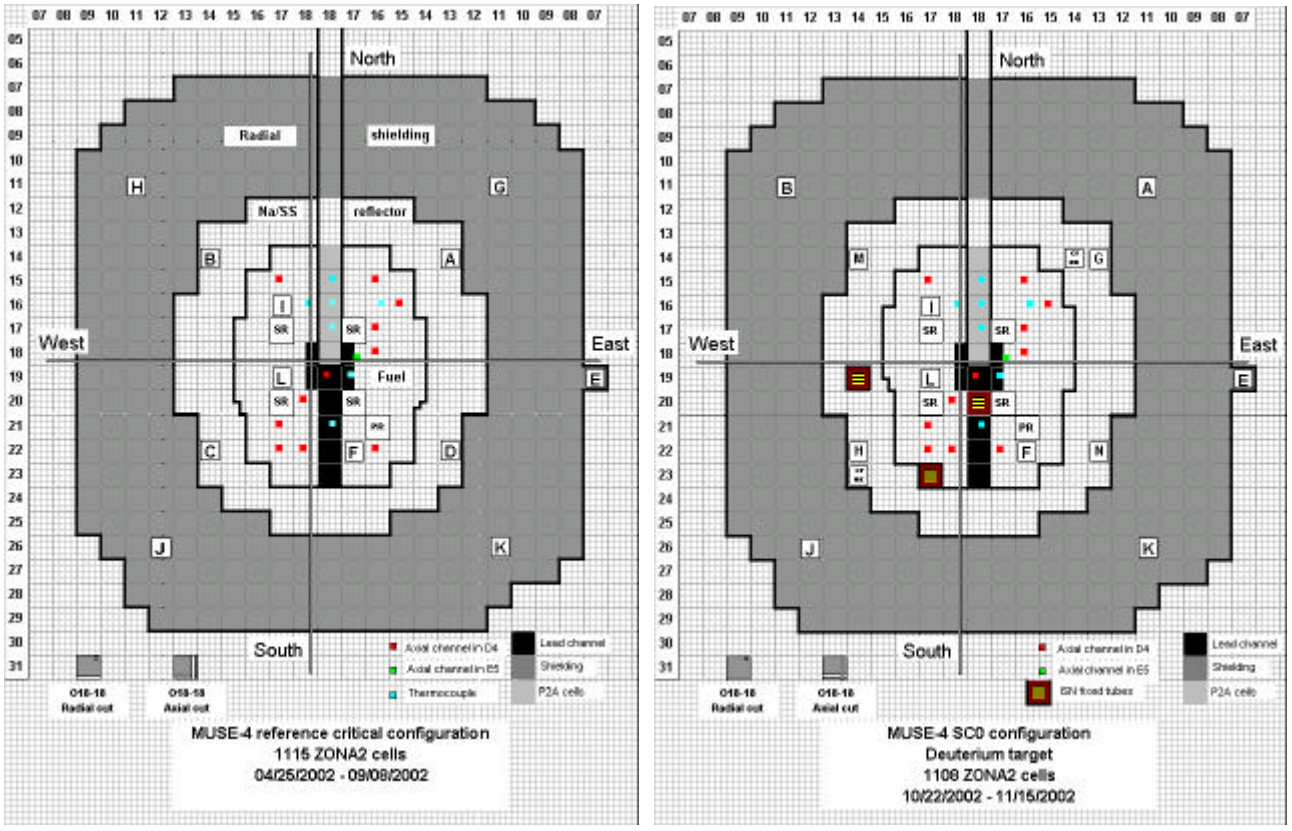

Fig. 5.1 (cont.): Radial cuts of the four main sodium cooled configurations

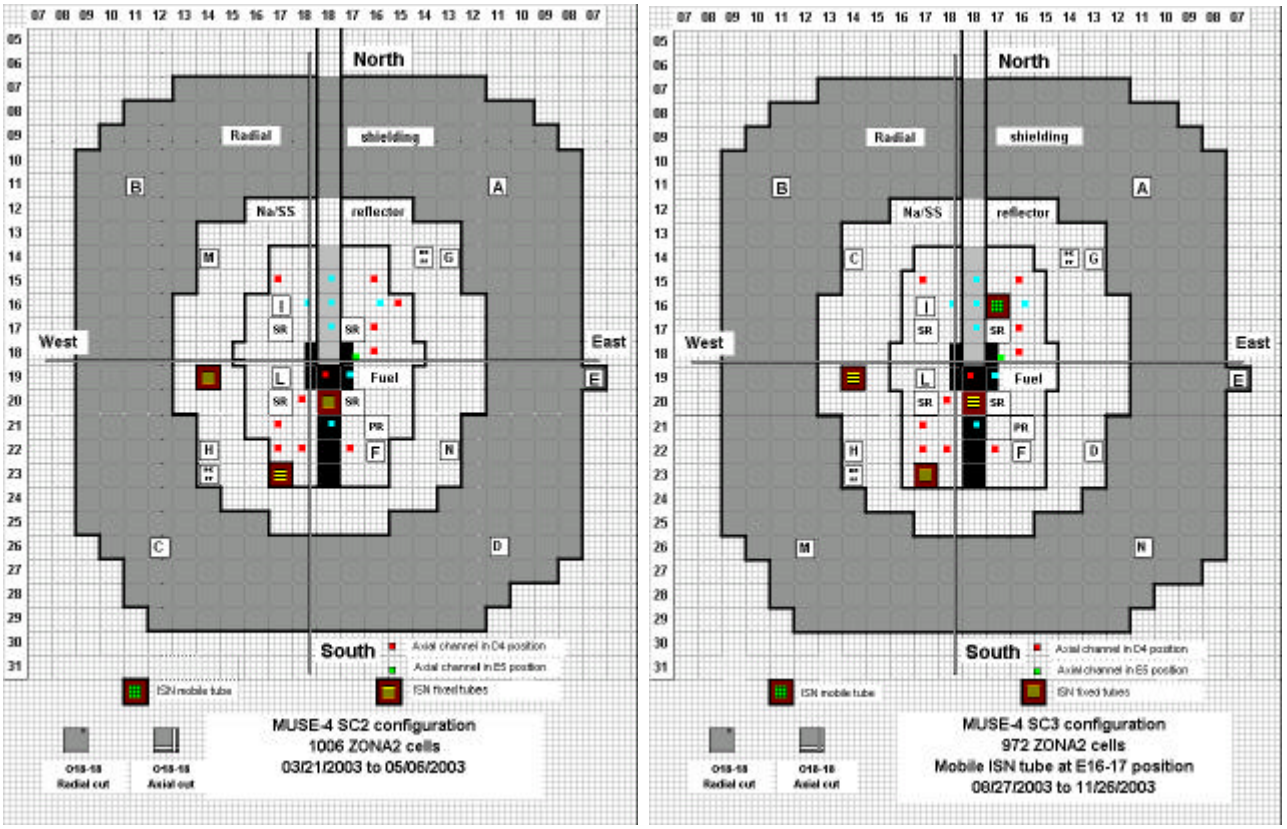

Fig. 5.2: Radial cut of the sodium/lead cooled configuration

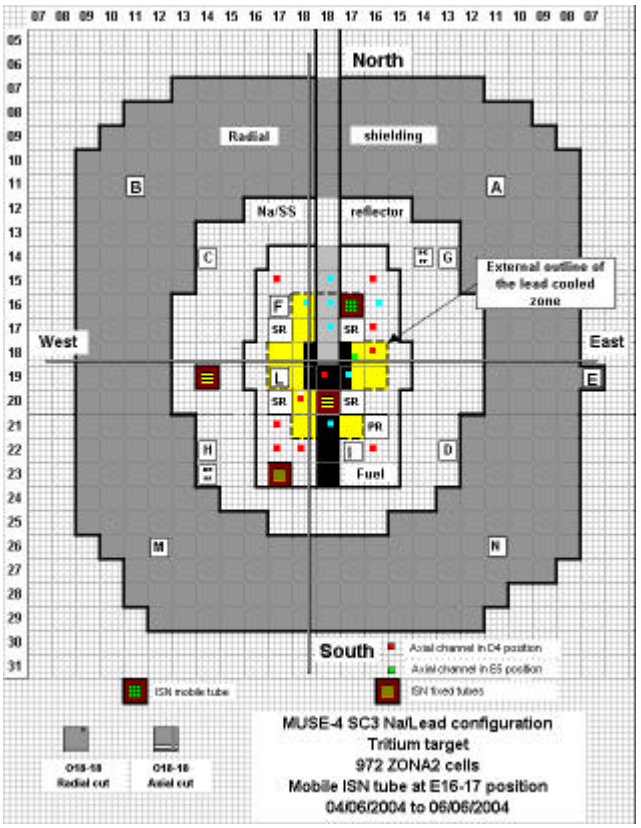

5.3 Coupling of GENEPI and the MUSE-4 cores

The GENEPI accelerator was designed and constructed by the ISN (newly LPSC) team at the IN2P3 GRENOBLE site from September 1996 (first studies and calculations) to December 1998 (end of building of the A track). The physical studies and qualification were performed during the year 1999. The removal took place in February 2000 in order to make the implantation in the MASURCA facility. The set up of the accelerator was completed at the end of June 2000 and the first D+ beam was delivered to an inert target in August 2000.

The TiD target was mounted in November and the first neutrons were produced in the beginning of March 2001. The safety tests (compatibility with the functioning of MASURCA) were realized in the same period.

The first coupling of GENEPI TiD target with MASURCA all rods up in a slight sub-critical level (SC0 1086 cells+ISN tube) was performed on the 27th of November 2001.

The first coupling of GENEPI – TiT target with MASURCA all rods up in a slight sub-critical level (SC0 1108 cells) was performed at the end of November 2002.

5.3.1 Absolute Source Calibration

To characterize the neutron source produced by the GENEPI accelerator, irradiation experiments were performed. Nickel foils were disposed on a target holder inserted vertically in MASURCA core, as close as possible (~10 cm) to the target producing neutrons under deuteron impact. These irradiations were performed with all the safety rods inserted and at a repetition rate of about 4 kHz in order to minimize the activation due to the inherent source. Several reactions on Ni were exploited.

After irradiation the activity of each Ni target was measured in the Low Activity Lab of the CNRS-INP2P3-LPSC, using a low background germanium detector. These activities, compared to MCNP simulations of the activation, allow deducing the number of neutrons per pulse. The results are as following: the neutron production rate of the deuterium target was found equal to $3.0 \pm 0.3 \times 10^{4}$ neutrons per pulse on the 5th of April 2001 (for a 60 mA peak current, oscilloscope measurement).

The neutron production with the tritium target was found equal to $3.3 \pm 0.3 \times 10^{6}$ neutrons per pulse (40 mA peak current) on the 22th of January 2003. By recording simultaneously the monitoring detectors, which consist in silicon detectors counting the charged particles associated to the neutron production, it was also possible to associate the number of these particle detected to the absolute neutron production, and then to have an online monitoring of the source. The detection rate was found equal to $1.92 \pm 0.20 \times 10^{-7}$ proton per source neutron ((d,D) source monitoring) and to $2.44 \pm 0.24 \times 10^{-7}$ alpha-particle per source neutron ((d,T) source monitoring). More details about these measurements and results can be found in [5.1].

A second calibration of the TiT target was performed on the 2nd of July 2003, which showed a decrease of the neutron production of about one third. In September 2003, a new TiT target was installed to increase the neutron production but it was not very different from the old one.

5.3.2 Monitoring of the Source

An electronic ammeter measures the deuteron beam intensity on the target. The neutron production is measured online with two backward silicon detectors which detect the charged particles associated to the nuclear reactions: one is detecting the α-particles and the protons produced by reactions on the tritium or the deuterium target (the proton being not associated to

neutron production but to a competing reaction on deuterium), and the other one detects only the protons, α-particles being removed by a aluminium stopping foil. The shape of the neutron pulse obtained by current and charged particles measurements is shown in Fig 5.3. The rather good agreement between these two methods appears. Fig. 5.4 shows a more precise time shape of the neutron pulse obtained with a silicon detector, and from which the FWHM is found equal to 400 ns.

By recording simultaneously the monitoring detectors it was also possible to associate the number of these particle detected to the absolute neutron production, and then to have an online monitoring of the source. The detection rate was found equal to $1.92 \pm 0.20 \times 10^{-7}$ proton per source neutron ((d,D) source monitoring) and to $2.44 \pm 0.24 \times 10^{-7}$ alpha-particle per source neutron ((d,T) source monitoring).

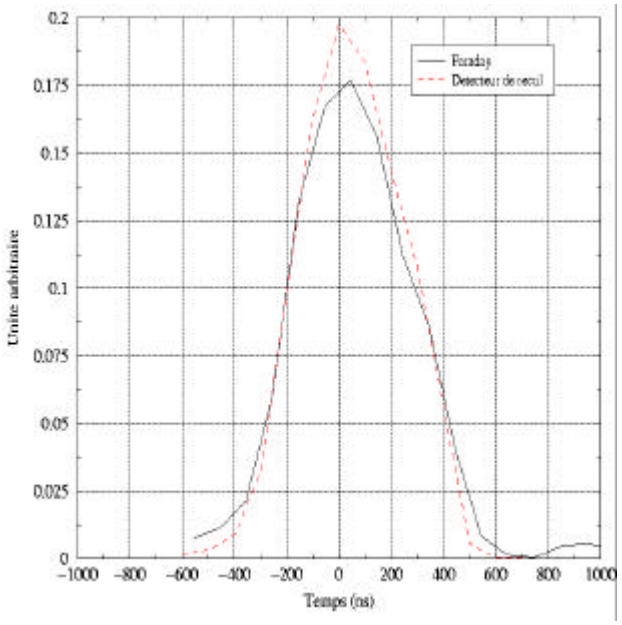

Fig. 5.3: Comparison of current and charged particles (correlated to neutron production) measurements

Fig. 5.4: Time shape of the neutron pulse obtained with a silicon detector. The gaussian fit of the pulse gives a FWHM of 400 ns.

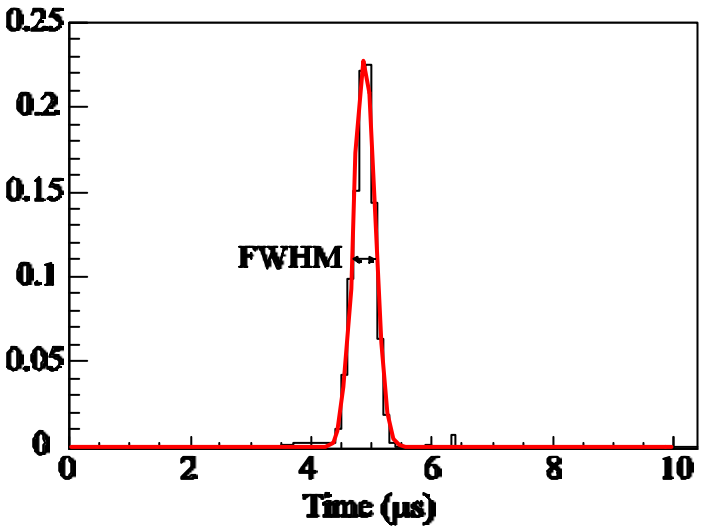

5.3.3 GENEPI Operating feedback

The GENEPI accelerator is an experimental device, which has changed during all the MUSE-4 experiment campaign [3.4].

In spite of the replacing of several components (hot filament, pump, electronic cards…) operating of GENEPI was satisfactory during the covered period: more than 10000 hours of pumping and 130 Coulombs integrated charge on the targets.

During the experimental programme 2 TiD targets and 2 TiT targets, produced by the SODERN company (subsidiary of EADS company), were used. A new target has been mounted each time we changed the nature of the deposit.

The main problems were the adaptation of the GENEPI accelerator to the MASURCA reactor environment:

- Constraining safety rules: adjunction of a fire protection and an earthquake protection.
- Make the GENEPI operation rules compatible to the MASURCA ones (access, remote control command…)
- Behaviour under neutron irradiation of the embedded electronic: change of several modules
- The use of tritium, even if it's confined as a titanium hydride: need of special detectors, gloves box and air flowed suits for target manipulation.
- Training of "local" technical people to run/operate the accelerator

5.3.4 Frequency modulation

The mean deuteron current and neutron production is controlled through the computer control by the pulse frequency from 10 Hz to 4,7 kHz without changing deeply the shape of the pulse.

For the part of the physics programme concerning the study of the delayed neutrons fraction evolution, the modulation of the source between two frequencies (typically from 300 Hz to 4 kHz) was used.

For safety reasons, the rise rate of the frequency has to be limited in order not to exceed the neutron doubling time of neutrons in the reactor (5 seconds) and prevent triggering the fall of the safety rods. So electronics of the pulse frequency control include a slow ramp for normal operation. Moreover measurement of the rise rate (log derivative) of the mean current on the target is used to detect doubling times shorter than usual, to reset the frequency to the lower value and then let it slowly recover. This device is useful after sparking when the beam recovers quickly from zero to the normal value and also if rising fronts of modulation are too fast.

5.3.5 Perspectives and Recommendations

The online monitoring of the neutron production could be upgraded to reach a better coherence between the beam current measurement and the neutron productions in term of signal shape and of absolute level.

This will allow the future experiments to take into account more accurately the neutron production fluctuations during the acquisitions. Indeed, it has to be noted that the target behaviour in term of load (Tritium or Deuterium) evolution during the use is not taken into account for the present experiments. It is the same for the deuterium pollution in the tritium target due to the deuteron implantation.

The preventive service operation frequency should be important to keep the accelerator in operation, in particular on the electronic and pumping devices.

A second GENEPI accelerator has been built in CNRS-INP2P3-LPSC facilities at GRENOBLE with the main improvement concerning the reduction of the pulse width. The pulse duration should be decreased under 500ns by using cable delay lines for the arc discharge and an IGBT crowbar to short circuit it. These improvements could be transferred to MASURCA.

5.4 Review of the measurements performed

Although many different configurations were studied in the framework of the MUSE-4 experiments [4.1], we will retain for reasons of simplicity only the major ones in certain parts of this final report. Besides the reference critical configuration, the four other configurations SC0, SC2, SC3 and SC3 Na/Pb can, in view of the experiments performed further, be categorized with respect to the type of driving source which was used. When the GENEPI accelerator is switched on, either a deuterium or a tritium target was installed. Certain types of measurements were performed with GENEPI turned off resulting in the intrinsic source as the driving source. Some measurements have been also carried out with a ^{252}Cf source emitting, via spontaneous fission, about 2. 10^9 neutrons per second with a spectrum close to fission one.

The different kind of measurements performed in the MUSE programme were either devoted to the characterization of the core or to the determination of the sub-criticality level:

- for the characterization of the core the following parameters were measured: critical mass, control rod reactivity worth (more especially for the pilot rod), reaction rate distributions (traverses), spectral indices by miniature fission chambers or foil activation, neutron spectrum by neutron spectrometry, flux importance traverses and kinetic parameters. All these measurements have been achieved with the four safety rods up. Most of them have been obtained with the pilot rod down and some with the pilot rod either at critical position or in high position.

- for the determination of the sub-criticality level, different kind of measurement techniques were employed: the Source Jerk technique; the Pulsed Neutron Source (PNS) technique based either on the Area approach, the fitting of the á-decay constant or the k_{prompt} method; the Rossi-á technique; the Feynman-á method and the Cross Power Spectral Density (CPSD) technique.

Tab. 5.2 gives an overview of the measurements performed by the different institutes in the different configurations.

Usual characterization measurements with FC (rod-drop experiments, fission rate traverses, spectral indices and source importance distributions) were primarily performed by CEA. Spectral and spatial index measurements using foil activation were managed by PSI with the assistance of CEA. Neutron spectroscopy and source modulation measurements have been achieved by CNRS/LPSC.

A major part of the experiments in the three sub-critical configurations SC2, SC3 and SC3 Na/Pb, on the other hand, aimed at the determination of the sub-criticality level. Several institutes (CEA, CNRS, SCK, CIEMAT, IRI) were involved in this programme . Since different institutes sometimes used the same techniques, the analysis procedure and reproducibility of the measurements can be examined.

For full details about these measures, refer to the experimental reports [4.1] and the list of publications.

Tab. 5.2: Overview of the measurements performed during the programme

		Configuration																
		Reference			SC0				SC2				SC3			SC3+		
	Coolant	Sodium														Sodium + Lead		
	State	Critical	Subcritical															
	External neutron source	-	-	^{252}Cf	-	^{252}Cf	D target	T target	-	^{252}Cf	D target	T target	-	^{252}Cf	T target	-	^{252}Cf	T target
	Power calibration	X																
Characterisation measurements	Rod drop (SR and PR)	X																
	Fission rate relative distributions	X	X				X	X				X			X			X
	Spectral indices (miniatures FC)	X	X					X				X			X			X
	Spectral indices (foil irradiations)	X					X	X				X						
	Neutron spectroscopy							X				X						
	Importance relative distribution (counts on monitors)		X	X	X	X			X	X			X	X				
	Kinetic parameters		X					X				X						
Reactivity measurements	Source jerk technique					X								X			X	
	Source multiplication methods		X		X				X				X			X		
	Pulsed neutron source technique (fixed frequency)						X	X			X	X			X		X	X
	Pulsed neutron source technique (source modulation method)							X				X						X
	Neutronic noise – current mode		X		X													
	Neutronic noise – pulse mode		X		X	X	X	X	X		X	X	X	X	X	X	X	X

5.4.1 Critical mass

First criticality has been obtained on January 9, 2001 with a 1112 fuel cell configuration. Then, critical configurations with 1114, 1115, 1119, 1125 and 1132 fuel cells have been also set-up in order to manage : the loss of reactivity due to the ^{241}Pu decreasing, the reactivity effect of the special tubes used for β_{eff} measurements and the reactivity effect of ISN (newly LPSC) measurement tubes.

5.4.2 Rod-drop experiments

In the MASURCA facility, the sub-critical level of the different configurations have been especially determined by the standard method used in critical reactors. At present time, this reference route is based on the set up of rod drop experiments coupled with the modified source method (more details in section). In this aim, rod drop experiments have been performed with the pilot rod. Considering the low reactivity effect caused by such a rod (negative reactivity effect < 0.5$), spatial effects can be neglected and thus it is not necessary to correct experimental values deduced from the inverse kinetics equations in the point model. These results are presented in Tab. 5.3.

Tab. 5.3: Core reactivity when the pilot rod is down

Date	Configuration	Reactivity (in cents)
15 January 2001	1112 cells	-25.6
29 June 2001	1114 cells	-16.3
06 February 2002	1115 cells	-19.4
9 April 2002	1115 cells	-37.1
19 April 2002	1115 cells	-37.9
11 September 2002	1132 cells	-25.1
26 September 2002	1125 cells	-24.9

5.4.3 Fission rate distributions

Validation of the deviation (from the critical reference) of fission rate distributions constitute an objective of prime importance regarding the definition of recommended calculation tools for the prediction of the neutronic features of future ADS's. Thus, fission rate relative distributions close to the beam guide, inside the lead buffer and in front of the target, have been first measured on the reference critical configuration with all SR up for a large sample of elements. The objective of such a measurement campaign was not only to quantify initial biases not depending of the external source, but also to allow the assessment of minor actinides nuclear data.

Tab. 5.4 gives the list of traverses performed on the reference configuration.

Tab 5.4: Fission rate relative distribution measurements performed on the reference configuration with 1115 fuel cells.

Position of the pilot rod	Critical position	Down
Reactivity (in dollars)	~0	~-0.37
Radial channels	N/S, W/E	N/S, W/E
Axial channels	E19-18, E16-15, W21-17, W20-18	E19-18, E16-15, W21-17, W20-18
Isotopes used	^{232}Th, ^{233}U, ^{235}U, ^{238}U ^{237}Np ^{238}Pu, ^{239}Pu, ^{240}Pu, ^{242}Pu ^{241}Am, ^{243}Am, ^{10}B	^{233}U, ^{235}U, ^{238}U ^{237}Np, ^{239}Pu, ^{10}B

Similar measurements were performed in subcritical configurations. Nevertheless, owing to the difficulties with the carrying out of the experiments and, above all, because of the increasing of the acquisition time duration due to the low counting rates when the core configurations are deeply subcritical, a limited number of measurements could be completed. The full list of fission rate traverses that we were able to perform on subcritical configurations is presented in Tab 5.5.

Tab. 5.5: List of fission rate traverses performed on subcritical configurations

Configuration	SC0					SC2			SC3			SC3 Na/Pb		
Reactivity (in dollars)	~ -1.9					~ -9.1			~ -13.6			~-11.1		
Position of the safety rods	Up					Up			Up			Up		
Position of the pilot rod	Down					Down			Down		Up	Down		
Target (D/T)	D		T			T			T			T		
GENEPI frequency	4.5 kHz		OFF	2 kHz	4 kHz	4 kHz	4 kHz	4 kHz	OFF	2 kHz	2 kHz	2 kHz	4 kHz	2 kHz
Channels	N/S	E/W	N/S	N/S	E/W	N/S	E/W	E19-18	N/S	N/S	E/W	N/S	E/W	E/W
Isotopes	^{235}U	^{235}U	^{235}U	^{235}U	^{238}U	^{235}U	^{235}U	^{235}U	^{235}U	^{235}U	^{235}U	^{235}U	^{235}U	^{235}U

Although we have few measurements in subcritical configurations, some effects caused by the source could be clearly highlighted. Fig. 5.5 and 5.6 shed on light the (D,T) source dominated mode when the core is deeply subcritical. Fig. 5 7 and 5.8 show on one hand the spectral effect caused by the 14 Mev neutrons provided by GENEPI with the tritium target and, on the other hand, the asymmetry produced by the presence of the beam guide.

Fig. 5.5: ^{235}U fission rate distribution in the N/S radial experimental channel

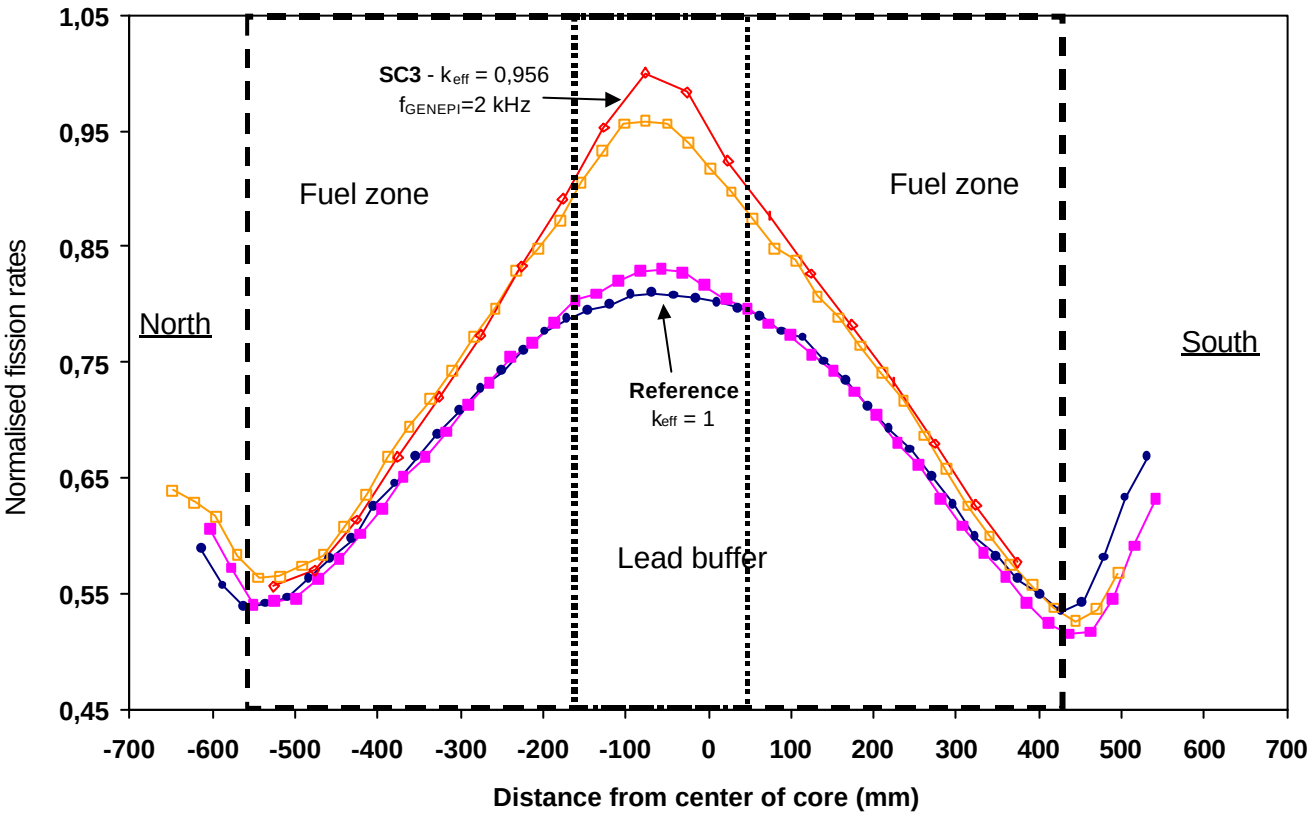

Fig. 5.6: ^{235}U fission rate distribution in the E19-18 axial experimental channel

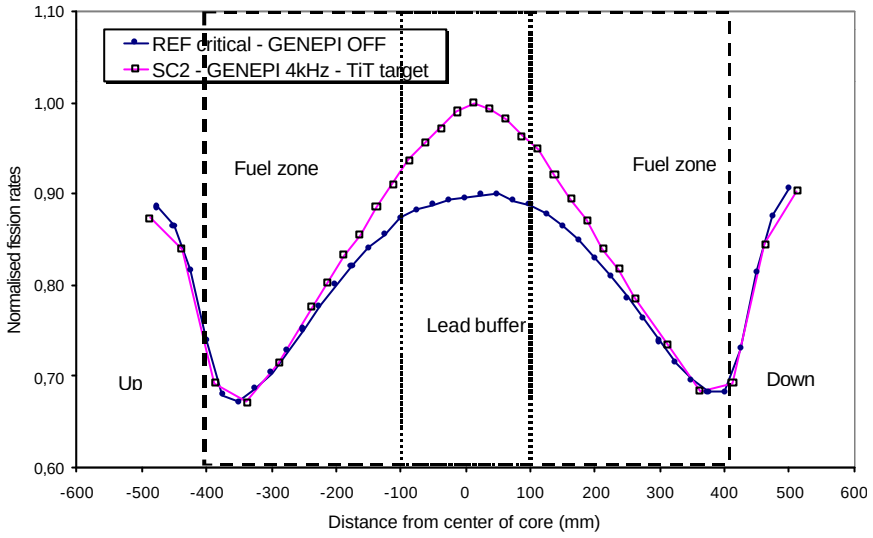

Fig. 5.7: ^{238}U fission rate distribution in the West/East experimental channel

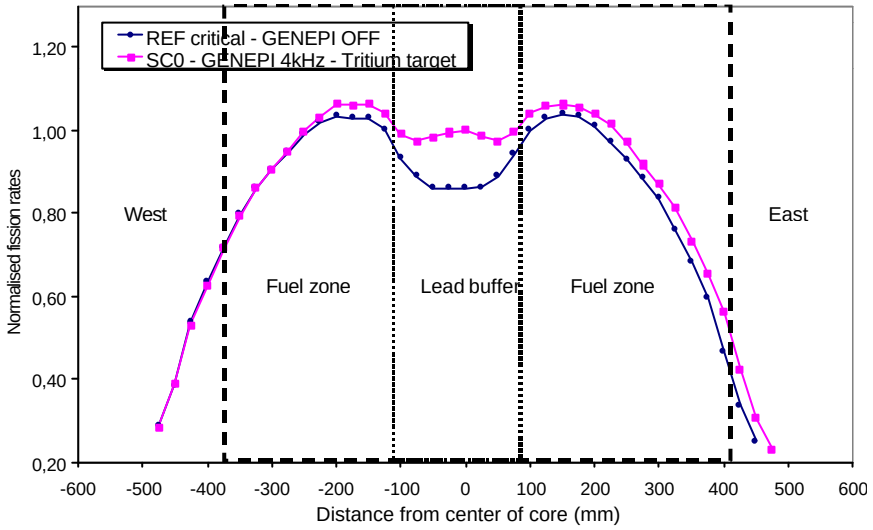

Fig. 5.8: ^{238}U fission rate distributions in the North/South experimental channel

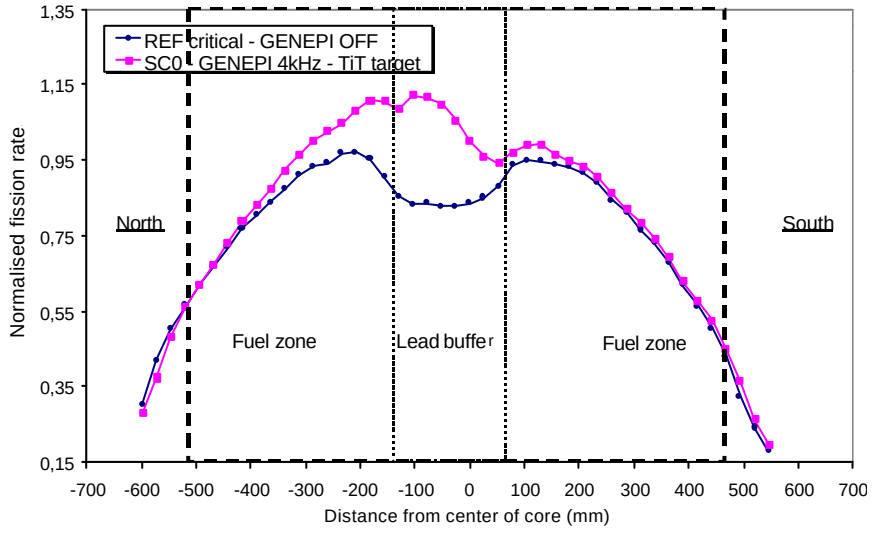

5.4.4 Spectral indices by miniatures fission chambers (FC)

Spectral indices by miniatures fission chambers have been performed for the main five configurations previously described.

When critical (either with the PR down or at critical position), the experimental channels and the isotopes were similar to those used for fission rate traverses. Measurements have been also conducted for ^{244}Cm in the N/W and E/W channels. Most of the time, three measurement points by experimental channel were acquired.

For SC0, SC2, SC3 and SC3 Na/Pb configurations, a reduced number of measurements have been achieved. Less isotopes were used (^{235}U, ^{238}U, ^{237}Np, ^{239}Pu, ^{240}Pu,^{10}B) and only two experimental points have been realized when it was possible (due to time constraints). Moreover, only measurements with GENEPI ON with the tritium target have been realized.

5.4.5 Spectral indices by foil activation

To permit a deeper study of the spectral variations due either to the new heterogeneities of such system (as the central lead zone or the accelerator tube) or to the external source, activation measurements were performed. The choice of foils has been guided mainly by the need to cover as wide a range of threshold energy values as possible. The full list of activation reactions employed is given in Tab. 5.6.

Tab. 5.6: List of special foils and reactions employed for spectral studies

Reaction	Threshold [MeV]	Reaction	Threshold [MeV]
$In^{115}(n,\gamma)$	-	$Ni^{58}(n,p)$	2.8
$Co^{59}(n,\gamma)$	-	$Zn^{64}(n,p)$	2.8
$Th^{232}(n,\gamma)$	-	$Fe^{54}(n,p)$	3.1
$Zn^{64}(n,\gamma)$	-	$Fe^{56}(n,p)$	6.0
$Au^{197}(n,\gamma)$	-	$Mg^{24}(n,p)$	6.8
$U^{235}(n,fis)$	-	$Pb^{204}(n,2n)$	~7
$Np^{237}(n,\gamma)$	-	$Th^{232}(n,2n)$	~7
$Np^{237}(n,fis)$	0.7	$Al^{27}(n,a)$	7.2
$Th^{232}(n,fis)$	~1	$Nb^{93}(n,2n)$	11.0
$In^{115}(n,n')$	1.2	$V^{51}(n,á)$	11.5
$Th^{232}(n,fis)$	1.3	$Ni^{58}(n,2n)$	13.5
$Co^{59}(n,p)$	2.0		

The list of measurements which have been performed is presented in Tab. 5.7. In definitive, more than 300 samples were activated.

Tab. 5.7: List of foil activation experiments

Irradiation	Date	Configuration	Foils irradiated
1	17 September 2001	Reference 1114 cells	In, Fe and U
2	9 October 2001	Reference 1114 cells	Ni, Nb, Co, Fe, Zn Va, Pb
3	14 March 2002	Reference 1115 cells	Ni, Al, Mg, Th
4	19 March 2002	Reference 1115 cells	In, Zn, Fe, Au, Np
5	25 June 2002	Reference 1115 cells	Mg, Au, Co, U
6	24 October 2002	SC0 1108 cells + D target	In, Np
7	13 November 2002	SC0 1108 cells + D target	In, Au
8	5 February 2003	SC0 1108 cells + T target	Ni, Mg, Nb, Pb
9	19 February 2003	SC0 1108 cells + T target	Va, In, Ni, U
10	04 March 2003	SC0 1108 cells + T target	Ni, In, Au, Al, Th
11	11 March 2003	SC0 1108 cells + T target	In, Ni, Co, Fe, Va, Zn, Np
12	9 April 2003	SC2 1006 cells + T target	In, Mg, Ni
13	15 April 2003	SC2 1006 cells + T target	Ni, In, Va, Al, Fe, Au

5.4.6 Neutron spectroscopy

Neutron spectroscopy measurements were performed in SC0 and SC2 configurations using ^{3}He proportional gas counters. These counters were inserted in the centre of the core region into special fuel tubes shielded from gamma rays by a 2 cm thick lead blanket. From the specific response of these detectors to mono-energetic neutrons obtained on Van de Graaff accelerator, it is possible to establish the response matrix of the detector and then, from the measured spectrum, by the mean of an iterative subtraction method (starting at 2.2 MeV), to extract the neutron energy spectrum from 100 keV up to 1.5 MeV. Compared to the expected flux obtained by MCNP simulations this method show good agreement in the considered energy range (SC2, in Fig. 5.9).

Fig. 5.9: Measured neutron flux compared to the flux simulated with MCNP.

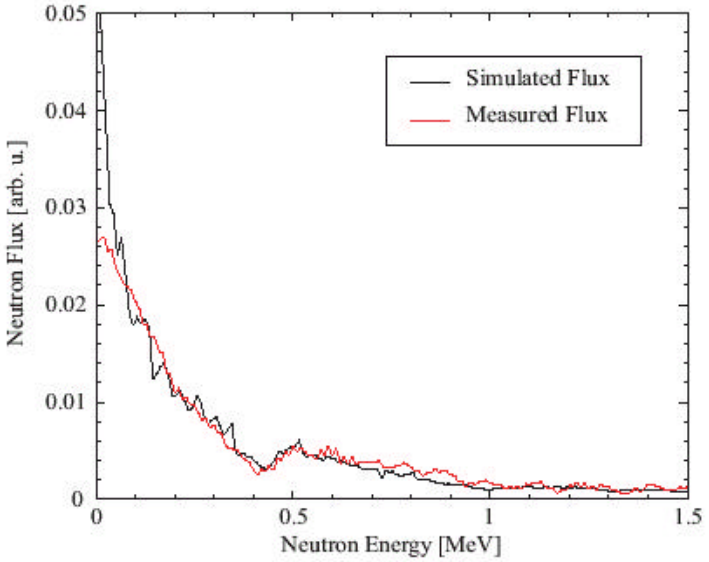

5.4.7 Source importance distributions

To estimate a traverse of source importance experimentally, a ^{252}Cf source is moved in an experimental channel and the counting rates of monitors are recorded for each position of the source. The relative adjoint flux traverse in then given by:

$$\frac{f_i^*}{f_0^*} = \frac{C_i - C_r}{C_0 - C_r} ,$$

where ϕ is the adjoint flux, C the average monitors counting rate, r denotes the measurement without the source, 0 describes the measurements with the source in the core centre and i the measurement with the source in position i.

During the programme , importance traverses have been worked out in the two radial experimental channels and in four axial experimental channels E19-18 (inside the lead buffer and in front of the GENEPI target), W20-18 (in a transition area between fuel and lead), E16-15 and W22-17 (not perturbed area). The ^{252}Cf sources were moved, using a specific device , with a precision better than 10 mm. These experiments are listed in Tab. 5.8. Fig. 5.9 shows a example of results that was obtained.

Tab. 5.8: List of importance traverse measurements

	Reference configuration with 1114 fuel cells		SCO 1108 cells	SC2 1006 cells	SC3 972 cells
Safety Rods	Up	Up	Up	Up	Up
Pilot rod	Down	600 mm	Down	Down	Down
Approximate reactivity (in dollars)	-0.24	-0.11	-1.9	-8.7	-13.6
^{252}Cf source (n/s)	$3.7\ 10^7$		$2.\ 10^9$ n/s		
Radial channels	N/S W/E		W/E	N/S W/E	W/E
Axial channels	E19-18 E16-15 W21-17 W20-18	E19-18 E16-15 W21-17 W20-18	-	-	-

Fig. 5.9: Adjoint flux traverse - E/W channel - SC2 configuration

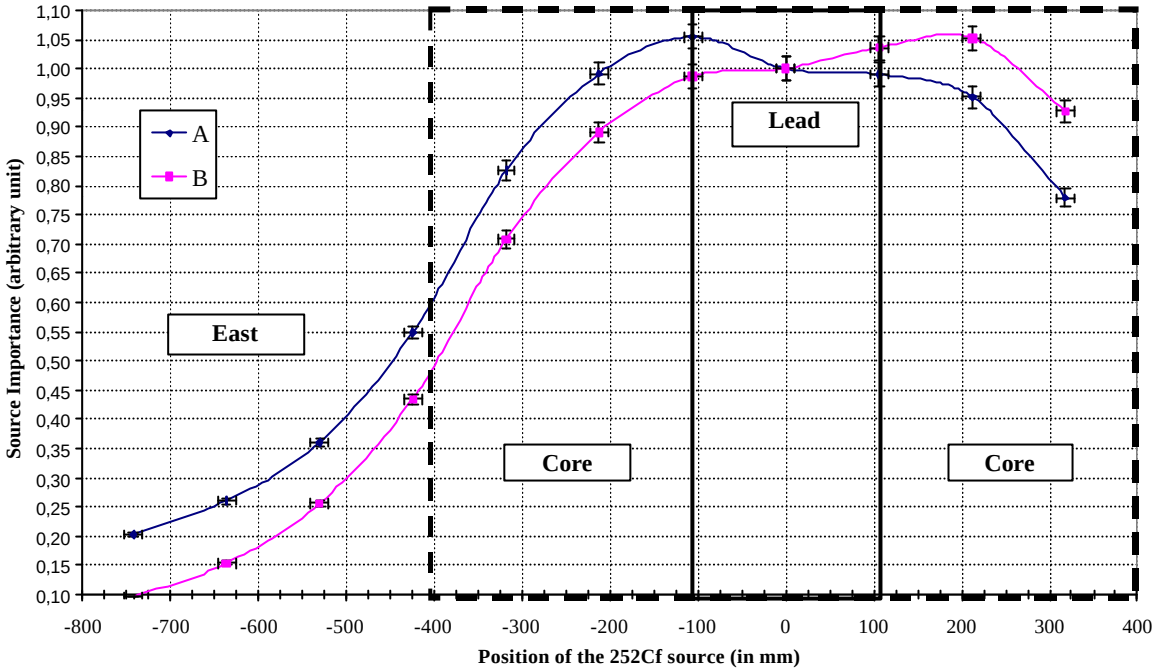

5.4.8 Kinetic parameters

Two assessments of the effective delayed neutron fraction have been performed close to criticality using both the CPSD and the Rossi-α methods. The results obtained are presented below (Tab. 5.9).

Tab. 5.9: β_{eff} measured values close to criticality

	Reference configuration	
Fuel cells	1132	1115
Reactivity in cents ($\rho_\$$)	$-24.6<\rho_\$<0$	-36.5
Method	CPSD (current mode)	Rossi α (pulse mode)
β_{eff} (pcm)	334 ± 6 (1σ)	317 ± 13 (1σ)
Λ (μs)	0.59 ± 0.01	0.55 ± 0.02

When subcritical, β_{eff} has been assessed using a combination of the k_{prompt} method and the source variation method. Results are presented below (Tab. 5.10).

Tab. 5.10: β_{eff} measured values in subcritical configurations

Configuration	SC0	SC2
k_{eff} (k_p method)	0.9925 ± 0.001	0.9706 ± 0.001
β_{eff} (pcm)	342 ± 32	313 ± 34

5.4.9 Source jerk techniques

These experimental techniques and the analysis methods associated are detailed in section 7.6. Here, we only present some raw experimental data obtained during the programme .

- **The Standard Source Jerk technique**

The standard Source Jerk technique is based on the fast removal of the source out of an initial stationary subcritical medium. In the MUSE experiments, we performed such measurements on SC0, SC3 and SC3 Na/Pb with a ^{252}Cf source located at the center of one of the W/E experimental channel. From these experiments one can deduce the reactivity expressed in dollars. Fig. 5.10 show a sample of experimental data obtained.

Fig. 5.10: Source jerk experiments with a ^{252}Cf continuous source for two subcritical levels

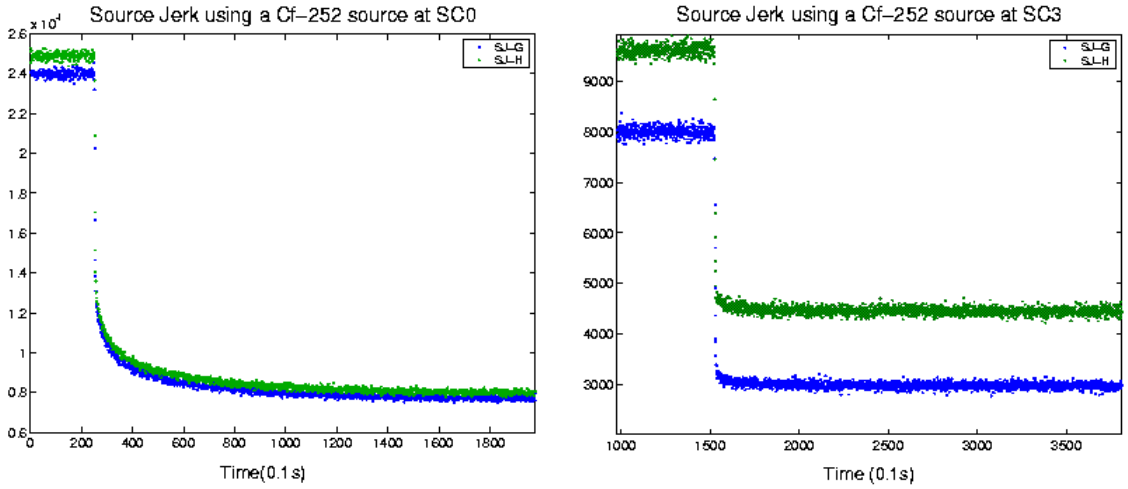

- **Source modulation method**

The Source Modulation technique is quite similar to the Source Jerk Method. For a given sub-critical level, the external neutron source rate is suddenly changed from a high count-rate level P_0 to a low count-rate level P_1.

During the MUSE-4 programme , this technique has been set-up by varying suddenly the frequency of the GENEPI pulsed source resulting in a decrease of the average count-rate. Given the return phase to the high frequency must be adapted to the reactor doubling time (5 s), on pain to cause a safety rod drop, the source is not switched-off but varies from a high value F0 (4 kHz) to a low value F1 (300 Hz) in order to decrease the time needed to reach F0 from the low frequency F1 (Fig. 5.11).

Fig. 5.11: Source frequency variation cycle and experimental neutrons counting rate for three cycles

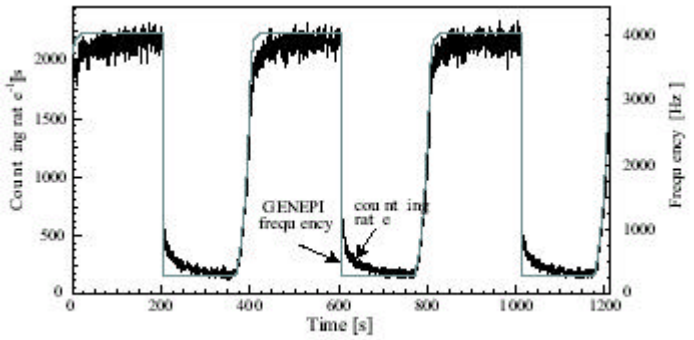

Such measurements have been performed on SC0, SC2 and SC3 Na/Pb configurations (Fig. 5.12). From this measure, one can infer the reactivity expressed in dollars. Combined with the k-prompt method (analysis strategy proposed by CNRS), β_{eff} can be deduced (section 5.7.8).

Fig. 5.12: Experimental counting rates measured with detector 4 for the SC0 and SC2 configurations

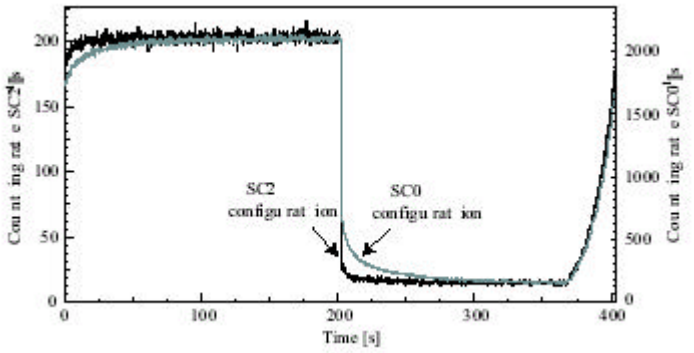

5.4.10 Pulsed neutron source experiments

The most direct method to study the response of the system to source intensity variations, is to inject a short neutron pulse and record the counting rate following the pulse of detectors distributed on different reactor positions. Depending on the method used, one can deduce an experimental value of respectively, the prompt multiplication factor $k_p=(1- \hat{a}_{eff})k_{eff}$, the prompt neutron decay constant $\alpha_p=(\hat{a}_{eff}- \tilde{n})/ \Lambda$, or the reactivity expressed in dollars $\tilde{n}_{\$}= \tilde{n}/ \hat{a}_{eff}$.

Taking advantage of the GENEPI device, this technique has been applied on all sub-critical configurations using both deuterium (SC0, SC2) and tritium target (SC0, SC2, SC3, SC3 Na/Pb) with frequencies of 0.5 to 4 kHz. Most of the measurements have been performed with all the SR up and the pilot rod down. Data have been also obtained with the pilot rod up in order to investigate the possibility of measuring small reactivity changes. Very deep subcritical configurations, achieved pulling down one SR or the 4 SR, were also studied. As a consequence, a huge amount of data have been acquired.

Looking at the reduced histograms (Fig. 5.13 and 5.14), we already could make several observations :

1- The shape of the histogram changes for different detector positions and reactivities,
2- In both cases, the shape of the histograms in the reflector and the shielding shows a much smoother increase in the counting rate and a rounded maximum, ≈10-20 µs after the GENEPI pulse. On the other hand, the signals from detectors in a given region (detectors in symmetrical positions) show very similar shape.
3- The change on the exponential decay rate is very sensitive to the reactivity.
4- For configurations close to criticality (SC0), similar decay slopes are observed for all the detectors (core, reflector, shielding) in the range 75-250 µs. The point kinetic model is valid in this case.
5- For deep subcritical configurations, reflector and shielding detectors on one hand, and core detectors on the other hand, have very different behaviours. The point kinetic model is no more valid and alternative analysis models have to be used (see section 7 for more details).
6- For deep subcritical configurations, all histograms, more especially for reflector/shielding detectors, exhibit a slope change after a few tenths of µs. This

behaviour is increased for very strongly subcritical configurations (configuration with the 4 safety rods inserted, for instance, has a k-effective lower close to 0.85). This effect occurs when two conditions are fulfilled : a) the neutron population can be divided in two groups of very different lifetime, b) the neutron population of the shortest lifetime group is larger than the other group. Then, after a certain time, the amplitude of both groups invert and produce the change in the slope of the time evolution. In addition, this effect can be amplified by the use of ^{235}U detectors. The large resonance of ^{235}U at 1 eV increases the measured amplitude of thermal neutrons respect to the fast and epithermal neutron population.

Fig. 5.13: Responses for detectors located in the core, the reflector and the shielding, for four reactivity levels

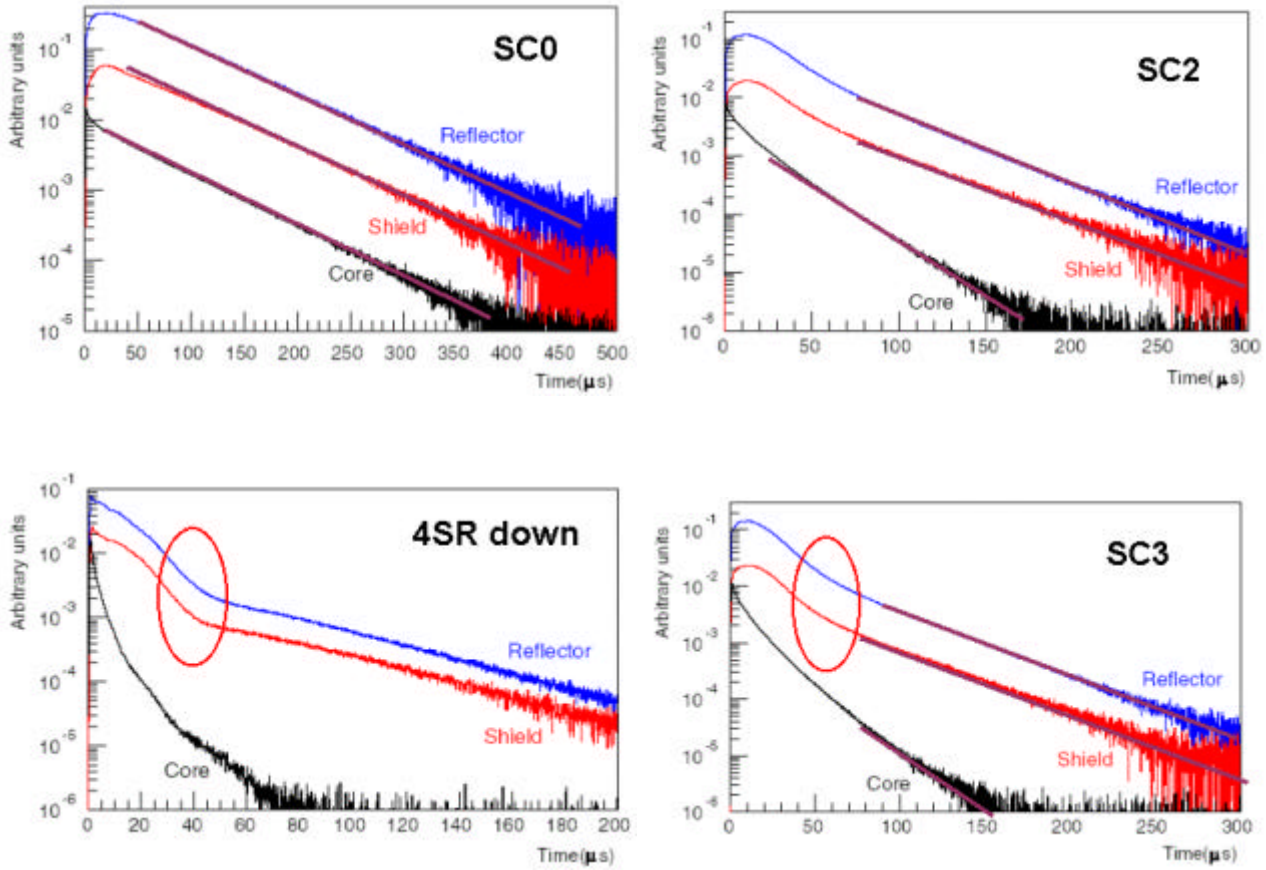

These measures also demonstrated that small changes of reactivity could be detected. Fig. 5.14 shows the time dependence of the counting rate measured for the three core configurations SC0, SC2, SC3 with the pilot rod inserted into or removed from the core, giving access to six different levels of reactivity. Since the PR reactivity worth is less than half a dollar (i.e. less than 160 pcm), we can see that the decrease of the counting rate clearly exhibits a sensitivity to such low reactivity effect.

Fig. 5.14: Shapes of the reduced time histograms for a detector in core for six different levels of reactivity

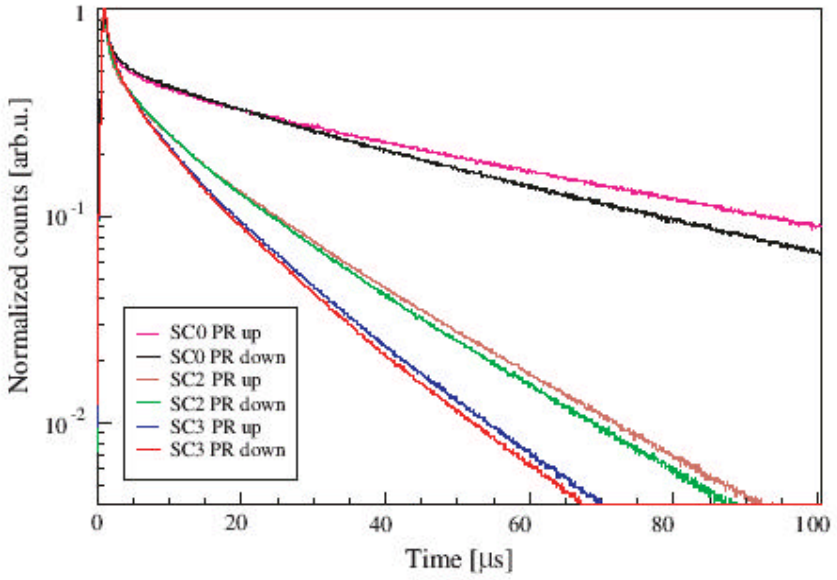

5.4.11 Noise measurements

Noise measurements have been performed with the intrinsic source of MASURCA core (≈1.4 10^8 n/s), the ^{252}Cf source used for source jerk measurements (≈2. 10^9 n/s), the pulsed source supplied by GENEPI with the deuterium target (≈1.2 10^8 n/s at 4 kHz) and the pulsed source obtained with GENEPI equipped with the tritium target (≈1.3 10^{10} n/s at 4 kHz with a fresh fuel). All configurations (critical with the PR or one SR inserted, SC0, SC2, SC3 and SC3 Na/Pb) were studied. Last, several analysis methods (Rossi-α, Feynman-α, APSD and CPSD) were applied.

Given the amount of experimental data acquired, this report cannot even summarizes the main results from the application of noise methods in the MUSE-4 configurations. In this report, only conclusions with respect to the applicability of individual noise techniques for the measurement of the reactivity in ADS are presented (section 7). For more details about these measures, refer to the list of publications.

5.5 Analysis and interpretation of the experimental data

5.5.1 Review of the calculation schemes used for the experiments analysis

The MASURCA mock-up is a zero-power nuclear reactor, which implies that thermal-hydraulic feedback do not play a role. Therefore, this section concentrates on the *neutronics* calculational methods which have been used by the different partners within the MUSE project to support the analyses of various experiments. The main aspects to be covered by the neutronics analyses are :

1. static analyses for critical configurations
2. static analyses for subcritical configurations
3. dynamic analyses for subcritical configurations

The first two types of analyses are "fundamental mode analyses"; they were used to obtain global information about the core configurations and time-integrated detector responses. The effect of the external neutron source is not taken into account. The main parameters to be calculated are the values of k_{eff}, $\hat{a}_{eff}$, Λ and reaction rate traverses.

Dynamic analyses explicitly take into account the time-dependent behavior of the external neutron source. The main results from these analyses are time-dependent responses for detectors located in various positions in the core, in the reflector and in the shield.

The basic ingredients for neutronics analyses are the description of the geometry of the problem and the cross sections describing the interactions of the neutrons.

Two types of approaches can be used for neutronics analyses :

1. microscopic methods.

These methods use a detailed description of the 3-dimensional geometry of the problem and a detailed *(i.e.* continuous-energy) description of cross-section data. Monte Carlo methods are the best-known in this category, although also finite-element methods exist.

2. deterministic methods.

These methods use effective data for the description of neutron interaction cross sections. This implies that information on the geometry of the problem is included in these (self-shielded) cross-section data. Therefore, an approximate description of the 3D geometry is used.

In the analyses of MUSE experiments both Monte Carlo and deterministic methods were used.

- **Nuclear data**

As mentioned above, nuclear data form a basic ingredient for all neutronics analyses. Several basic nuclear data evaluations exist; the most important ones are the European JEF-2.2 evaluation [5.2], the American ENDF/B-VI.5 evaluation [5.3] and the Japanese JENDL-3.2 evaluation [5.4].

It should be noted, that during the MUSE project for each of these evaluations new versions were issued (JEFF-3.0, ENDF/B-VI.8 and JENDL-3.3). However, most partners within the MUSE project kept using the older evaluations in order not to confuse the comparison of calculational results.

- **Validation**

In order to be able to rely on the results of neutronics analyses carried out for the MUSE configurations a validation of the calculational approach (the combination of codes and data) is required. In the MUSE core a relatively large amount of ^{239}Pu is present, while a fast neutron spectrum is created in the core. A dedicated validation of the calculation tools for such a configuration was felt to be necessary. Therefore, a simplified calculational benchmark was defined, which still contains the main features of the MUSE core. Initially, large discrepancies were observed between the results from different participants. However, finally it appeared that an update was needed in the nuclear data for ^{239}Pu. After correction of these data consistent results were obtained by the participants to this benchmark [4.5].

As a sequel a realistic calculational benchmark was defined [4.6]. This benchmark contains 3 descriptions of MUSE cores: one is a specification of a core which has already been built (COSMO) and the remaining two definitions represent MUSE critical and subcritical configurations, although the "as built" specifications slightly differ from the benchmark

description. An overview of the main conclusions of this benchmark is reported in next section.

- **Calculation schemes used by BNFL**

BNFL supported the MUSE-4 experimental programme using the reference French calculation system ERANOS [5.5] (European Reactor Analysis Optimised System).

Nuclear data based on the JEF-2.2 evaluation were used throughout the work.

Both 3D (TGV) and 2D (BISTRO) 33 energy group neutronic models of the MUSE-4 cores were constructed and the resultant flux solutions and group constants were then processed using functions embedded within the overall ERANOS calculational scheme.

- **Calculation schemes used by the CEA**

The CEA Cadarache contributed to the analyses with deterministic calculations carried out with ERANOS. Monte Carlo analyses with MCNP [5.6] were used for the interpretation of $\hat{a}_{eff}$ measurements and to obtain cross checks for the deterministic analyses.

In the deterministic analyses performed by CEA cross-section data are used, which are based on the JEF-2.2 evaluation. Probability tables are included for the 37 main isotopes in the unresolved resonances energy range.

For the Monte Carlo analyses data based on the JEF-2.2 evaluation and on ENDF/B-VI.5 were used.

The 1968 energy group library resulting from the pre-processing was subsequently used in the cell code ECCO. This code provides multigroup, self-shielded, P1 anisotropy order cross sections. A fine-group, heterogeneous Pij calculation is performed, which yields spatially homogenized data condensed to 62 energy groups.

The code TGV/VARIANT solves the XYZ transport equation with the variational nodal method in the SP3 (simplified spherical harmonics) approximation. The exact core geometry is treated and 62 energy groups are used.

- **Calculation schemes used by CIEMAT**

CIEMAT contributed to the interpretation of the results with Monte Carlo analyses carried out with MCNP.

Throughout the CIEMAT analyses nuclear data based on the ENDF/B-VI.5 evaluation were used.

- **Calculation schemes used by CNRS**

CNRS contributed to the analyses with Monte Carlo simulations carried out with MCNP. Throughout the analyses, nuclear data based on the ENDF/B-VI.5 evaluation were used.

- **Calculation schemes used by ENEA**

The ENEA participated both to the MUSE benchmark and to MUSE-4 interpretation of the kinetics experiments by means of the ERANOS deterministic codes system.

Cross-sections processing at different energy groups (33, 50 and 175) was carried out by means of ECCO cell code starting from the 1968 fine energy groups JEF-2.2 reference nuclear data library.

In order to take into account the core-reflector interface effects, the macrocell option was used [5.7].

k_{eff}, spectral indices and several reaction rate traverses were calculated by using the BISTRO and TGV/VARIANT modules in order to solve respectively 2D and 3D transport problems.

With the aim to analyze the MUSE-4 kinetics experiments, two calculation procedures were developed and validated using ERANOS code by means of a static approach in order to evaluate the prompt-á value of the system and to simulate the PNS area method for different MASURCA subcritical configurations with DT external source (SC0, SC2 and SC3) [4.4, 5.8].

- **Calculation schemes used by FZJ**

FZJ contributed to the MUSE project with Monte Carlo analyses. The neutron cross section data used in the FZJ analyses were mainly taken from the MCNP library ENDF60 which is based on the nuclear data file ENDF/B-VI Release 2. Furthermore, the more recent libraries ENDF66 (ENDF/B-VI Release 6) and ACTI (ENDF/B-VI Release 8) were used. For test purposes, calculations were made in which the ENDF/B-VI based probability tables of Pu-239 were replaced by those obtained with JEFF-3.0.

The Monte Carlo analyses for the OECD/NEA benchmark problems were carried out with the Monte Carlo code MCNP. A private TALLYX subroutine was used within MCNP in order to calculate the reaction rate traverses, spectral indices and neutron spectra in specified positions of the MUSE core on the basis of surface tallies.

The Monte Carlo calculations to the analysis of the MUSE-4 experiments were performed by the MCNPX code [5.9]. The reaction rate traverses in different experimental channels and the spectral indices at specified positions were determined by the use mesh tallies.

- **Calculation schemes used by FZK**

The neutronics analyses performed by FZK were carried out with the KAPROS/KARBUS deterministic code system [5.10].

The libraries for KAPROS/KARBUS are based on the JEF-2.2 evaluation.

- **Calculation schemes used by KTH**

KTH made calculations with MCNP and MCNPX of the relative source efficiency ö*. A procedure was developed [5.11] to calculate this quantity with standard outputs of MCNP.

- **Calculation schemes used by NRG Petten**

NRG Petten contributed to the MUSE project with detailed Monte Carlo analyses with a modified version of MCNP and participated in the benchmarks carried out in the framework of the project.

The default cross-section library used in the NRG Monte Carlo analyses is based on the JEF-2.2 evaluation. In order to determine the sensitivity to the nuclear data used in the

analyses, NRG also carried out a series of calculations in which data from different evaluations were used. Among others, data were used which were produced within the HINDAS 5th Framework project by Koning et al. [5.12]. Very recent uranium evaluations proposed for inclusion in the ENDF/B-VII evaluation were also used.

A new method was developed by NRG with which the value of the effective delayed neutron fraction, $\hat{a}_{eff}$, can be calculated in an MCNP analysis without any approximations [5.13].

- **Calculation schemes used by SCK**

SCKCEN contributed to the MUSE project with static calculations for the MUSE benchmark. The analyses were carried out with MCNP.

The cross-section data used in the MCNP analyses were based on the ENDF/B-VI.5 and JEF-2.2 evaluations.

- **Calculation schemes used by TUD/IRI**

IRI contributed to the MUSE project by time-dependent Monte Carlo simulations of detector responses carried out with the code MCNP-DSP [5.14].

Cross-section data in the IRI analyses were based on the ENDF/B-VI.5 evaluation.

5.5.2 Feedback from the MUSE-4 benchmark

In 2001, the reactor physics and safety subgroup of the NEA/OECD WPPT (Working Party on Scientific Issues in Partitioning and Transmutation), jointly with the MUSE-4 project, decided to propose a computational benchmark based on the MUSE-4 experiments [4.6]. The intention was to create a benchmark, which in addition to the comparison between codes and calculation schemes, would take advantage of some experimental results available. The objective was to provide the guidance on the evaluation of systematic uncertainties and indications of future development required both, in the simulation codes and the associated nuclear data bases.

Since large experience is available on the simulation of fast critical reactors, the benchmark proposed to divide the exercise in three phases.

In the first phase, a typical liquid metal cooled fast critical reactor, the COSMO reference critical configuration studied at MASURCA in 1998/1999, was proposed for the simulation. Geometrical fluence distributions, spectral indices and global parameters as the k_{eff} and kinetic parameter values were studied and compared with the available experimental results.

In the second phase, the MUSE-4 reference critical configuration with 1112 fuel cells was simulated requesting the same kind of evaluations as in the COSMO case.

Finally, the third phase proposed the study of the former SC2 configuration (with an expecting number of fuel cells equal to 976) resulting in a subcritical system with k_{eff} close to 0.97, and with an external neutron source based on the D-T reaction with the tritium target placed in the MASURCA core centre. The simulation of this configuration included the calculation of the same parameters of the critical configurations with additional attention on two specific aspects of the subcritical systems: the propagation and multiplication of the source inside the multiplication assembly, and the kinetic behaviour of the coupled system.

In the two later phases, the simulations have been made blindly before the experimental results were available.

The large participation in this benchmark has allowed the comparison of many combinations of simulation methods, including deterministic and Monte Carlo methods, and nuclear data bases. For the comparison of calculations versus experimental data, several differences between the configurations simulated in the benchmark. and those really studied during the MUSE-4 experiments, eventually needed to apply corrections. This made also more complex the analysis and limited the conclusions drawn from this exercise.

- **k_{eff} and global parameters**

The inter-comparison among the different codes for the effective delayed neutron fraction and mean neutron generation time, shows that there are difficulties with the definition and understanding of the requested parameters. In addition, it has been found that very different methods have been used to evaluate the requested parameters, leading to very different calculation uncertainties. Both effects have introduced severe difficulties on the comparisons and identification of code and nuclear data libraries effects on these global parameters. Nevertheless, the average value of the delayed neutron fraction in MUSE reference configuration is very close to the experimental value. On the other hand, the interpretation of calculation results for the mean neutron generation time with Monte Carlo codes has proven to be difficult and no satisfactory result was obtained.

For the neutron multiplication or criticality constant, large differences are found between different solutions, reaching 2% in the k_{eff} value. After a careful selection of nuclear data and simulation methods, a reduced dispersion of 600 pcm is found on the absolute evaluation of k_{eff} using ENDFB6 versus JEF2.2 libraries. However, the results of probabilistic and deterministic codes using the same data library are in agreement. Finally, irrespective of the nuclear data library used, the computed change of reactivity between two configurations (100 pcm on 3200 pcm) is nearly the same. Comparing with the experiment, we observe that JEF2.2 based libraries provide better estimations of the reactivity. On the other hand, experimental results for the subcritical configuration are characterised by a large uncertainty compared with the dispersion of the simulation codes. Hence, no definitive conclusions can be extracted in this case except that the reactivity variation between the two configurations is consistently predicted by the codes.

The computed total power of the source subcritical simulation shows a large spread that can be explained by the dispersion in computed k_{eff} values and small differences in neutron source efficiency calculations (4%).

- **Reaction rates spatial distributions**

In general, the reaction rates spatial distributions are rather well reproduced by the simulations, with dispersions typically lower than 5% in the fuel core region, away from the interfaces. The precision of the simulation get worse (typically within ±10%) in two cases, when describing the detector response in the reflector or shielding and when describing the regions very close to the neutron source. The first point seems to be related to the difficulty of describing correctly the neutron spectra in the reflector, and the second might be related to the high neutron energy (14MeV) of the D-T source and its transport.

Comparing with the experimental values, one observes, in general, good predictions by the simulation codes typically within the experimental uncertainties.

- **Spectral indices and fluence spectra**

Small but relevant discrepancies between simulations performed with different nuclear data bases in the critical configurations are observed, indicating significant differences on the cross sections between ENDFB6, JEF2 and JENDL3 libraries.

For ^{239}Pu, ^{241}Pu, ^{235}U, all simulations provide results in good agreement (< 5%) with the experiments when available, except in the case of the ^{239}Pu in the subcritical configuration in the E-W channel, where all simulations overestimate the spectral index a 15%.

For ^{240}Pu, ^{242}Pu, ^{241}Am and ^{243}Am the simulations based on JEFF2.2 provide good results (<5%) but the simulations based on ENDFB6 overestimate the reaction rate between 5% and 10%. No clear status for JENDL3, since the 2 available solutions show different behavior.

For ^{238}U: the simulations based on ENDFB6 provide good results (<5%) but the simulations based on JEFF2.2 underestimate the reaction rate up to 5%. No clear status for JENDL3, since the 2 simulations show different behavior. In subcritical, large discrepancies (exceeding 40% in some cases) are observed. This is be produced by a different description of the neutron source among the simulations as observed in the neutron spectrum.

For ^{238}Pu, all simulations overestimate the experimental data between 5% and 10%.

For the capture in ^{55}Mn and ^{115}In the difference ranges between 30 and 40%.

For the subcritical MUSE-4 configuration, there are two kinds of solutions: source driven and eigenvalue calculations. Close to the source, the two types of calculations present large discrepancies that can be attributed to a different evaluation of the fast and high energy fraction in the neutron fluence. The effect is most pronounced near the source, inside the lead buffer. In addition, the solutions with source and with the same basic library, show significant discrepancies that are consistent, comparing different isotopes and different positions, and can not be justified by statistical or computation uncertainties. Pending further analyses, these differences are attributed to differences in the transport (including multiplication) of the high energy (14 MeV) neutrons from the source. re experimental results. All these effects have essentially disappeared at 34 cm from the source where results very similar to the critical case are recovered.

The large fluctuations in the subcritical simulations do not allow us to confirm the smaller differences induced by the choice of nuclear data library, but the large effects for the ^{55}Mn and ^{115}In spectral indexes are still observable.

Experimental results cannot allow us to extract further conclusions due to the experimental uncertainties and the large dependence of the spectral indices with the distance to the source at positions very close to the source (centre of the E-W and N-S channels).

- **Time evolution of the neutron flux after a short neutron pulse**

A clear correlation is observed between the k_{eff} value and the logarithmic slope of the counting rate decay of the ^{235}U fission detectors located in the fuel core at medium times, 50-120 μs, after the source pulse. Similar decay rate is observed in the reflector and shield in this time interval, although the large uncertainties do not allow to reach clear conclusions. At shorter times the time evolution is very different at different locations.

This correlation between k_{eff} and the logarithmic slope could be used to evaluate the reactivity of the system. No difference is observed between the MCNP and ERANOS time evolutions until 150 μs, however a slightly higher equivalent Λ value is predicted by LOOP.

Due to the dependence of the logarithmic slope with the reactivity, no direct comparison can be performed with the experimental data. However, from simulations performed in configurations similar to the experiments, it has been observed that, a) the core region is well reproduced for equivalent reactivity, and b) none of the simulations can reproduce the behaviour at long times in the reflector and shield regions, resulting in an underestimation of the fission rate. A possible explanation, related with the capture cross section of ^{56}Fe at energies below 1 eV, has been proposed in [5.15].

- **General benchmark conclusions and recommendations**

The simulation of fast neutron sources (14 MeV) inside a subcritical reactor introduces slightly larger uncertainties on the reactor behaviour. This is probably related to a number of factors, including: uncertainties on the nuclear data in the region between 0.5 and 20 MeV, model deficiencies on some codes and lack of experience on the application of the codes to this kind of problems.

In addition, the exercise has been very helpful to identify the points of the different simulation methodologies that should be improved: calculation of β_{eff} and Λ in MCNP, significant discrepancies between different nuclear libraries, possible underestimation of ^{56}Fe capture cross section, etc.

Last, MUSE does not provide the answer to all the discrepancies, and additional comparisons between simulation and data will be very interesting and helpful, in particular paying attention to the external fast neutron source propagation within the multiplier media and transport of low energy neutrons in large nearly transparent reflectors.

5.5.3 Analysis results and interpretation

The analysis of the experiment and the comparison of measurements with deterministic and stochastic calculations have given the following conclusions [4.3]:

- Critical mass

There is an excellent agreement between measured and calculated reactivities from critical to k_{eff} = 0.95, with both sodium or lead coolant; deterministic (ERANOS) and stochastic (MCNP-X) calculations provide comparable results (given the uncertainties) as shown in Tab. 5.11:

Tab. 5.11: k_{eff} Measurements and Calculations (in pcm)

	Number of fuel cells	Experiment (MSM) (1$ = 331 pcm)	ERANOS Calculation	MCNP-X Calculation
Cross Section Library			ERALIB1	JEF+La150n+ Pu239JEFF3
Reference Configuration	1115	-80 ± 5	- 40 ± 315	+ 11 ± 18*
SC0 Configuration	1108	-616 ± 36	- 594 ± 315	- 689 ± 19*
SC2 Configuration	1006	-2884 ± 201	- 2873 ± 315	- 3036 ± 18*
SC3 – Na Configuration	972	-4493 ± 313	- 4464 ± 315	- 4126 ± 19*
SC3 – Pb Configuration	972	-3661 ± 291	- 3604 ± 315	-

(* statistical uncertainties only)

- Kinetic parameters

Measurements were performed in near-critical conditions, and also for the SC0 and SC2 configurations where a combination of the kp-method and the source modulation method was applied.

For the critical configuration, the agreement between measurements and calculations is good for the delayed neutron fraction β_{eff} for both deterministic and Monte Carlo codes within the reported uncertainties. For the generation time Λ (Tab. 5.12), there is also a good agreement between experiment and deterministic calculations within the reported uncertainties. However, the calculation of the mean neutron generation time based on Monte Carlo methods remains an open problem, since the interpretation of the MCNP removal times/lifetimes in view of a mean neutron generation is still under discussion. With regard to the validity of the standard measurement interpretation methods and the appropriateness of the used calculational schemes for the determination of â$_{eff}$ and Ë in deep subcritical conditions, the MUSE results don't allow to draw specific conclusions.

Tab. 5.12: Measured and Calculated β_{eff} – Critical configuration

	Experiment		Calculation			
	Pile noise)	Rossi α	CEA, BNFL,PSI	NRG	SCK	FZJ
Code			ERANOS	MCNP	MCNP-X	MCNP-X
Library			JEF2.2	JEFF3.0	JEF+La150n Pu239 JEFF3	ENDF/B-VI
β_{eff} (pcm)	334 ± 6	317 ± 13	326 ± 10	333 ± 2.5*	-	348 ± 3*
	average value = 331 ± 6					
Λ (µs)	0.59 ± 0.01	0.55 ± 0.02	0.52 ± 0.01	-	0.63*	0.62 ± 0.005*
					(these values correspond in fact to the mean lifespans of neutrons inducing a fission)	

(* : statiscal uncertainties only)

For subcritical configurations, further experiments and studies will be also necessary before drawing meaningful conclusions. In Table 5.13, we only reported the β_{eff} value experimentally measured on the SC2 configuration with the D-T source (using the combination of the kp-method and the source modulation method), and the values calculated for the 976 fuel cells configuration considered in the MUSE benchmark.

Tab. 5.13: Measured and Calculated β_{eff} – Subcritical configuration

	Experiment (combination of the k_p method and the source variation method [5.16])	Calculation (NRG [4.6])		
Configuration	SC2 1004 cells	976 cells		
K eff	0.97060	0.96829		
Code	-	MCNP		
External source	(d,T)	(d,T)	-	
Method	-	SDEF	KCODE	
Library	-	JEFF3.0	JEFF3.0	JENDL-3.3
β_{eff} (pcm)	313 ± 34	333.7 ± 6.2	326.7 ± 2.5	320.0 ± 2.2

- φ* parameter

The value of φ* is higher with the (d,T) source of 14 MeV than with the (d,D) source of 2.6 MeV, because of the (n,2n) reactions above 7 MeV, which increase the neutron multiplication. With the (d,D) source, the value of φ* is still greater than one, indicating that this source is more efficient than the fission source.

- Fission rate traverses

For the critical case, the C/E for fission rate traverses is very good (see Fig. 5.15), except in the center of the EW channel (owing to the position of this channel) and for isotopes with high thermal cross section near the reflector (see Fig. 5.16). Some measurements show up to 7% underestimation of the calculated fission rate. The origin of these discrepancies close to the reflector is a well-known problem and arises from the difficulties for deterministic codes to reproduce space-energy correlated phenomenon at such an interface [5.8]. A solution is under study at this time and should be implemented in ERANOS soon. The MCNP calculations match the measurements better (Fig. 5.16 - right), although residual discrepancies indicate that the nuclear data concerned by reflector effects could be ameliorated

Fig. 5.15: Fission rate traverse for the reference critical configuration
(circle=measurement, square=calculation)

Th232 – NS radial channel

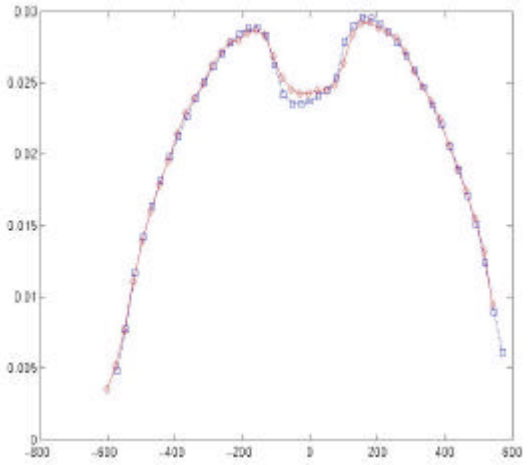

Np237 – W21-17 axial channel

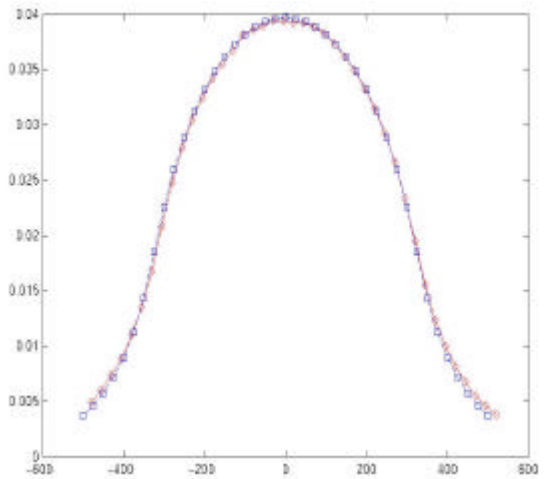

U238 - E19-18 axial channel

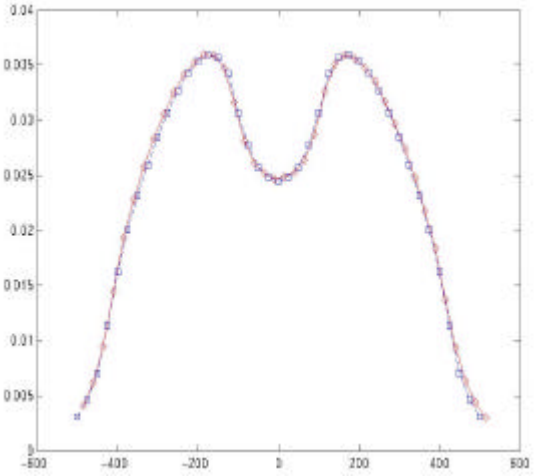

Am243 - EW radial channel

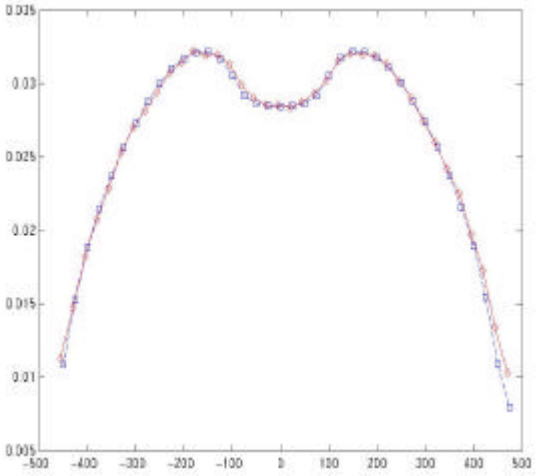

Fig. 5.16: Fission rate traverse for the reference critical configuration (circle=measurement)

U233 – W20-18 axial channel

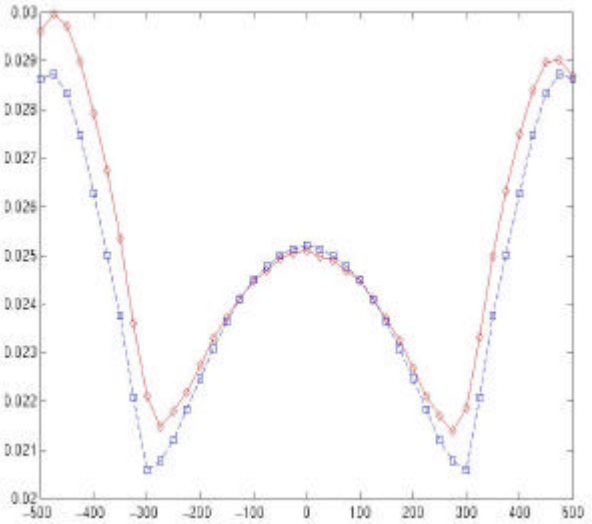

Pu239 – E/W radial channel

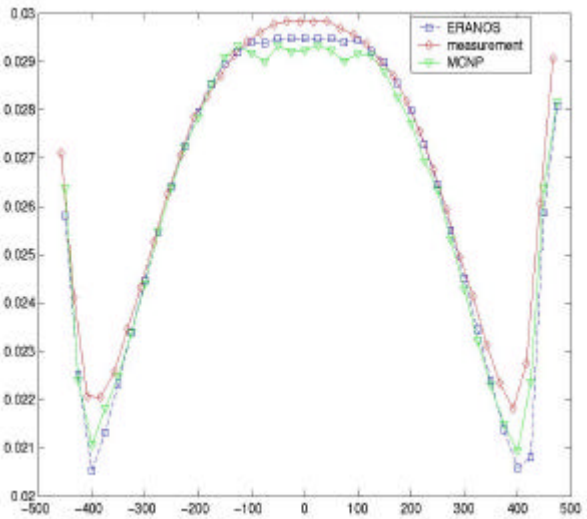

For subcritical configurations, ^{235}U fission rate traverses in the NS and EW channels show a very good C/E agreement better then 2% (Fig. 5.17). For SC0 (D,T), the ^{238}U fission rate traverses in the EW and NS channels show a very high C/E (Fig. 5.18). The cause of this discrepancy is the difficulty to reproduce in the calculation the exact level of subcriticality. Fig. 5.19 show that the ^{238}U flux shape in the centre of the MUSE-4-SC0 (D,T) configuration is very sensitive to the exact level of subcriticality in the calculation [5.17].

Fig. 5.17: ^{235}U Fission Rate traverse, calculated and measured, in NS Experimental Channel for the SC3-Na-DT configuration

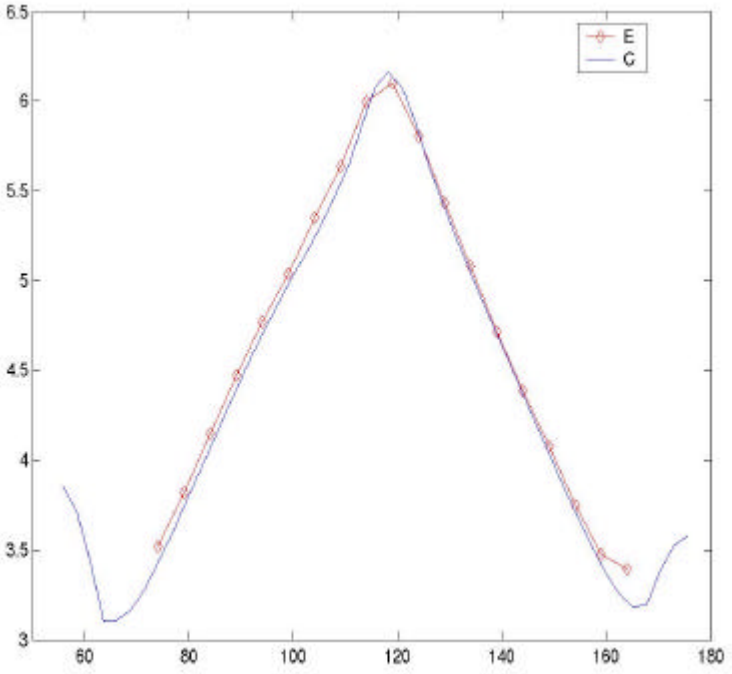

Fig. 5.18: ^{238}U Fission Rate traverse, calculated and measured, in NS Experimental Channel for the SC0-Na-DT configuration

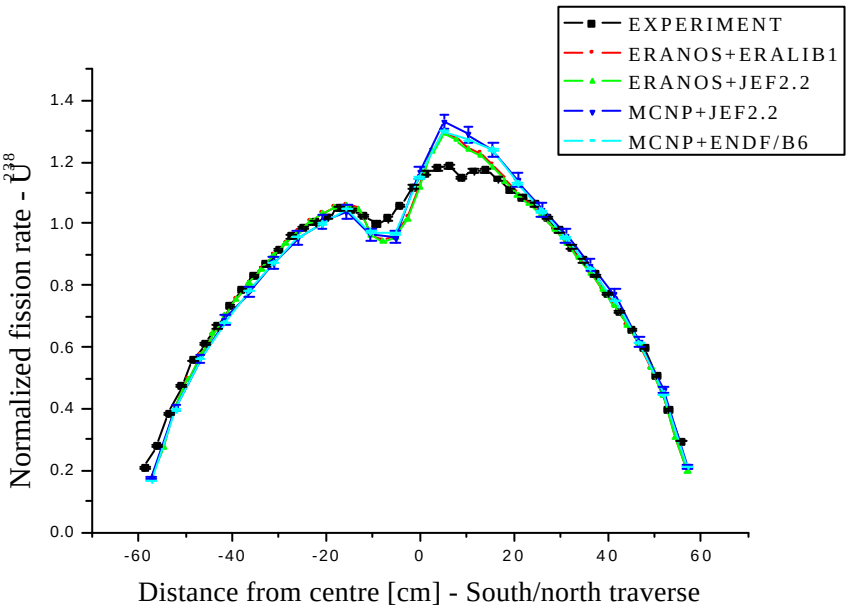

Fig. 5.19: Sensitivity of the shape of ^{238}U fission rate traverse to the subcriticality level

EW radial channel

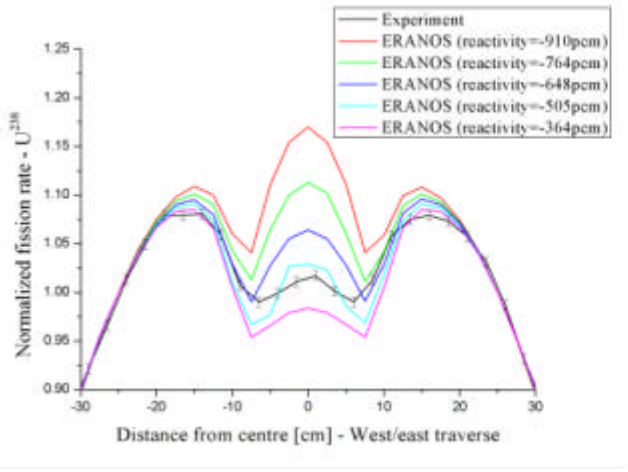

NS radial channel

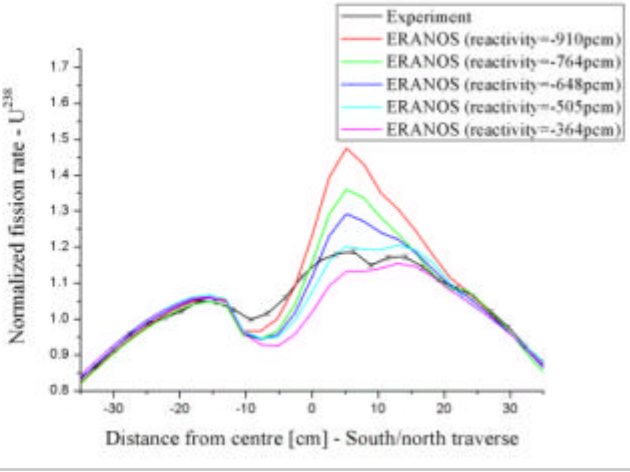

- Spectral indices

The spectral indices are well calculated in the fuel but unsatisfactory close to the lead; we have identified a high sensitivity of these quantities to the elastic and inelastic cross sections of lead (see Fig. 5.20), which seem to be overestimated.

Fig. 5.20: sensitivity of the $^{238}U/^{235}U$ fission index in the E19-18 channel located in lead

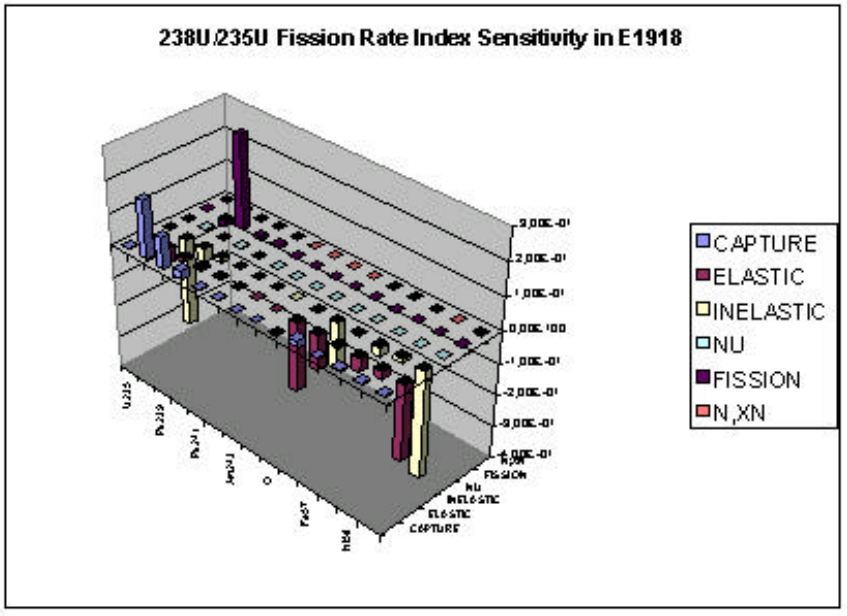

- Spatial Indices

Foil activation measurements [5.17, 5.18] reveal the impact of the central ADS-type heterogeneities on calculation accuracy. In particular, the difficulties of reproducing correctly spectral variations at high neutron energies, in and around the central lead region, have been brought out clearly. The influence of the external source is significant only to predict threshold spatial indices. Additionally, this effect appears just in the proximity of the external source. Some particular aspects have been quantified as the streaming effect along the accelerator channel.

- Sensitivity to lead cross-sections

Several different response parameters in the MUSE-4 configuration show a rather large sensitivity to the high energy part of the lead cross sections, especially for the (n,2n) and the inelastic cross sections [5.19].

- Kinetics

Codes and data are capable to predict the time dependent behavior in the core only. The deviation at long times in the reflector and shielding (see Fig. 5.21) has been attributed to low energy neutrons and may be related to a bad characterization of the thermal capture cross section of ^{56}Fe [5.15]. Therefore, only PNS area method seems to be reliable for what concerns the order of magnitude of the spatial correction factors (see Tab. 5.14) [4.4, 5.8]. Concerning its application, it does not allow an on-line subcritical level monitoring in ADS, but can be used as "calibration" technique with regards to some selected positions in the system to be analysed by alternative methods, like Source Jerk/Prompt Jump.

Tab. 5.14: Reactivity evaluation of the SC0 configuration by means of PNS area method: comparison between the experimental and calculated values

	Reactivity ($)		Dispersion in comparison to the expected values		
Detector	Exp.	Cal.	Exp.	Cal.	(E-C)/C (%)
I	-14.3	-13.1	1.14	1.06	+7.5
L	-12.9	-13.0	1.03	1.03	-0.6
F	-11.9	-11.8	0.95	0.94	+0.7
M	-12.7	-12.8	1.01	1.02	-0.8
G	-13.0	-12.4	1.04	0.99	+5.0
N	-12.1	-11.8	0.96	0.94	+2.2
H	-12.6	-12.1	1.00	0.96	+4.3
A	-12.7	-12.4	1.01	0.98	+2.8
B	-13.0	-12.8	1.04	1.01	+1.9

Fig. 5.21: Comparison between experimental and MCNP calculated ^{235}U time-responses

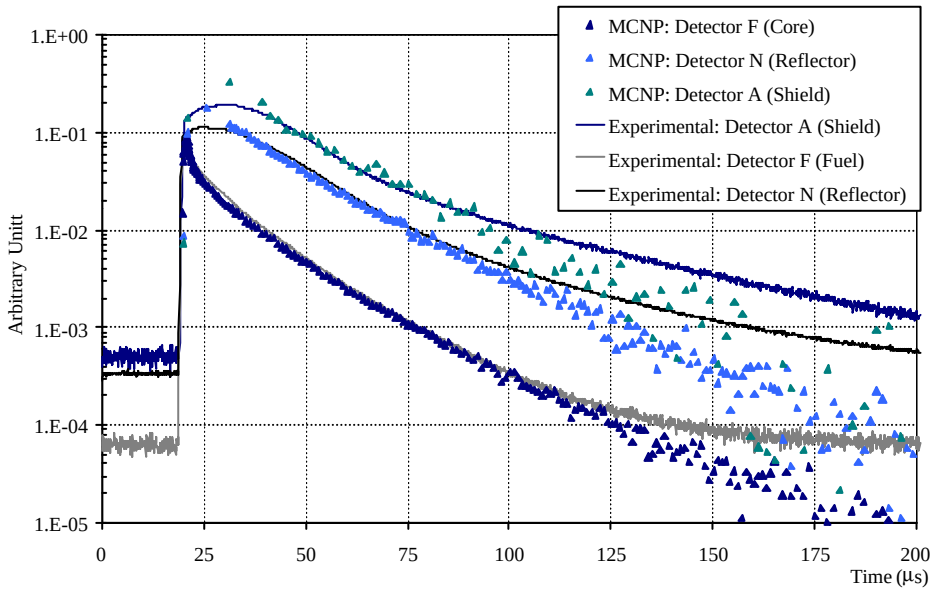

5.6 Monte Carlo simulations of neutron spectra and neutron source efficiency

One of the objectives of the studies presented in this section was to study the representativity of the MUSE experiments of a future ADS, by comparing the effects from the GENEPI-generated (D,D)- and (D,T)-neutron sources with the effects from a proton-induced spallation source [5.11]. All of the sources were coupled to the second sub-critical state of MUSE-4 (SC2). MCNP was used for all calculations with the (D,D)- and the (D,T)-sources, while MCNPX was used to simulate the configurations involving the 1000 MeV proton-induced spallation source.

5.6.1 Neutron energy spectra

Neutron leakage energy spectra from the lead buffer

One way to investigate the neutron source effects is to first study the sources without the multiplicative medium present and to compare the different neutron leakage spectra. For this purpose, the surrounding fuel and shielding were temporarily removed, as shown in Fig. 5.22. For the simulation of the spallation source, the lead buffer/target in the model was extended by one extra sub-assembly towards the proton beam, replacing part of the accelerator tube. Using MCNPX, 1000 MeV protons were directed towards the lead target, generating the spallation source.

Fig. 5.22: Configuration of only the lead buffer region. To the left: (D,D)- or (D,T)-source neutrons emitted at the centre of the core. To the right: 1000 MeV protons accelerated towards the extended lead buffer creating a large number of spallation source neutrons.

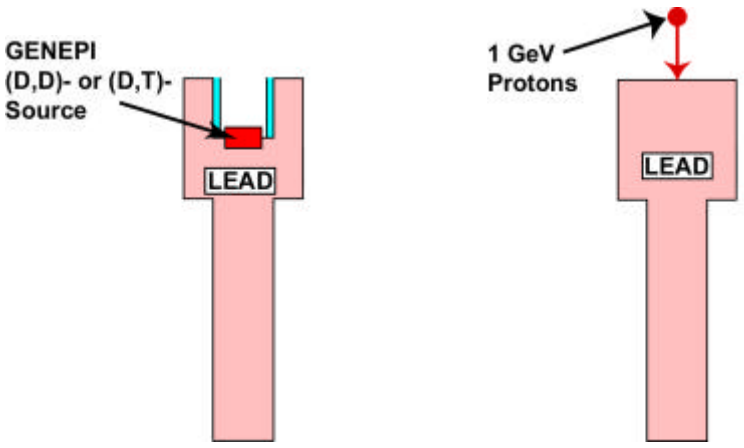

The energy spectra of the neutrons exiting the lead buffer are plotted in Fig. 5.23 and it is seen that the spectrum from the (D,D)-source has a large peak between 2 and 3 MeV, which is the energy range with which the neutrons are emitted by the GENEPI generator. Hence, only a small fraction of the source neutrons have lost their initial energy. This is an expected result, since the energy loss by elastic scattering of neutrons in lead is quite small. However, for the (D,T)-source, the energy of the neutron spectrum has decreased significantly, which is explained partly by the (n,2n)-reactions in the lead buffer, induced by the 14 MeV neutrons. The (n,2n)-reaction in lead has a threshold at about 7 MeV, explaining why there is no such effect for the (D,D)-source. However, about 35 % of the neutrons exiting the lead buffer have not interacted with the

lead and are still in the 14-MeV peak. For the spallation source, most of the source neutrons have rather low energy compared to the initial proton energy, with the maximum density at a little less than 2 MeV. This is a typical neutron leakage spectrum for 1000 MeV protons impinging on a lead target of this size. About 7 % of the spallation neutrons, however, still have energy higher than 20 MeV.

The GENEPI-generated neutron sources in the MUSE experiments were surrounded by a lead buffer with the purpose to simulate the neutron diffusion of an actual lead (or lead-bismuth) target in an ADS. The comparison of the neutron leakage spectra shows that the neutrons from the (D,T)-source in MUSE-4 have a rather similar energy spectrum as the neutrons from the spallation source have, and can from this point of view be considered more representative for a spallation-driven system than the (D,D)-source.

Fig. 5.23: Neutron leakage spectrum from the lead buffer/target for a (D,D)-source, a (D,T)-source and a spallation source (1000 MeV protons).

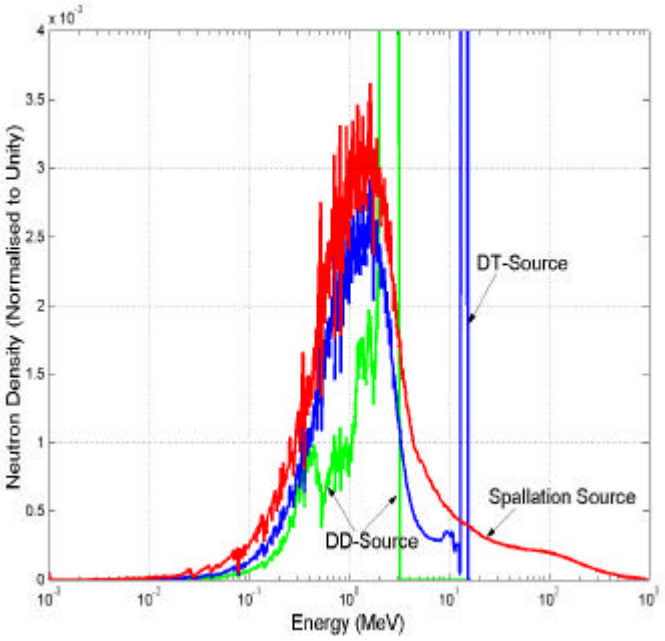

Neutron energy spectra in the core

The neutron energy spectra for the three different sources have been computed with the entire core present. The spectra were calculated in two different positions; one in the lead buffer and one in the fuel.

In Fig. 5.24, the neutron energy spectra for the three different sources calculated in the lead buffer are plotted. The spectra are very similar to each other, the energy density being maximal at about 500 keV. Several spectrum characteristics of the multiplying fuel can be recognized, for example the two dips in the neutron fluxes caused by the scattering resonances in sodium (~3 keV) and oxygen (~0.4 MeV). This indicates that the neutron spectrum in this position is rather dominated by the fission multiplication in the fuel and that many of the neutrons from the fuel enter into the lead buffer. However, a smaller fraction of the neutrons have energies different from the average behavior and the two peaks representing the origins of the GENEPI-generated neutron sources and the high-energy tail of the spallation source are very clear in this position. It should be noted that the position in the lead buffer where the energy spectra have been calculated is only about 5 cm from the position where the GENEPI source neutrons are emitted.

In Fig. 5.25, the neutron spectra in the fuel at a point located 21 cm from the center of the core and about 10 cm into the fuel are depicted. Naturally, the fuel spectrum characteristics in this case are even more pronounced than in the lead buffer. The three different curves are very similar and almost no traces from the origins of the external neutron sources can be observed. Only about 0.15 % of the (D,T)-source neutrons are still in the 14 MeV peak and about 0.04 % of the neutrons in the spallation-driven system have energies higher than 20 MeV. The spectra for the other sub-critical states (SC0, k_{eff} ~0.994 and SC3, k_{eff} ~0.95) are not shown here, since they are similar to the spectra of SC2. However, as there is less fission multiplication for larger sub-criticalities, the origin of the sources becomes a little more pronounced in SC3 and vice versa in SC0.

The computed neutron spectra show that the energy spectra in the core, originating from the three different external sources are very similar to each other. These results indicate the validity of one of the basic hypothesis of the experiments, namely that the choice of using a spallation source or the source neutrons produced by the (D,D)- or the (D,T)-reactions, will affect very little the neutron spectrum in the fuel. Only inside the lead buffer and at the buffer/core interface some differences are observed. We therefore conclude that, for the purpose of computing neutron spectrum-weighted quantities, the energy distribution of the external source can be neglected beyond a few centimeters into the fuel.

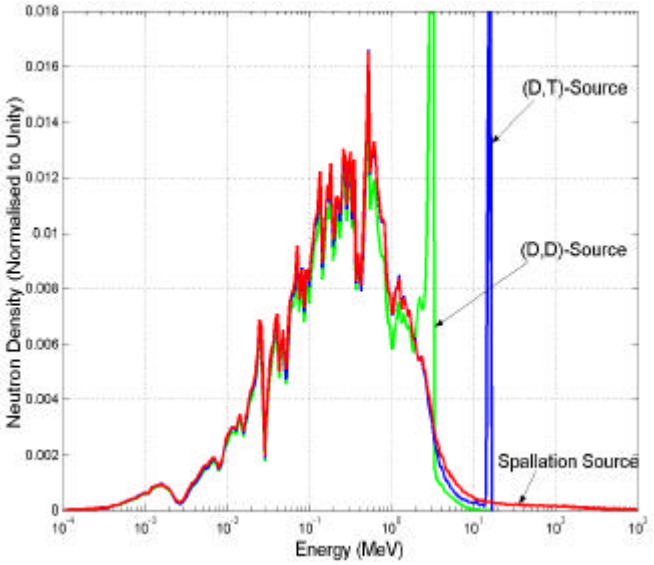

Fig. 5.24: Neutron energy spectra in the lead buffer.

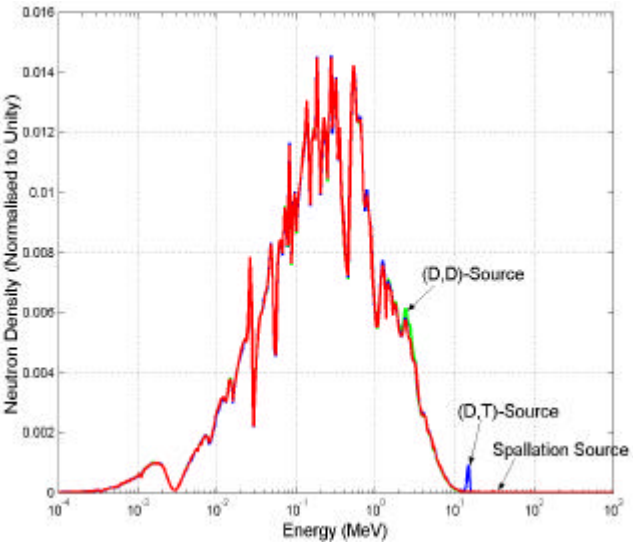

Fig. 5.25: Neutron energy spectra in the fuel.

5.6.2 Neutron source efficiency

The neutron source efficiency (φ*) was determined for the GENEPI-generated (D,D)- and (D,T)-neutron sources, both of them coupled to the second sub-critical state (SC2). φ* represents the relative efficiency of the external source neutrons and can be expressed according to the following equation;

$$\boldsymbol{j}^* = \left(\frac{1}{k_{eff}} - 1 \right) \cdot \frac{< \boldsymbol{F} \boldsymbol{f}_s >}{< S_n >} \ .$$

$< \boldsymbol{F} \boldsymbol{f}_s >$ is the total production of neutrons by fission and $< S_n >$ is the total production of neutrons by the external source. The relation shows that, for given values of k_{eff} and $< S_n >$, the larger φ*, the larger the fission power produced in the system. The quantities on the right hand side of the equation are standard outputs from MCNP. The results, including statistical error estimates, are listed in Tab. 5.15. The neutron source efficiency obtained for the spallation source was not included in this report, due to the ambiguity in defining the external neutron source in a system where the actual source particles are protons and not neutrons. The neutron source can be defined in several different ways and the results are directly dependent on the choice of definition. Therefore, completely different values of φ* are often observed, due to the different choices of external neutron source definition.

Tab. 5.15: Neutron source efficiency for the (D,D)- source and the (D,T)-source in the MUSE-4 SC2 configuration and in a centrally lead-cooled configuration.

Source	k_{eff}	φ*
(D,D)-Source	0.97285 (± 18 pcm)	1.36 (± 0.010)
(D,T)-Source		2.17 (± 0.020)
(D,T)-Source (centrally lead-cooled core)	0.97382 (± 27 pcm)	2.39 (± 0.030)

The energy of the emitted (D,D)-source neutrons (2-3 MeV) is only slightly larger than the average energy of a neutron produced by fission. Since φ* is 1.0 for an average fission neutron, the value for the (D,T)-source is therefore expected to be equal or slightly larger than 1, which is indeed the case. For the (D,T)-source, the reason for the higher values of φ* is the larger fission rate, part of which coming from fissions induced by the neutrons multiplied by (n,2n)-reactions in the lead buffer. The number of fission neutrons per source neutron is large, approximately 59% larger than for the (D,D)-source. The (n,2n)-multiplication of the 14 MeV neutrons increases the number of neutrons leaking out into the fuel and inducing fission chain reactions, thus enhancing the neutron source efficiency. In average, about 1.5 neutrons leave the lead buffer per initial 14 MeV neutron, compared to about 1 neutron for each (D,D)-source neutron.

In an extended phase of the MUSE-4 experiments, a configuration with 22 of the central sodium-cooled fuel sub-assemblies replaced by lead-cooled sub-assemblies was studied. In order to maintain the same reactivity for the two configurations, some of the peripheral fuel sub-assemblies were removed. As is shown in Tab. 5.15, the source efficiency for the lead-cooled configuration is significantly higher than for the sodium-cooled configuration, 2.39 compared to 2.17. The reason for this difference is again the (n,2n)-multiplicative effect in lead. Since there is more lead in the central part of the core in the lead-cooled configuration, where there are still many neutrons with energy higher than about 7 MeV, there is more (n,2n)-reactions. These circumstances enhance the neutron multiplication, as well as φ*. Since the source efficiency relates the source intensity to the power produced in the system, we conclude that, for a constant

source intensity, the replacement of sodium coolant by lead coolant in the 22 central fuel sub-assemblies increases the power by approximately 10%.

5.6.3 Proton Source Efficiency

An important factor when designing a real ADS, driven by a high-energy proton beam, is to optimize the beam power amplification, i.e. the core power over the accelerator power, given that the reactor is operating at a certain sub-critical reactivity level. Therefore, optimizing the source efficiency and thereby minimizing the proton beam requirements can have an important impact on the overall design of an ADS and on the economy of its operation. The neutron source efficiency parameter φ* is commonly used to study this quantity, since it is related to the number of fissions produced in the core (which is proportional to the total core power) by an average external source neutron. However, calculating φ* introduces some problems, since the actual source particles are protons and not neutrons. With the purpose of providing a simple means for studying the core power over the beam power, a new parameter, the "proton source efficiency" (ψ*) has been introduced [5.20]. ψ* refers to the number of fission neutrons produced in the system by each source proton and is expressed in the same way as φ*, only with the replacement of $<S_n>$ by $<S_p>$, according to

$$\psi^* = \left(\frac{1}{k_{eff}} - 1 \right) \cdot \frac{<\nu\Sigma_f \phi>}{<S_p>}.$$

$<\nu\Sigma_f \phi>/<S_p>$ is the total production of neutrons by fission over the total number of source protons. Hence, ψ* also represents the product of φ* and the number of source neutrons generated per source proton (Z), i.e. $\psi^* = \varphi^* \cdot Z$. In order to optimize the core power over the beam power, the proton source efficiency has been studied conceptually as a function of several different system parameters, such as the target radius, coolant material, axial proton beam impact position, proton beam energy and fuel composition [5.20, 5.21, 5.22]. A rather strong dependence was found for all of these parameters, in particular for the target radius.

In the profound study of different measurement techniques for reactivity monitoring in an ADS, performed within in the MUSE-4 programme , the method based on the current-to-flux reactivity indicator has appeared to be the major candidate for on-line monitoring (see Chapter 9). The ratio between the neutron flux monitored in a detector (Φ) in the core and the proton beam current (i_p) can be expressed by the following relation,

$$\frac{\Phi}{i_p} \propto \frac{k_{eff}}{1 - k_{eff}} \cdot \varepsilon \cdot \psi^*,$$

where ε is the efficiency of the detector. Hence, assuming that the reactor is operating at a constant reactivity and that the detector efficiency does not change, ψ* is the proportionality factor between the monitored neutron flux and the proton beam current. By studying the dependence of ψ* on different possible variations of the target-core properties, a good estimation of the stability of the current-to-flux reactivity indicator can be obtained. Possible transients that might affect ψ* are, for instance, a change in the beam direction or the beam impact location, the proton energy or the target temperature. Over longer periods, the change in isotopic composition of the fuel due to burnup, or the modification of the core geometry during reloading, might change the source efficiency. In order to assure the reliability of the reactivity indicator, these

factors, potentially able to affect the proton source efficiency or the detector efficiency, should be monitored continually or checked on a regular basis.

5.6.4 Conclusions

From the computed neutron spectra, the two following conclusions can be drawn. First, the energy spectrum of the neutrons leaking out from the lead buffer for the (D,T)-source is rather similar to that of the spallation source. Therefore, from this point of view, the (D,T)-source can be considered more representative of an ADS than the (D,D)-source. Second, the fact that the fission multiplication dominates at distances past a few centimeters into the fuel implies that, for the purpose of core studies, the presence of the source may be ignored in the calculation of spectrum-weighted quantities and the MUSE experiments can, from this point of view, be considered representative of an ADS.

The calculations of φ^* for the different sources yield a considerably higher value for the (D,T)-source than for the (D,D)-source, which is explained by the (n,2n)-multiplications of the 14 MeV neutrons in lead. Moreover, the proton source efficiency parameter ψ^* has been defined and studied, in order to provide a basis for the optimization of the core power over the beam power and for the evaluation of the stability of the current-to-flux reactivity indicator.

6 Characterization of spallation targets bombarded by a high energy proton beam

In this part of the report are described the measurements and calculations performed within the frame of the SAD project (see sections 4.3 and 4.4.3). These experiments and analyses, carried out from 2000 to 2004 (annex 4), aimed at the verification of codes and data bases applied in modeling of: a) integral and differential characteristics of hadron field around a spallation target and, b) transmutations in target and construction materials and their resulting radioactivity.

Ad. a) Experimental investigation of neutron spectra at angles of 45^0, 75^0 and 105^0 to the proton beam was done with the use of Bonner spheres spectrometer detector. Neutron spectra were unfolded and compared with the calculated ones. A combination of the LAHET code with different nuclear models and the MCNP code was applied. The best agreement between measured and calculated spectra was observed in the 0.1 - 3 MeV neutron energy range. The largest differences occurred in the highest energy region (> 50 MeV) and between 5 and 20 MeV. An inherent imperfection of the Bonner spheres method for the former region (weak dependence of response functions on neutron energy) resulted in the discrepancy.
In order to improve the situation, an experiment with the use of track detectors with heavy metal (Ta, W, Au, Bi, and Pb) radiators was conducted. Its aim was the evaluation of the high energy particle induced fissions in radiators and their application to fast neutron (~30 – 500 MeV) spectrometry i.e. unfolding the neutron spectrum, basing on known excitation functions of threshold reactions of heavy metal fission. As a result of the measurement and theoretical analysis the near-linear dependence of the fission yield in these metals on the maximum value of their fission cross-section and computer simulated density of fission reactions was found. The idea needs further development.

Ad. b) The reaction rates in samples of the main elements composing the spallation target and surrounding construction materials, such as Mg, Al, Cr, Mn, Fe, Ni, Cu, Nb, W, Bi and Pb, were measured. In the experiments a cylindrical Pb targets were applied. As a result of extensive measurements of induced radioactivity a number of nuclides were identified. The majority of them are short-lived with half-lives, below 1 month. There are also some exceeding 1 month half-lives and even longer than 1 year. One can expect that among the produced but not measured (due to low activity) more long-lived nuclides are present.
In order to take into consideration both, proton and neutron induced reactions for broad energy range the following spatial distributions of induced activity in different elements were determined experimentally:
- Angular distribution around the target in samples of polyester (for C) and Al.
- Distribution on the Pb target surface in samples of polyethylene (for C) and Al.
- Axial distribution inside the Pb target and on its front and back surfaces.
- Radial distribution in Bi samples for three cross sections of the Pb target.

In the measurements of axial distributions of radionuclide activity in the Pb target three types of distribution shapes were distinguished: distribution of Bi isotopes, distributions of medium mass nuclides (most possibly products of fission or/and “deep” fragmentation), distributions of heavier mass nuclides (products of spallation of Pb nuclei). The most interesting are the distributions of Bi isotopes (^{207}Bi, ^{206}Bi, ^{205}Bi) obtained from Pb, thus only in proton induced reactions like (p,xn). They reveal a sharp characteristic peak about 30 cm inside the target in the region where proton energy decreases to 30 – 80 MeV. It results both from the decrease of proton energy with the penetration depth in lead and from the shape of the excitation function of respective reactions. These distributions are properly

reproduced in calculations by all applied codes (LAHET, MCNPX and FLUKA) and model options. The observed good agreement of calculation and measurement at the target front and near the end of primary proton range is observed. It results most probably from the fact that in both cases the activation stems mainly from reactions induced by the primary protons and for their energy ranges where the applied reaction models work properly. On the other hand, between the target front and the end of primary protons range increases the role of secondary protons and neutrons and their transport in lead. Thus, one can suppose that in this case worse performance of respective models is responsible for the discrepancy.

For all axial distributions some general regularities were found when comparing the calculated and measured results: too low values of calculation for fission fragments, better ones for heavier nuclides (A > 170). At the worst, the comparison shows the agreement within one order of magnitude. Almost always the C/E ratio is between 3 and 1/3. For he activity of the whole target even differences below 10% are observed, in particular for the nuclides - products of spallation with $\Delta A \approx 10$ - 30. However, one can not point out a single code and/or nuclear reaction model yielding good results for all examined nuclides. The model of Cugnon gives the best agreement with our experimental values - about 70 % of results within 30 % difference.

Verification of the computer evaluations, of integral and differential characteristics of hadron field and the radionuclide production around a spallation target in the whole energy range by comparison with the experimental data is one of the important tasks of the project SAD. All the described experiments were devoted to these subjects

6.1 Experiments

Different cylindrical Pb targets were applied and different types of measurements performed:

- Measurement of neutron spectra around the Pb target with the use of Bonner spheres method [6.1, 6.2],
- Application of track detectors for assessment of fast neutron induced fissions in heavy elements (excluding actinides),
- Activation measurements of angular and surface distributions of hadrons around the target [6.1, 6.2],
- Measurement of specific activities of threshold activation detectors in front and behind the target [6.3 to 6.9],
- Measurement of axial and radial distributions of the radionuclides activity induced in the target.

The proton beam intensity and distribution on the targets front surface has been monitored with the use of ionisation chamber, Al activation detectors, matrix of thermoluminescent detectors and profilometer.

6.1.1 Measurement of neutron spectra around the Pb target with the use of Bonner spheres method

The spectra of neutrons emitted from a thick target bombarded with high-energy protons have a very wide energy range, starting at the initial proton energy of hundreds of MeV, down to the energies of the order of keV. Experimental investigation of such neutron spectra is thus a valuable source of data for validation of the computer methods of their simulation. In the presented research neutron spectra at the angles of 45^0, 75^0 and 105^0 (to the proton beam direction) (Fig. 6.1) were measured with the use of Bonner spheres spectrometer (BSS).

Fig. 6.1: Layout of the experiment for the determination of neutron spectra

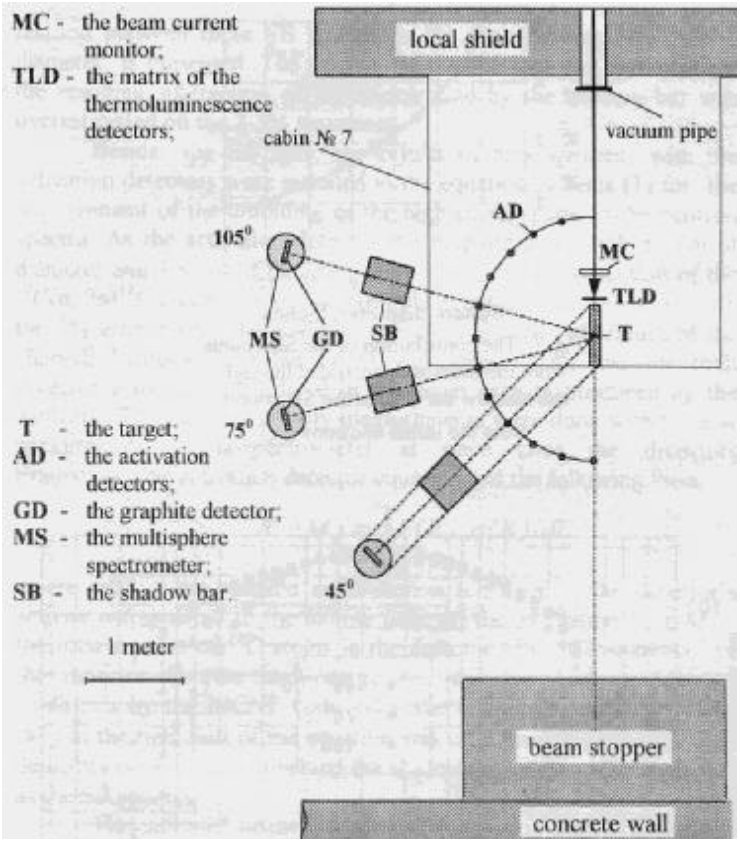

Neutron spectra were unfolded with the use of the 2-nd kind Fredholm formula

$$N_i = \int_{E_{min}}^{E_{max}} F(E) j(E) dE$$

where:

E - neutron energy [keV], $F(E)$ - neutron flux density [$cm^{-2}s^{-1}$], $f(E)$ - response function of i-th sphere [cm^2], N_i - the i-th sphere signal [s^{-1}].

The neutron spectra were also numerically evaluated taking into account the detailed experimental conditions. Two methods were used. In the first one a combination of the LAHET Code System [6.10] (for the nuclear cascade calculation at energies above 20 MeV) and the MCNP4B code [6.11] (for the neutron transport evaluation below this energy threshold), and in the second the MCNPX code [5.10], were applied. The calculated values are energy dependent neutron fluences averaged over a sphere corresponding to the volume of spherical moderator of the BS spectrometer. An example of results of the comparison of calculated and experimental neutron spectra is presented in the Fig. 6.2. All calculations with the LAHET code assuming different nuclear models produced very similar shapes of the spectra. Thus, only the results from the Bertini model are shown in the graph. The relative statistical errors of the calculated results amount to 2÷3%, except of the highest energy interval, above 50 MeV. The largest differences between measured and calculated spectra occur also in this region and between 5 and 20 MeV. The main reason of discrepancy at high energies is the weak dependence of BSS response functions on the neutron energy in this region, resulting in the poor ability of the technique to unfold respective

spectra. It is an inherent imperfection of the method. An improvement requires precise knowledge of the experimentally verified BSS response function at neutron energies above 20 MeV.

The experimental and calculated fluences (per initial proton) in the whole energy range from $3\cdot 10^{-2}$ to 650 MeV, at 277 cm distance from the target centre are presented in Tab. 6.1. As can be seen the calculation with MCNPX results in slightly better agreement with measurement for 45^0 and slightly worse for the larger angles. In both calculations the differences amount to 17 - 33 % and the higher values correspond to smaller angles.

Fig. 6.2: Experimental and calculated neutron spectra at 75°

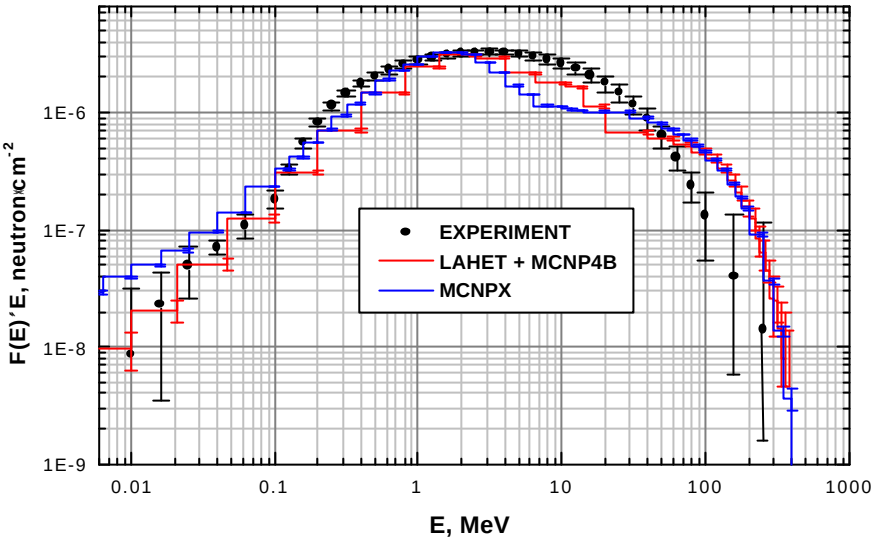

Tab.6.1: Experimental (Bonner Spheres Method) and calculated neutron fluence at the selected angles

Angle	45^0	75^0	105^0
Experiment	$(1.40 \pm 0.05)\cdot 10^{-5}$	$(1.42 \pm 0.06)\cdot 10^{-5}$	$(1.26 \pm 0.07)\cdot 10^{-5}$
Calculation by:			
MCNPX	$(9.647 \pm 0.019)\cdot 10^{-6}$	$(1.070 \pm 0.002)\cdot 10^{-5}$	$(1.013 \pm 0.002)\cdot 10^{-5}$
LAHET + MCNP4B	$(9.391 \pm 0.193)\cdot 10^{-6}$	$(1.046 \pm 0.022)\cdot 10^{-5}$	$(1.053 \pm 0.276)\cdot 10^{-5}$

6.1.2 Application of track detectors for assessment of fast neutron induced fissions in heavy elements (excluding actinides).

In order to improve the accuracy of measurements of the neutron spectra in the high energy region, an experiment with the use of track detectors with heavy element (Ta, W, Au, Bi, and Pb) radiators was conducted. Its aim was the evaluation of the high energy particle induced fission densities in radiators and their application to fast neutron (~30 – 500 MeV) spectrometry i.e. to unfolding of the neutron spectrum, based on known excitation functions of the threshold fission reactions.

During the irradiation with 660 MeV proton beam sandwiches consisted of the heavy element radiators between two track detectors, were placed behind the Pb target, where no primary protons could run in. After exposition and etching of the detectors, the numbers of fission fragments tracks resulting from reactions induced mostly by high energy neutrons (~99%) in radiators, were counted and their surface densities evaluated. Also the track dimensions were measured. Example of the dimensions distribution is presented in Fig. 6.3.

Fig. 6.3: Distributions of track diameters for the Au radiator

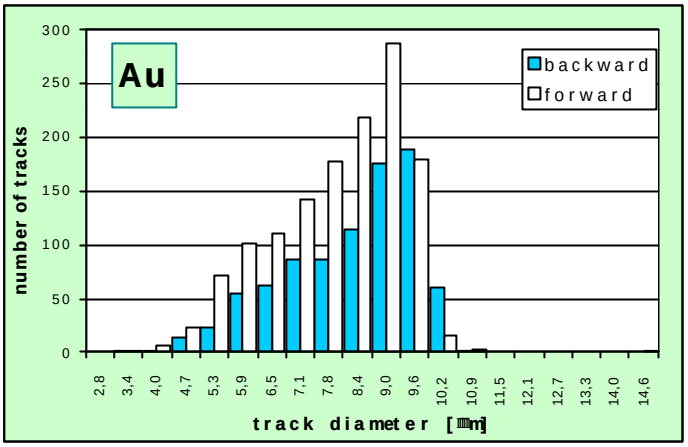

Application of a simplified theoretical approach gives the following approximate formula for the surface density of tracks (D [cm^{-2}]) from a particular radiator:

$$D = \frac{n_f R}{2} f = \langle \Phi s_f \rangle \frac{N_A r c R}{2A} f$$

Where:

n_f - volume density of fission fragments in a radiator [cm^{-3}], R - range of the average fission fragment in the radiator [cm], f - correction factor for the improper assumptions, s_f - maximum value of the neutron fission cross section [cm^2], F - fluence of neutrons [n/cm^2], A - atomic mass of the radiator [g], c - content of the radiator element, r - density of radiator [g/cm^3], N_A - Avogadro's number [at/mol].

The results show (see Fig. 6.4) that the normalised surface density of tracks counted in the backward direction (in this way the tracks from recoil nuclei are avoided), is proportional to the calculated fission density and/or to the maximum cross section for fission of a given radiator.

Fig. 6.4: Normalised density of tracks counted in the backward direction versus calculated fission density and neutron fission cross-sections for saturation energy (~380 MeV).

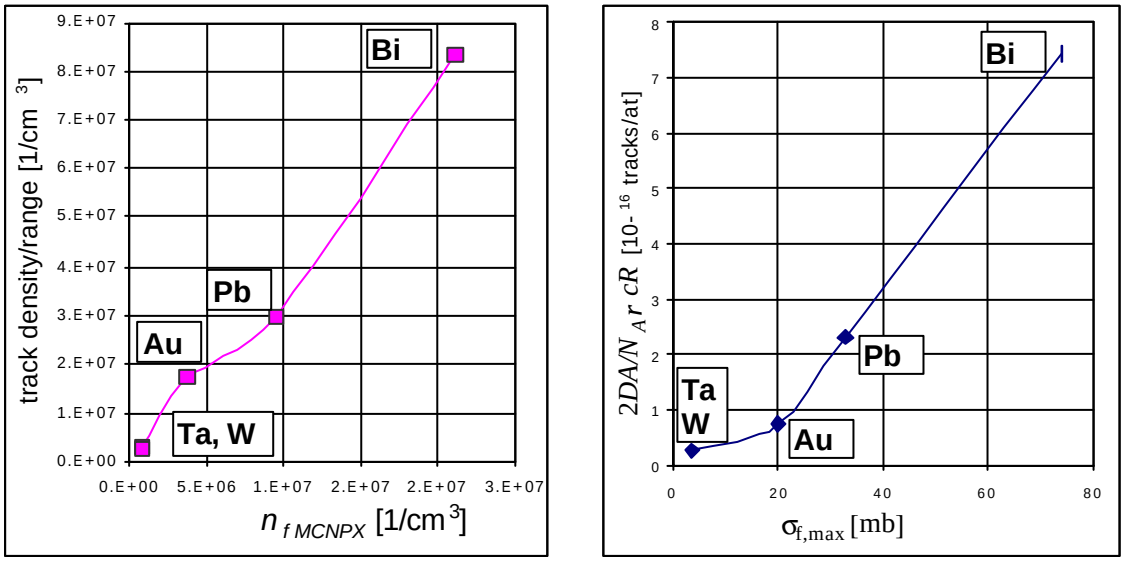

The obtained result is promising but the idea of the detection of tracks of heavy element fission fragments for fast neutron spectrometry needs further development.

6.1.3 Activation measurements of angular and surface distributions of hadrons around the target.

This part of the experiment consisted of two measurements. In the first one, the activation detectors of carbon and aluminium were applied for investigation of hadrons leaking from the lead target. The detectors were arranged around the target at the distance of 1 m from its centre in the horizontal plane of the target axis at the angles from 0° to 165° to the axis (Fig. 6.1). The absolute activities of ^{18}F, ^{11}C and ^{24}Na, induced in the detectors with reaction thresholds of 40, 20 and 6 MeV, respectively, were measured. The angular distributions of measured activities per one detector atom and one source proton, normalised to saturation values, are presented in Fig. 6.5 where they are compared with respective results of calculations. Total error of the presented experimental results ranges from 6% for the points near the distributions maximum up to 15% at their minimum. Angular distributions of the specific activity were simulated with the MCNPX code. The total activities were obtained as the sums of the two reaction channels the proton and neutron induced ones. Errors of the simulated activities are determined mainly by the uncertainty of reaction cross-section data.

Fig. 6.5: The angular distribution of the specific activity of the C and Al detectors positioned around the Pb target

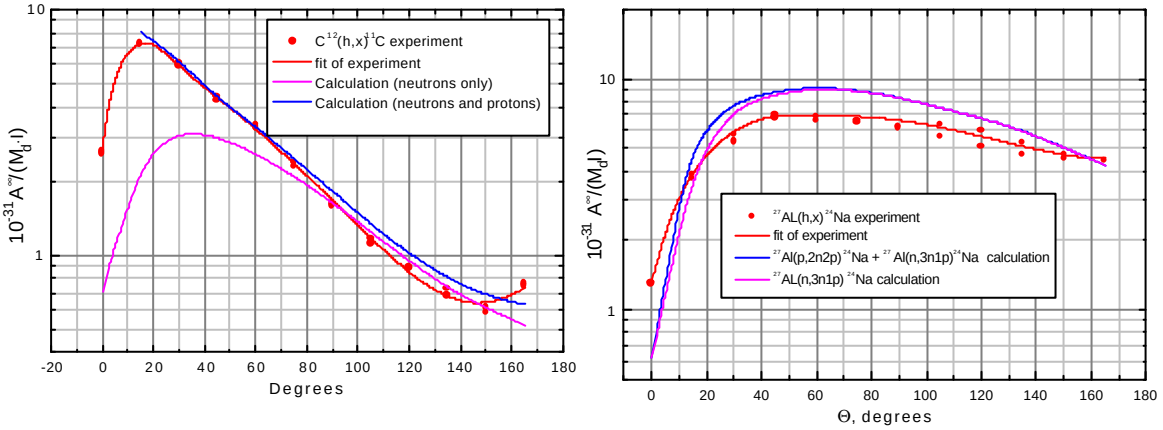

In the second measurement the longitudinal distribution of hadron yields was assessed. For this the lead target was wrapped with layers of activation detectors (AD) i.e. aluminium and polyethylene foils (Fig. 6.6).

Fig. 6.6: Activation detectors (AD) positioned on the side-surface along and at the ends of the lead target. The distance along the target in cm

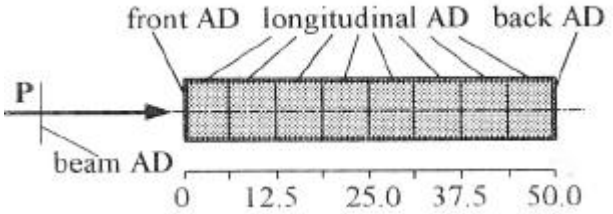

The results of measurements compared with calculations are presented in Fig. 6.7 in the same way as the angular distributions.

Fig. 6.7: The distribution of specific activity of the C and Al detectors positioned on the surface of a Pb target

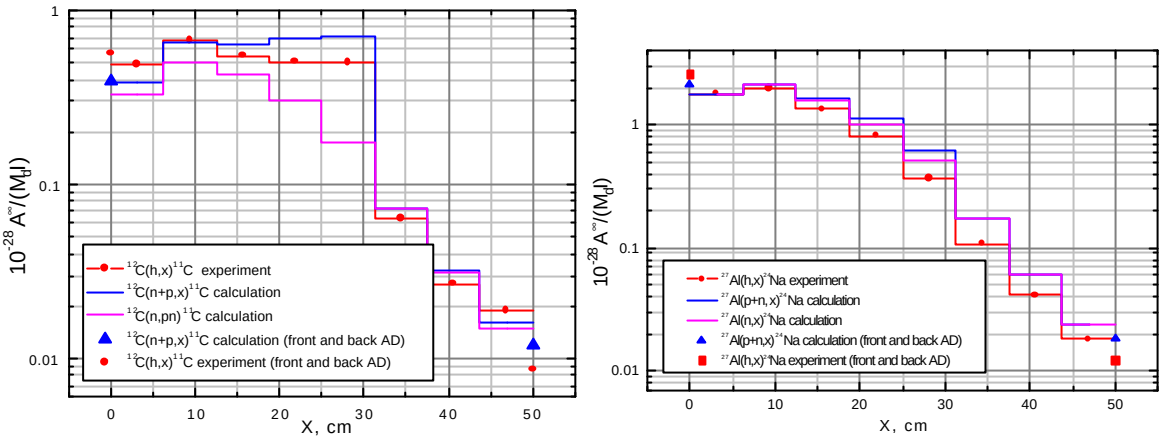

The respective experimental errors were estimated to remain between 6 and 15 % for different parts of the distributions. Generally, the calculated and experimental angular distributions show fair agreement with the exception of the back angle (165^0) where the low energy protons scattered from the target front may be underestimated in calculations. Also for the longitudinal distribution of activity the calculation results are similar to the experimental ones. The differences remain within the limits of total uncertainty of the results. It can be seen in the graphs that the proton contribution to the activities grows with the decrease of energy.

6.1.4 Measurement of specific activities of threshold activation detectors in front and behind the target.

In this initial experiment the samples of different metals were placed directly in the proton beam of 650 MeV in front of the target, and in the neutron field behind the target. One measurement was devoted to testing of the applied irradiation and counting procedure. The samples of Al, Fe, Cu, Nb and Pb were irradiated directly in the proton beam without the lead target. Based on the irradiation of Fe sample, the cross sections for the primary proton production of some residue radionuclides in natural Fe were determined and compared with other results. The obtained values agree within experimental errors with the results of earlier experiments for such nuclides as: ^{41}Ar, ^{42}K, ^{46}Sc, ^{48}V, ^{51}Cr and ^{52}Mn. For ^{24}Na our result fits better to the expected excitation function than the one of Lavrukhina [6.12].

In this way the applied procedure of the proton beam intensity monitoring and the absolute detection efficiency determination was tested and positively verified. The evaluated average relative determination error amounted to ~5 %. However, the accuracy can be still improved, mainly by better monitoring of the number of protons.

As a result of extensive measurements of activity induced in samples of main elements (Mg, Al, Cr, Mn, Fe, Ni, Cu, Nb, W, Bi and Pb) composing the typical construction materials around 200 radionuclides were identified. The majority of them have short half-lives, below 1 month. However, there are also some with half-life exceeding 1 month or even 1 year. One can expect that among the produced but not measured (due to low activity) nuclides the proportion is similar and some more long-lived nuclides are present.

6.1.5 *Measurement of axial and radial distributions of the radionuclides activity induced in the target.*

For assessing the axial distribution the spallation target was built of several pieces of 5 cm and 1 cm thick cylindrical parts and of 31 pieces of 1mm thick lead samples all 80 mm in diameter (Fig. 6.8). The Pb samples were placed along the target in such a way that to best reproduce the characteristic distribution of proton induced activity of Bi radionuclides (evaluated earlier with the use of LAHET code).

Fig. 6.8: Structure of the lead target: (diameter - 80 mm, length - 308 mm). Sample thickness - 1 mm

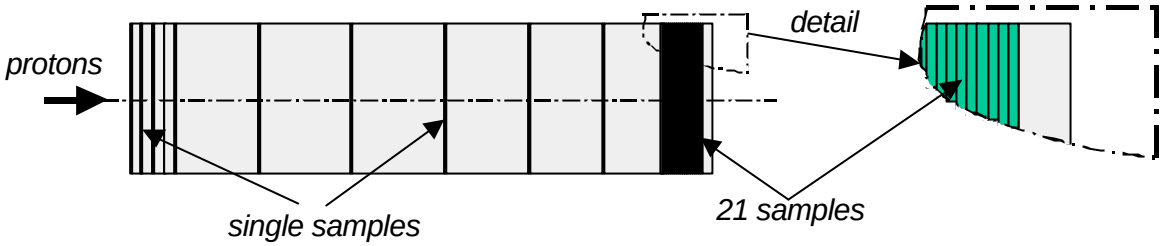

All parts of the target plus samples together with proton monitors were irradiated and then the samples and monitors were counted with the use of HPGe coaxial detector. For quantitative evaluation some nuclides were selected from the ones with the identified lines in the measured γ-spectra and for which axial distributions inside the Pb target were obtained. Examples of the results are presented in the Fig. 6.9.

Majority of calculations simulating the experiment was done with the code MCNPX (versions 2.5b and 2.5d) [6.13]. Different model options were applied in calculations of the induced activity. For the sake of example, the following representatives of nuclides: ^{83}Rb (fission), ^{185}Os (spallation) and ^{207}Bi (p,xn), resulting from different types of reactions, were selected for comparison of the experiment and calculations. This comparison is presented in Figs. 6.10, 6.11. One can observe that in some cases the new model option called INCL4-ABLA yielded results in better agreement with the experiment than other model options of MCNPX, for instance the distribution of ^{207}Bi. Comparisons for other nuclides have been presented in earlier reports from our investigations [6.14] as well as results of our calculations with the code Fluka [6.15].

The axial distributions of the Bi isotopes 205 and 206 have been used for ADS validation work in a diploma thesis at the University of Karlsruhe [6.16].

Fig. 6.9: Distributions of the specific activity of radionuclides along the Pb target irradiated with 660 MeV protons.

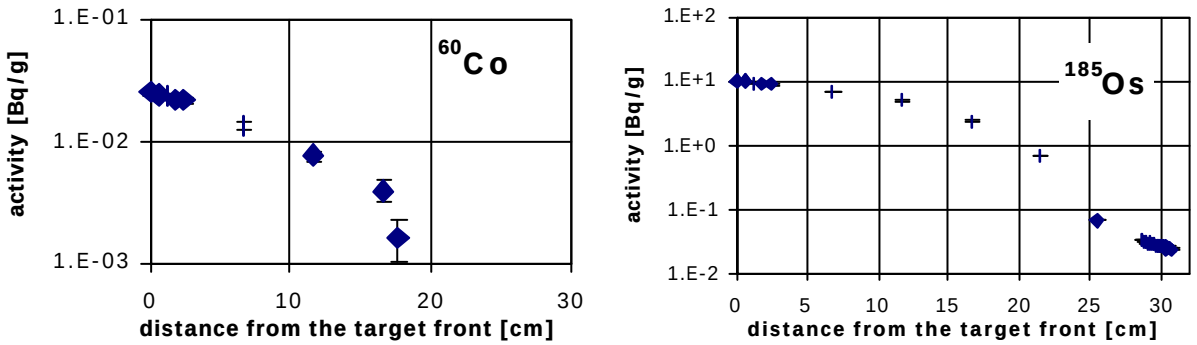

Fig. 6.9 (cont.): Distributions of the specific activity of radionuclides along the Pb target irradiated with 660 MeV protons.

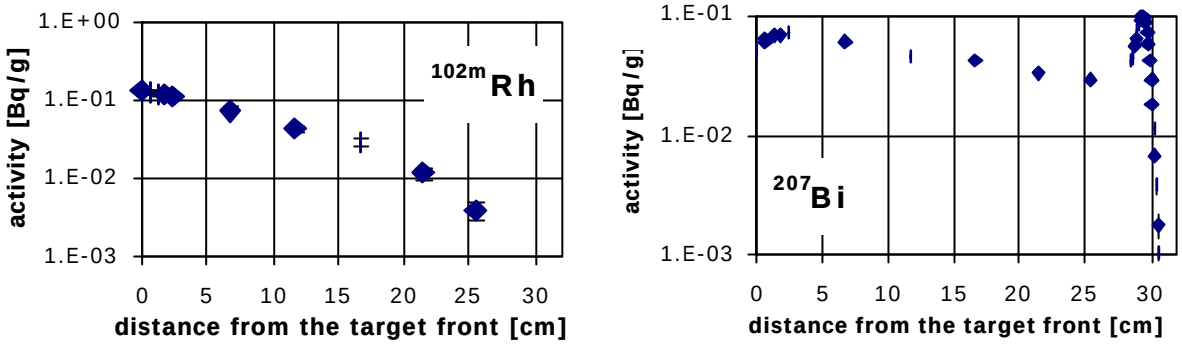

From the practical point of view evaluation of the total homogenised target activity can be of interest, especially for the liquid metal one. Such evaluation has been done on the basis of both the experiment and calculations (MCNPX and FLUKA). The experimental and calculated values were compared and the results of comparison are presented in Table 2.

Tab. 6.2: C/E (calculation/experiment) ratios for selected radionuclides.

BABL - Bertini + Abla, Bdef - Bertini default, CABL - CEM + Abla, CEM - CEM default, ISABL - Isabel, ISDRE - Isabel + Dresner

		Exp.	Uncert.	BABL	Bdef	CABL	CDRE	CEM	ISABL	ISDRE	FLUKA
fission products	^{60}Co	148	6	0,50	0,48	0,60	0,60	0,46	0,46	0,50	0,38
	^{65}Zn	274	8	0,87	1,71	0,77	0,67	2,04	0,82	1,64	0,78
	^{83}Rb	3540	170	0,49	0,43	0,59	0,63	0,50	0,53	0,37	0,68
	^{85}Sr	1644	85	0,66	0,58	0,80	0,80	0,77	0,75	0,51	**0,90**
	^{88}Y	6050	160	0,45	0,45	0,53	0,54	0,56	0,53	0,42	0,73
	^{95}Zr	5070	58	0,89	0,57	1,59	1,67	0,57	1,26	0,57	1,20
	^{102m}Rh	905	39	0,60	0,38	0,76	0,80	0,36	0,76	0,37	0,77
	^{110m}Ag	3460	92	0,44	0,39	0,73	0,75	0,19	0,59	0,24	0,59
	^{121m}Te	1580	44	0,63	0,78	**0,90**	0,85	0,57	0,78	0,71	0,54
spallation prod.	^{173}Lu	6640	120	1,42	1,86	0,54	0,55	**1,03**	**0,94**	1,33	0,07
	^{175}Hf	13350	450	1,14	1,32	0,52	0,51	0,89	0,80	**1,03**	0,10
	^{183}Re	32950	830	1,55	1,63	**1,02**	**1,03**	1,42	1,37	1,53	0,56
	^{185}Os	63770	890	1,27	1,15	0,89	0,89	1,20	1,17	1,13	0,51
	^{194}Au	435	41	**1,08**	**0,97**	**1,06**	**1,06**	1,28	1,15	**1,05**	1,34
	^{203}Hg	4480	33	1,30	1,28	1,59	1,60	0,48	**1,01**	**1,01**	0,68
p,xn	^{207}Bi	825	18	**1,06**	1,41	1,18	1,18	1,67	1,86	2,21	1,17

< 10% 10% < < 20%

Fig. 6.10: Examples of measured and calculated distributions of the specific activity of radionuclides along the Pb target irradiated with 660 MeV protons; eq = 1 and eq = 0 means: with and without taking into account the pre-equilibrium evaporation in the decay of excited nucleus.

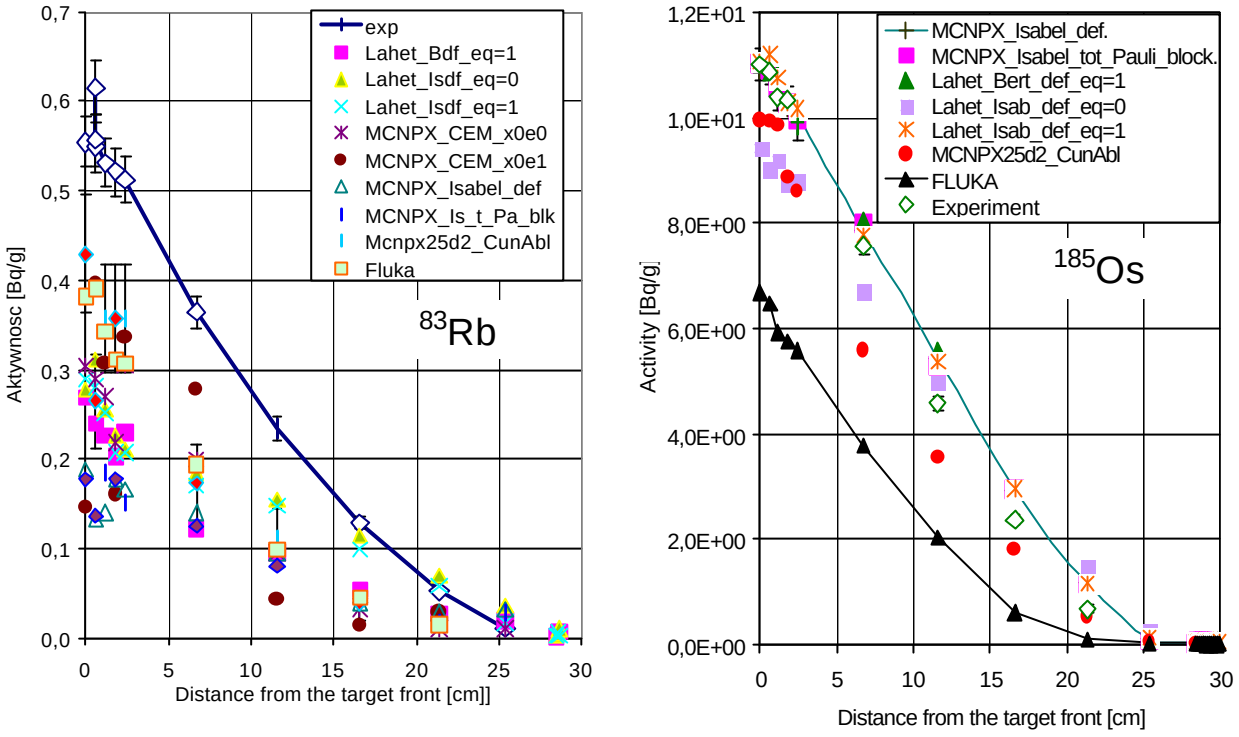

Fig. 6.11: Example (^{207}Bi) of measured and calculated production rate distribution of Bi radionuclides along the Pb target irradiated with 660 MeV protons

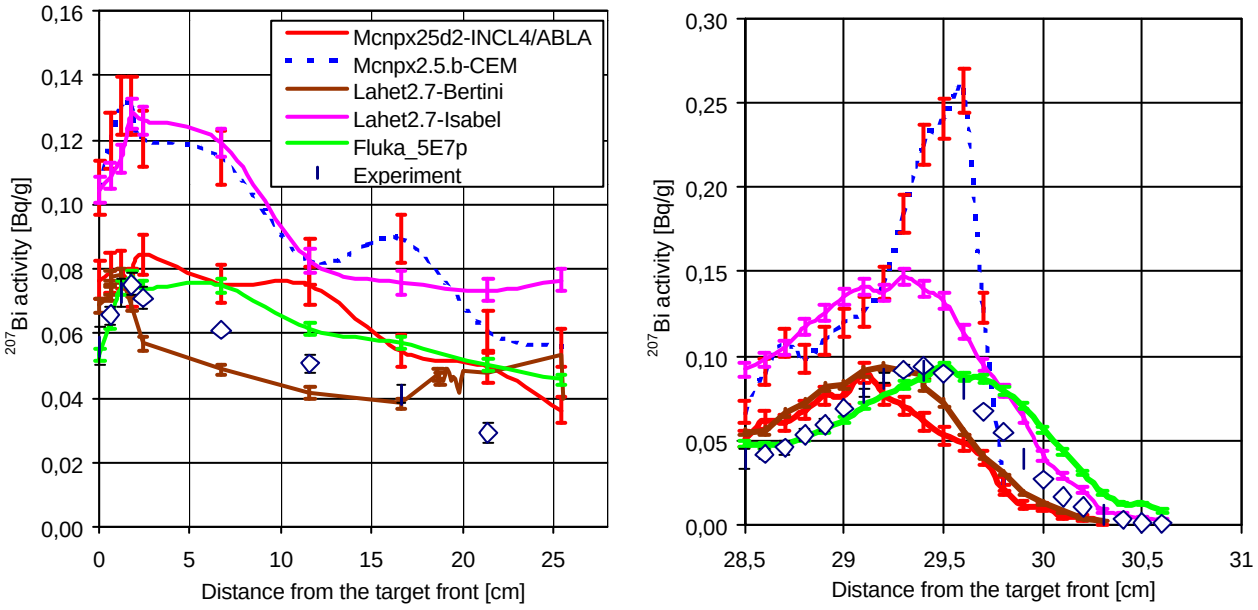

For the assessment of radial distributions two methods of detection were applied:

- Measurement of radioactivity induced in Bi samples irradiated in the Pb target.
- Application of track detectors for assessment of fast neutron induced fissions in heavy elements (excluding actinides).

In this case the spallation target consisted of 6 Pb cylinders 5 cm thick and 16 cm in diameter. Between the first 4 cylinders: the sample holders made of lead, Cu foils and track detectors of the same diameter as the target were introduced. Between the last 3 segments only Pb discs and track detectors were inserted.

All parts composing the target and the sets of samples are sketched in Fig. 6.12.

Fig. 6.12 :Layout of the Pb target and the holder of Bi samples

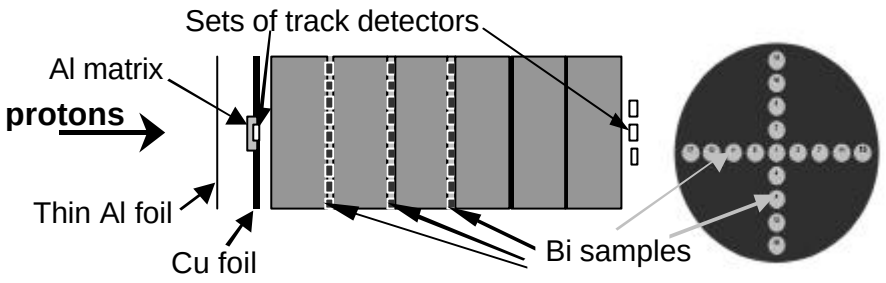

The measured activity of radionuclides induced in Bi samples was compared with the simulated one. Calculations were done with the use of MCNPX and FLUKA codes. The radial distribution of activity generated in lead was also studied. An example of the last results, for ^{207}Bi, is presented in Fig. 6.13. The measurements of tracks surface density distributions both axial and radial allowed for visualisation of the change of proton beam shape with the depth of penetration in lead (see Fig, 6.14).

Fig. 6.13: Experimental radial distribution of ^{207}Bi activity in the Pb target, 5 cm from its front

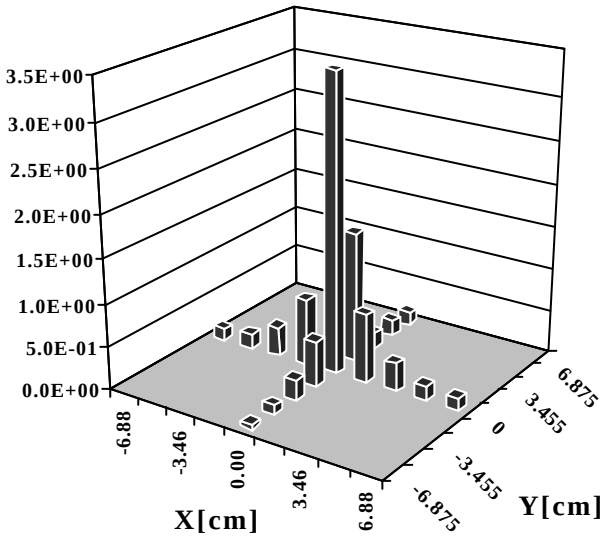

Fig. 6.14: Experimental radial distributions of fission fragments track density in the Pb target at 5, 10, 15, 20 and 25 cm depth

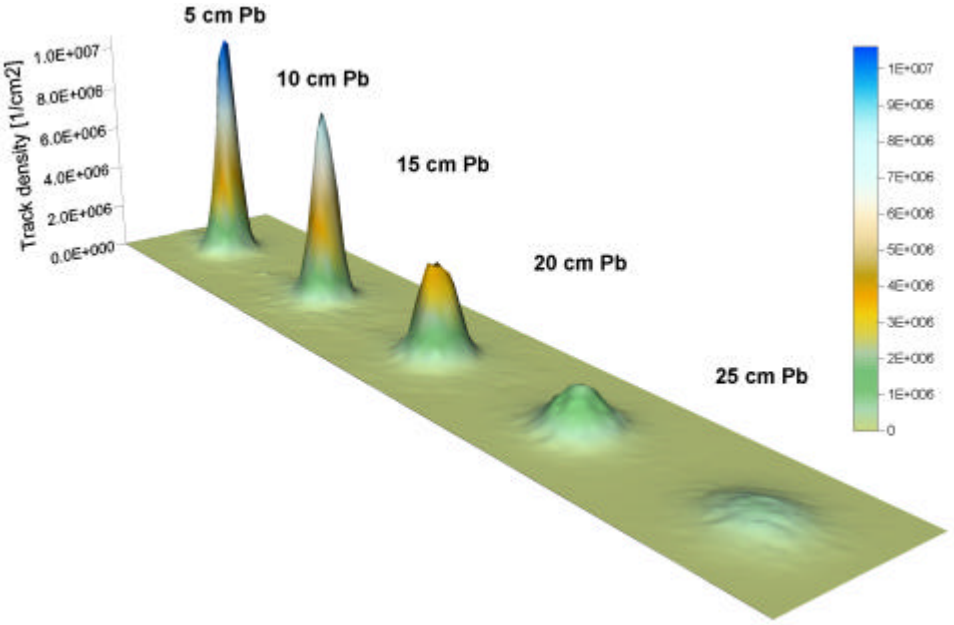

6.2 Discussion of results, conclusions

6.2.1 Activation measurements

The measurements of hadron angular distribution around the Pb target exposed to 660 MeV proton beam show a fair agreement with the calculated ones (6 - 15 % relative uncertainty). The agreement is worse only for the back angle (165^0) where the low energy protons backscattered from the target front may be underestimated in calculations. Also the calculation results for the activity on the Pb target surface agree with the experimental ones. The differences remain within the limits of total experimental uncertainty (6 - 15 %).

In the measurements of longitudinal distributions of radionuclide activity in the Pb target three types of distribution shape were distinguished (see Fig. 3.9):

- that of Bi isotopes,
- that of medium mass nuclides (most possibly products of fission or/and “deep” fragmentation),
- that of heavier mass nuclides (products of spallation of Pb nuclei).

The most spectacular are the distributions of Bi isotopes (^{207}Bi, ^{206}Bi, ^{205}Bi), which can be produced from Pb in proton induced reactions solely (e.g. (p,xn)). They reveal a characteristic sharp peak about 30 cm inside the target in the region where proton energy decreases to 30 – 80 MeV. The maximum results from the energy spectrum of protons, changing with distance passed in lead, coinciding at this depth with the maximum of the excitation function of respective reactions (Fig. 6.15).

Fig. 6.15: Cross section for reaction Pb(p,xn)^{206}Bi [6.17].

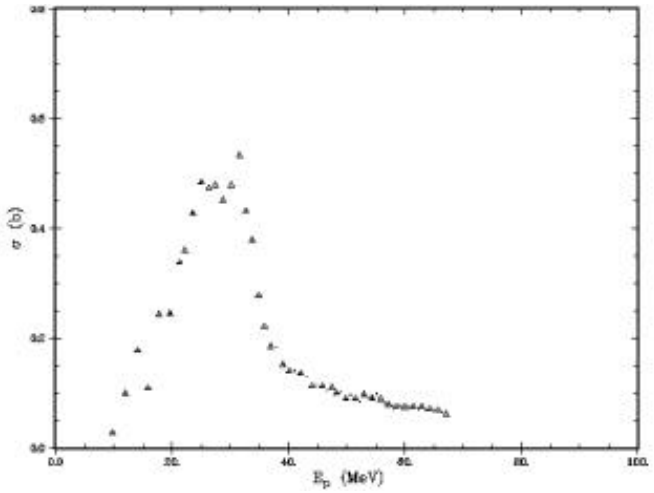

The distributions of Bi isotopes are properly reproduced in calculations by all applied codes and model options (LAHET, MCNPX, FLUKA), however one can observe better or worse compliance with the experimental results (see Fig. 3.11). In the peak of distribution one can distinguish the most deviating calculation results from the LAHET2.7-Isabel and the MCNPX2.5b-CEM options. Similar situation occurs for the continuum part of the distribution, between the target front and the place where the peak is observed. The worst performance is shown also for the LAHET2.7-Isabel and the MCNPX2.5b-CEM options. A good agreement of calculation and measurement at the target front and near the end of primary proton range is observed. It results most probably from the fact that in both cases the activation comes mainly from reactions induced by the primary protons and for their energy intervals where the applied reaction models work properly. On the other hand in between increases the role of secondary protons and neutrons and their transport in lead. Thus, one can suppose that in this case worse performance of respective models is the reason of the discrepancy.

For the medium mass nuclides (e.g. ^{83}Rb) – most probably fission products – the distributions decrease abruptly when proton energy drops below the respective reaction threshold. Their spatial distribution agrees with the one of beam protons in the target and their production ends practically at the depth of 20 - 30 cm in the target. A comparison with calculations (in the Fig. 3.10) shows that in the first half of the target length, where the energy of primary protons is high (450 - 660 MeV), the agreement is poor independently of the applied model of the excited nucleus decay. On the other hand the shape of experimentally determined distribution complies very well with the excitation function of the respective reaction (Fig. 616).

Fig. 6.16 : Comparison of the experimentally determined distribution of ^{83}Rb along the Pb target (irradiated with 660 MeV protons) with excitation function for the Pb(p,x)^{83}Rb reaction. The end of ^{83}Rb distribution - at ca. 29 cm – corresponds to 80 MeV energy of primary protons.

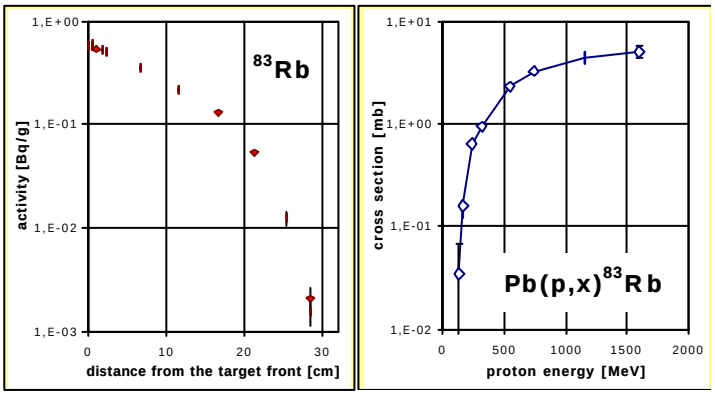

For the heavier nuclides (e.g. ^{185}Os) - residuals of the spallation process – the distribution is similar to that of medium mass nuclides, however, sometimes after the decrease of activity there is still observed a measurable low level activity until the end of target (see Fig. 3.9). It seems to result from neutron or secondary proton induced reactions. The experimental distributions and computed ones (Fig. 6.10) agree relatively well in the whole target length except for the results of FLUKA code (see example in Fig. 6.17).

Fig. 6.17: Comparison of measured and calculated activities [Bq/q] of ^{185}Os along Pb target for two options of the applied codes. a) MCNPX2.5b_CEM df_0e1 and b) FLUKA

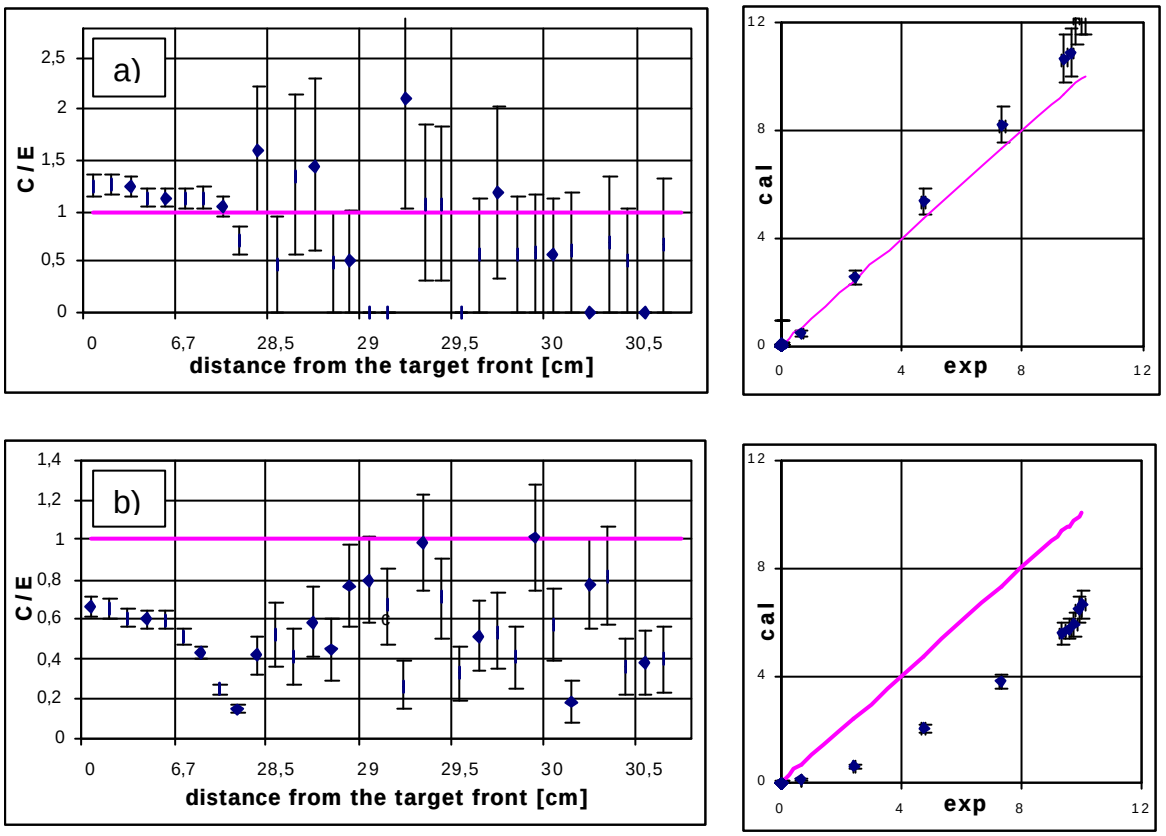

For all axial distributions some general regularities were found when comparing the calculated and measured results: underestimated in calculations values for fission fragments, better ones for heavier nuclides (A > 170). At the worst, the comparison shows the discrepancy within one order of magnitude. Almost always the C/E ratio remains between 3 and 1/3. For the activity of the whole target the differences even below 10% are observed (see Table 2), in particular for the nuclides - products of spallation with $\Delta A \approx 10$ - 30. However, one cannot point out a single code and/or nuclear reaction model yielding good results simultaneously for all examined nuclides. The model of Cugnon gives the best agreement with our experimental values - about 70 % of results remain within 30 % difference.

6.2.2 Track detectors

The application of track detectors for measurement of fission product intensity is a well-known technique in case of spontaneous and low energy neutron induced fission. In the presented experiments the technique was used for the neutron induced fission of heavy elements, like Ta, W, Au, Hg, Pb, Bi etc, with high values of threshold energy practically ranging from ~40 to ~100 MeV. This was aimed at the development of an inexpensive method of neutron

spectrometry for energies above 30 - 50 MeV when the unfolding based on the measured fission reaction rates would yield the neutron spectrum.

The first measurements and simulations yielded promising results. The "infinite" thickness of heavy element radiators (i.e. thicker radiators than the fission fragments range) was applied. A linear relation of the measured (with the use of selected plastic detectors) surface density of fission fragment tracks with the calculated in computer simulation (MCNPX) volume density of fission rates for 5 heavy metals (Ta, W, Au, Pb, Bi) was observed. This can be treated as a confirmation of the feasibility of the technique application for quantitative determinations.

Also were measured the distributions of track diameters (the shortest and the longest) and from them were deduced angles of incidence of fission fragments on the detector surface. The efforts to obtain respective and similar distributions in computer simulations brought only a partial success and were not presented in the report. The overcoming of this obstacle needs further investigations as well as the final application of the method for neutron spectrometry

7 Experimental techniques and analysis methods for the determination of the reactivity of an ADS

One major objective of the MUSE experiments is to determine which experimental technique or combination of experimental techniques could be used to control and monitor the reactivity of an ADS. To this end, many experimental methods are used to assess reactivity levels in various subcritical configurations without the need to perform a critical configuration. Such techniques are the source jerk techniques, pulsed neutron source experiments and noise techniques. The reactivity values determined with these techniques are then compared to these obtained with the reference experimental route based on rod drop experiments coupled with the (modified) source multiplication method (MSM).

In this section, the basic characteristics of the different techniques are recalled. Section 8 summarizes the main results obtained with these measurement methods when section 9 deals with the applicability of the different techniques for application in future ADS and finally proposes a methodology for reactivity monitoring in ADS.

7.1 Reference method for critical reactors

The reference method which is commonly used for critical reactors uses first a rod-drop experiment to determine the first reactivity level. This rod-drop experiment is performed from an initial critical reactor by means of a rod with a small reactivity weight. This small reactivity is necessary to limit the perturbations and to be able to apply the point kinetics equations. Subsequent reactivity levels are obtained by a Source Multiplication technique where the counting-rates of two subcritical states are compared to infer the reactivity ratio of the two reactor states. Since the first reactor state was determined with the rod-drop technique all other reactivity can hence be derived.

7.1.1 Rod-drop technique

The rod-drop technique [7.1] is based on the rapid insertion ("drop") of a control rod from a well-defined reactivity state, mostly the critical state. The subsequent time evolution of the neutron population is recorded. From the recorded time evolution of the neutron population it is then possible to infer the reactivity by the inverse point-kinetics method.

The inverse point-kinetics method [7.2] is a well-known method to determine the reactivity worth of the control rods in nuclear reactors. It is based on measuring the power of the reactor by neutron counters and solving the point-kinetics equations to calculate the dynamic reactivity $r(t)$:

$$r(t) = b + \Lambda \frac{d}{dt}\left[\ln n(t)\right] - l\,b \int_{-\infty}^{t} \frac{n(t')}{n(t)} \exp\left[-l\,(t-t')\right] dt' - \Lambda \frac{s(t)}{n(t)} \quad (1)$$

In this equation, b and l are the effective delayed neutron fraction and the corresponding precursor decay constant, and Λ is the neutron generation time. Often the source strength $s(t)$ is not known, although methods exist to determine the source strength from measurement.

For fast reactors with a very short generation time Λ, the above expression can be simplified using 'micro kinetics'. The result for the reactivity in dollars $\tilde{r}(t) = r(t)/b$ reads:

$$\tilde{r}(t) = \frac{1}{n(t)}\left[n(t) + n_0\left(\tilde{r}_0 - \exp[-lt] \right) - l\int_0^t n(t')\exp\left[-l(t-t')\right]dt' \right]. \quad (2)$$

Compared with the first equation this expression has two advantages. First, it does not require the external source strength to be known (although the value of the initial reactivity $\tilde{r}_0$ might seem as hard to get as s_0), and secondly it makes no use of the generation time. The latter is a consequence of the fact that use is made of prompt fission chains, instead of individual fissions, which is only valid if the reactivity does not change during a prompt fission chain. For fast reactors, and certainly for MASURCA, this limitation poses no problem. As stated above, a prompt fission chain takes less than 1 μs, while a safety rod drop that reduces the reactivity with about 10$ takes more than one second. This means that the reactivity changes about 0.001$ during a prompt fission chain, which indeed is negligible. For a sub-critical reactor, the duration of a fission chain is even shorter. For six delayed neutron groups, this equation reads:

$$\tilde{r}(t) = \frac{1}{n(t)}\left[n(t) + n_0\left(\tilde{r}_0 - \sum_{j=1}^{6}\frac{b_j}{b}\exp\left[-l_j t\right] \right) - \sum_{j=1}^{6} l_j \frac{b_j}{b}\int_0^t n(t')\exp\left[-l_j(t-t')\right]dt' \right] \quad (3)$$

From this equation, it can be seen that two set of input data are needed for the analysis: the initial reactivity $\tilde{r}_0$ and the delayed neutron data (l_j, b_j) for six families. The effective delayed neutron yields and the corresponding precursor decay constants for the six families can be calculated with standard neutronic codes. The initial reactivity $\tilde{r}_0$ can be derived from the experiments by the following procedure: If the delayed neutron data is calculated for a specific state of the reactor, e.g. (virtual) critical, and if the reactor is held at that state for a certain period of time, the reactivity obtained from the inverse point-kinetics procedure should be constant for that same period too. This leaves one degree of freedom to fix the initial reactivity $\tilde{r}_0$. Because the delayed neutron data were calculated for a critical reactor (see next section), the initial reactivity is obtained by forcing the reactivity to a constant value before the rod drop.

Due to the insertion of the rod a strong local perturbation of the flux can be present. This disturbance of the power profile can be so large that the inverse point-kinetics analysis is not valid anymore, especially for the detectors close to the safety rods. Better values can be obtained when the influence of the spatial flux distribution on the count-rates of the detectors is taken into account by means of spatial correction factors.

7.1.2 Source Multiplication method

7.1.2.1 Approached Source Multiplication (ASM) method

The Approached Source Multiplication (ASM) method [7.1] is based on the subcritical multiplication in a multiplying medium. The number of neutrons per second *N* which are present in the reactor is proportional to the injection and multiplication rate, and is given by:

$$N = \frac{S}{1-k} \quad (4)$$

If we measure this neutron population with a neutron detector having a detector efficiency $\mathring{a}_n$, the detected count-rate C is given by:

$$C = e_n \frac{S}{1-k} \quad (5)$$

When the effective neutron multiplication factor of the core is modified and the neutron driving source is unchanged, the ratio of the count-rates in both situations equates to:

$$\frac{C_1}{C_2} = \frac{1-k_2}{1-k_1} \quad (6)$$

Based on this equation and the knowledge of the initial reactivity level (by rod-drop) the reactivity associated to the new reactor state can easily be obtained by the following relation:

$$\frac{r_2}{r_1} = \frac{k_2 - 1}{k_1 - 1}\frac{k_1}{k_2} \approx \frac{k_2 - 1}{k_1 - 1} = \frac{C_1}{C_2} \quad (7)$$

By means of this expression one can easily relate different reactivity levels, if a reference reactivity level was determined with another independent technique such as the rod-drop technique.

7.1.2.2 Modified Source Multiplication (MSM) method

If the neutron source does not have the same spatial and spectral distribution as the induced fission source, which in practice is usually the case, the subcritical multiplication will not be described by the effective neutron multiplication factor but by the source neutron multiplication factor k_S. To account for this a correction factor $ö^*$ has to be introduced as given by the following expression [7.3]:

$$N = \frac{S}{1-k_S} = j^* \frac{S}{1-k} \quad (8)$$

This correction factor, known as the "source importance factor" accounts for the fact that the source neutrons do not have the same importance in general as the fission neutrons. The expression for the "source importance factor" is given by [7.3]:

$$j^* = \frac{1-k}{1-k_s} \approx \frac{\dfrac{\left\langle j_0^+, S \right\rangle}{\left\langle S \right\rangle}}{\dfrac{\left\langle j_0^+, nFj_s \right\rangle}{\left\langle nFj_s \right\rangle}} = \frac{\overline{\Psi_s}}{\overline{\Psi_f}} \quad (9)$$

One notices that the "source importance factor" to a good approximation can be described as the ratio of the importance of a source neutron to the importance of a fission neutron. When we take this correction factor into account together with the expression for the detection efficiency $e_n = \dfrac{\left\langle s_D j_s \right\rangle}{\left\langle nF j_s \right\rangle}$, the ratio of reactivities is given by:

$$\frac{\rho_2}{\rho_1} = \frac{\varepsilon_2}{\varepsilon_1}\frac{j_2^*}{j_1^*}\frac{C_1}{C_2} = \frac{\varepsilon_2}{\varepsilon_1}\frac{\overline{\Psi_{f_1}}}{\overline{\Psi_{f_2}}}\frac{C_1}{C_2} = \frac{\langle \sigma_D \varphi_s \rangle_2}{\langle \sigma_D \varphi_s \rangle_1}\frac{\langle \varphi_0^+, \nu F \varphi_s \rangle_1}{\langle \varphi_0^+, \nu F \varphi_s \rangle_2}\frac{C_1}{C_2} = f_{MSM_{1\to 2}}\frac{C_1}{C_2} \quad (10)$$

Based on this expression one can relate one reactivity level to another by measuring the count-rates if the MSM correction factor has been calculated. When this MSM factor equates to 1, the MSM method reduces to the ASM method.

7.1.3 The current-to-flux reactivity indicator

The current-to-flux indicator is closely linked to the source multiplication methods. The major difference between both techniques results from the fact that the current-to-flux indicator prerequisites an accelerator as the external source, because the beam current is measured. Hence, the current-to-flux indicator can be seen as a source multiplication technique dedicated for ADS.

In a subcritical multiplying medium the flux level φ is related to the effective multiplication constant k_{eff} (or reactivity level ρ_{PI}) and the accelerator current I by means of the proportionality constant c as given by [7.4]:

$$\varphi = c'\frac{S}{1-k_{eff}} = c\frac{I}{1-k_{eff}} = c\frac{I(1-\rho_{PI})}{-\rho_{PI}} \qquad (11)$$

From expression (11), we can derive the following expression for the current-to-flux reactivity indicator:

$$\rho_{PI} = -\frac{c\frac{I}{\varphi}}{1-\frac{cI}{\varphi}} \approx -c\frac{I}{\varphi} \qquad (12)$$

By monitoring the ratio of the beam current and the flux level, one can evaluate the deviation of the actual reactivity from the reference reactivity and take appropriate actions, when specified limits are being attained. Since both parameters, flux level and beam current, can be followed on-line, the current-to-flux ratio provides an on-line indicator for the subcriticality level.

7.2 Pulsed Neutrons Source (PNS) methods

The Pulsed Neutron Source methods [7.5] all rely on the existence of a pulsed neutron source as the driving source of the subcritical multiplication. The pulsed character of the source makes it possible to investigate the response of the reactor to a Dirac-shaped impulse which is repeated with a fixed frequency. Due to the high repetition rate, good statistics can be obtained in a minimum measurement time.

Different techniques can be applied:

- the PNS prompt decay fitting method which aims to fit the measured prompt neutron decay curve to one or a sum of exponentials according to an interpretation model; based on this

model the fundamental-mode decay $\alpha = \frac{r-b}{\Lambda}$ constant is identified from which the reactivity is inferred.

- the k_p-method which allows to obtain the prompt neutron multiplication constant by fitting the recorded response to an interpretation model that makes use of a calculated fission time distribution.

- the PNS area method which is based on the ratio of the separated areas in the response function and allows to obtain the reactivity in dollars $\rho_\$ = \rho/\beta$

7.2.1 The prompt decay fitting method

The fitting of the time response in PNS can be based on several models depending on the different physical phenomena taken into account. The complexity of fit-function is of course closely related to the interpretation model. Depending on the choice of the interpretation model, the following fitting functions for the prompt neutron decay were considered:

- a mono-exponential based on the point-kinetics model
- two exponentials based on a two-region (core-reflector) kinetic model
- three exponentials based on a three region – three energy group model

The first, most straightforward model is based on the point-kinetics assumption which supposes the validity of the complete separation of the time dependence of the flux from the spatial, energy and angular dependence. It is thus assumed that the fundamental eigenmode flux remains present during the time variations after a source impulse. This interpretation model results in a mono-exponential decay for the neutron population after the source impulse. The decay constant is the well-known eigenvalue prompt decay constant given by $\alpha = \frac{r-b}{\Lambda}$

Preliminary measurements (see Fig. 7.1) in MUSE already pointed out that the fitting of the recorded to a mono-exponential is not possible, especially for the first microseconds. This is due to the fact that in subcritical systems the point kinetics approximation can no longer be applied as such. Depending on the subcriticality level, the fundamental mode will be more or less pronounced and the total subcritical flux can be approximated by a series of eigenmodes. When a source impulse is applied to a subcritical system, all these spatial eigenmodes will have an individual time response with a characteristic prompt decay constant. Since the prompt decay constants of the higher eigenmodes are always significantly larger than the prompt decay constant of the fundamental eigenmode, a clear separation of the fundamental eigenmode is present in the time response. The generation of the higher eigenmodes in a subcritical system will therefore add a rapid changing contribution in the beginning of the time response, which will die out at later response times (see Figure 1). Hence, the complex problem could be in a first approximation be described by point kinetics for sufficiently large response times (compared to the slowest decay of the higher eigenmodes). In this way, an interpretation model based on a single exponential function could still be applied.

Fig. 7.1: Time response to a Dirac impulse in a subcritical fast core reactor with a moderating reflector

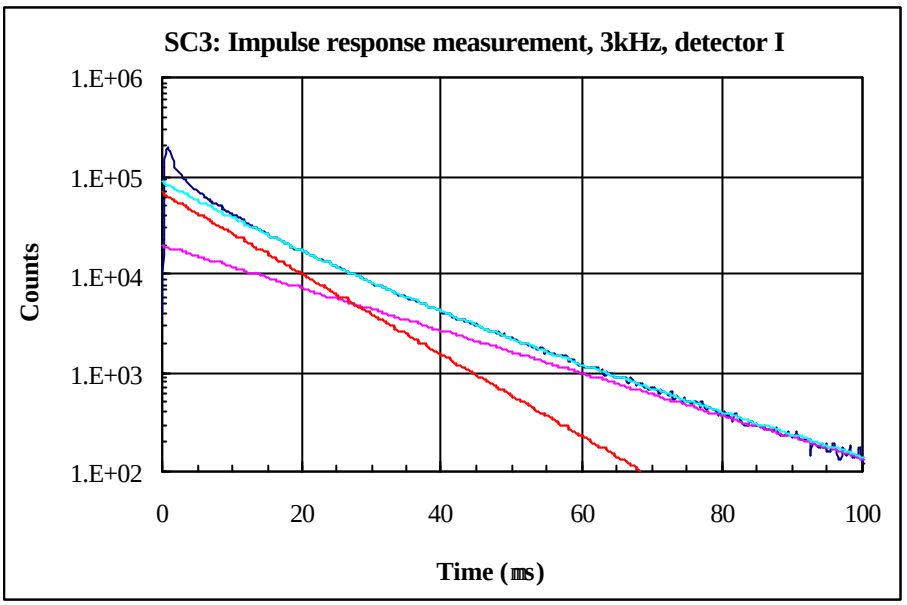

In addition to the higher mode excitation, there can exist a significant deviation from the point kinetic model due to the moderation of neutrons in the reflector. It is known that for fast core systems that are surrounded with a moderating reflector the mean neutron lifetimes in the core and in the reflector can be significantly different. Due to the moderation of the neutrons in the reflector, the mean neutron lifetime in the reflector can be one or even several orders of magnitude larger than the mean neutron lifetime in the core. This second reflector time constant will consequently be present in the time response (see Fig. 7.1) and distort the mono-exponential behaviour in simple point-kinetics.

Since a fraction of the neutrons in the reflector will return to the core, the apparent system mean neutron lifetime (seen from simple point kinetics) will be larger than the core mean neutron lifetime. Such fast systems surrounded with a moderating reflector as in the case of MUSE can therefore not adequately be treated with one region point kinetics and two region kinetics (core and reflector) has to be considered. Such a two region point kinetics model was developed by Avery and Cohn and further on simplified by Spriggs et al [7.6]. In this model, the reactor is represented by two regions: the core and the reflector. Neutrons in the core region can undergo absorption or fission reactions and are allowed to leak to the reflector. Neutrons in the reflector are either absorbed or leak back to the core or are lost from the system. Based on these simple considerations the following set of coupled differential equations is obtained:

$$\begin{aligned}
\frac{dN_c}{dt} &= \left(k_c(1-b)-1\right)\left(\frac{N_c}{t_c}\right) + f_{rc}\left(\frac{N_r}{t_r}\right) + \sum_i l_i C_i + S \\
\frac{dN_r}{dt} &= f_{cr}\left(\frac{N_c}{t_c}\right) - \left(\frac{N_r}{t_r}\right) \\
\frac{dC_i}{dt} &= k_c b_i \left(\frac{N_c}{t_c}\right) - l_i C_i
\end{aligned} \qquad (13)$$

When we apply the Laplace transform to these equations, we obtain for the determination of the time constants the following modified Nordheim-equation:

$$\rho = \omega\frac{\tau_c}{k_{eff}(1-f)} + \omega\frac{f\tau_r}{k_{eff}(1-f)(\tau_r\omega+1)} + \sum_i \frac{\beta_i\omega}{\omega+\lambda_i} \quad (14)$$

In this equation the effective multiplication factor k_{eff} of the complete system is related to the effective multiplication factor k_c of the core (thus without reflector) and the return-fraction $f=f_{cr}.f_{rc}$ according to:

$$k_{eff} = \frac{k_c}{1-f} \quad (15)$$

The values of the three different roots (in the case of one precursor group) are system-dependent. One of the roots is related to the decay of the precursor population. The aim is then to relate one of the two remaining roots to a k_{eff}-related parameter. In this way, the fitting of the recorded prompt neutron decay to the sum of two exponentials will yield two decay constants where one of the two contains information on the neutron multiplication constant of the system (core).

Since there was not always a perfect agreement between the recorded prompt neutron decay data and the fitted sum of two exponentials, an interpretation model based on the sum of three exponentials was proposed. This model is based on two systems (core and reflector-shield – 3 regions) and three energy groups (fast, epithermal and thermal) with strong coupling [5.15]. When physical conditions are imposed, this leads to a description of the flux response with three decay constants, which must be the same for the two systems. For the MUSE-4 subcritical configurations, the decay constant with the highest absolute value is very closely related with the prompt decay constant of the coupled reactor, and as in the case of the two-region kinetic model, in first approximation can be considered as the equivalent of the á eigenvalue in the point kinetic model for a simple reactor. However, a correction is necessary to obtain the effective multiplication factor k_{eff} of the complete system. This correction is formally equal to equation (15), but the definitions of k_c and f are different as shown in reference [5.15]. The lowest decay constant, in absolute value, is related to the low energy neutron lifetime in the second system, which is not multiplicative, so it is independent of the reactivity of the system. This method relies on the simultaneous fitting of all detector responses in the core and the reflector/shield to this sum of three exponentials. In this way, a complex fitting procedure is required to extract a reliable value for the á eigenvalue parameter and the associated reactivity. In addition, to obtain the complete system reactivity, several Monte Carlo calculations are required to calculate the correction factor f.

7.2.2 Kp method

Since the exact description of the reactor cannot be made by simple point kinetics, one can choose to make use of calculation tools to provide more detailed information.

Several approaches based on detailed Monte Carlo simulations are being explored to improve the precision of the PNS evaluation of the reactivity. The aim is take into account the spatial and spectral effects which cannot be modeled by simple point-kinetics.

According to the point kinetic model, when a pulsed neutron source is injected into the core of a subcritical reactor the neutron population decays like a pure exponential, when the delayed neutrons and the inherent source are ignored:

$$N(t) = N_0 e^{-\frac{1-k_p}{l}.t} = N_0 e^{-a.t} \quad (16)$$

with k_p being the prompt multiplication factor and l being the average generation time of a neutron.

When the reactor is close to criticality this decrease, which can be measured through the reaction rate of a detector located into the core, exhibits a constant slope. But for a subcriticality level relevant for an ADS (typically k_{eff}= 0.96), the slope becomes time dependent.

This behaviour can be explained by the fact that when the multiplication factor is low the neutrons from the first generations become relatively more important than the ones of the later generations. That means that an average generation time is not sufficient to describe the neutron creation. Therefore a more sophisticated model [5.16, 7.7, 7.8] was proposed which takes into account the distribution of the neutron generation times following a fission P(ô), ô being the time elapsed since the creation of the neutron that will give birth to the next generation. This distribution can easily be obtained by Monte-Carlo simulation for a stabilized neutron source.

From that definition we deduce that

$$\int P(t)dt = k_p \quad (17)$$

and thus we can normalise P(ô) to k_p = 1. With that normalised distribution P'(ô), we have access to the number of neutrons in the core at any time for any k_p value, summing the contribution of each generation:

$$N(t) = k_p P'(t) + k_p^2 P'(t) * P'(t) + k_p^3 P'(t) * P'(t) * P'(t) + .. \quad (18)$$

where * denotes the convolution operator. The decrease rate á$_{kp}$(t) can then be calculated for different k_p values from the logarithmic derivative:

$$a_{kp}(t) = \frac{1}{N}\frac{dN}{dt} \quad (19)$$

These different functions $a_{kp}(t)$ can then be compared with the one obtained from the experimental N(t) distribution. The one which fits best the experiment determines the k_p value of the reactor.

7.2.3 The Area method

The area method [7.1, 7.5], which is also referred to as the Sjöstrand method, is a well-known technique for the measurement of the subcriticality level. The technique is essentially based on the separation of the prompt area response from the total area response after an impulse.

The here proposed pulsed neutron source analysis is based on the fact that the source can be adequately represented by a series of Dirac pulses, since the pulse width of a neutron pulse is about 1µs. The time response of the reactor to a Dirac input pulse is given by the expression:

$$n(t) = n_0 \left(e^{-\frac{-r+b_{eff}}{\Lambda}t} + \frac{l\, b_{eff}\, \Lambda}{(-r+b_{eff})^2} e^{-\frac{(-r)\,l}{-r+b_{eff}}t} \right) \quad (20)$$

Expression (1) contains two different contributions as illustrated in Fig. 7.2. A first fast component (PN) due to the decay of the prompt neutrons introduced by the GENEPI source and a second slow component (DN) due to the decay of the precursors emitting delayed neutrons.

Fig. 7.2: The time response of the reactor to a Dirac pulse.

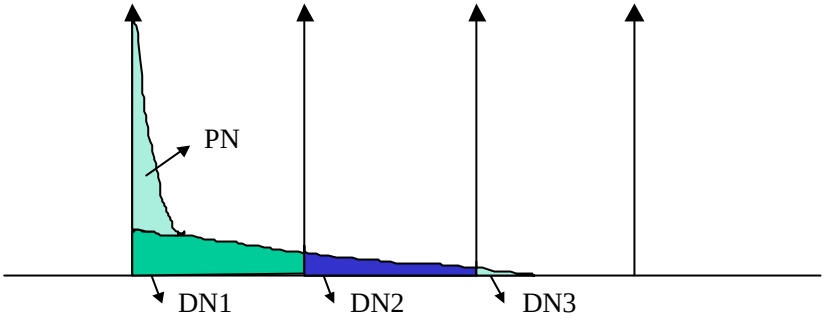

Integration of the prompt neutron component over the time interval [0,+∞[results in the following expression:

$$PN = n_0 \frac{\Lambda}{-r + b_{eff}} = \frac{n_0}{a} \quad (21)$$

By integrating the delayed neutron component over the time interval [0,+∞[the following expression is obtained:

$$DN = DN1 + DN2 + DN3 = n_0 \frac{b_{eff}\Lambda}{(-r + b_{eff})(-r)} \quad (22)$$

The ratio of both surfaces allows one to determine the reactivity expressed in dollars by the relation:

$$\frac{PN}{DN} = \frac{(-r)}{b_{eff}} = r_{\$} \quad (23)$$

When using a pulsed neutron source with a duty cycle frequency larger than the smallest frequency of the response function, the integration of the delayed neutron component cannot simply be performed as illustrated in Fig. 7.2. Fig. 7.3 shows that the emission of new neutron pulses during the decay of the precursors creates an overlap of the different responses and hence the response of a single neutron pulse can no longer be distinguished.

Fig. 7.3: Accumulated response to a series of Dirac pulses

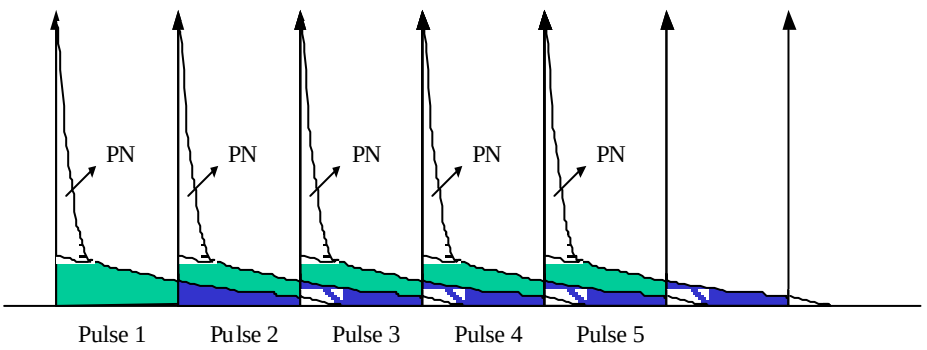

When however examining the obtained response into more detail, one notices that the time window between two Dirac pulses contains a sum of contributions from previous pulses. The sum of the contributions (DN1 of pulse i, DN2 of pulse i-1, DN3 of pulse i2, ..) in such a window, becomes identical to the total delayed neutron contribution DN. This is only true if the number of neutrons created with every Dirac pulse is constant over time. Since this number can be reproduced with an uncertainty of 1%, this condition is satisfied. Hence, by subtracting the prompt neutron contribution PN from the total response observed in the pulse window, the delayed neutron contribution is obtained.

The determination of the ratio of the prompt neutron contribution *PN* and the delayed neutron contribution *DN* allows determining in a straightforward way and without any input from code calculations the reactivity level expressed in dollars.

Monte Carlo and deterministic codes [5.8, 5.15] have shown that spatial effects may be needed to take into account when analyzing the area method reactivity results. The spatial dependence of the reactivity implies that a correction may be needed to obtain the effective multiplication of the system. In references [4.4] and [5.8] two procedures based on simulation codes to correct the reactivity are proposed, one based on Monte Carlo MCNP. The other based on deterministic ERANOS code.

7.2.4 PNS Investigation of SAD kinetics: the reflector/shield effect

Since the main experimental facility in MUSE - the MASURCA core has been driven by the 14 MeV neutron generator GENEPI, the project SAD [3.5] has been a natural completion to MUSE. It uses a typical for real ADS spallation neutron source (driven by the beam of 660 MeV protons). In this framework, calculations were performed for examining the influence of core, reflector and shielding parameters of the SAD versions on the kinetics in PNS methods [4.2].

The calculations based on the LAHET (partcicles with an E> 20 MeV) code and MCNP (neutrons with E < 20 MeV) code showed that the properties of the shield have a strong influence on the lifetime of long lived neutrons. As a result, it affects the shape of neutron pulse decay and thus possibilities and conditions of planned measurements of the system parameters on the basis of the all PNS methods. In consequence particular efforts were aimed at the reduction of the influence of shield presented in [7.9, 7.10]. In the efforts aimed at decoupling (i.e. at reduction of significance of the core surroundings) strong neutron absorbers (Cd, B) have been added to the concrete and reflector and the properties of such system have been evaluated.

Fig. 7.4: Neutron field decay after the δ-shaped neutron pulse in the SAD model

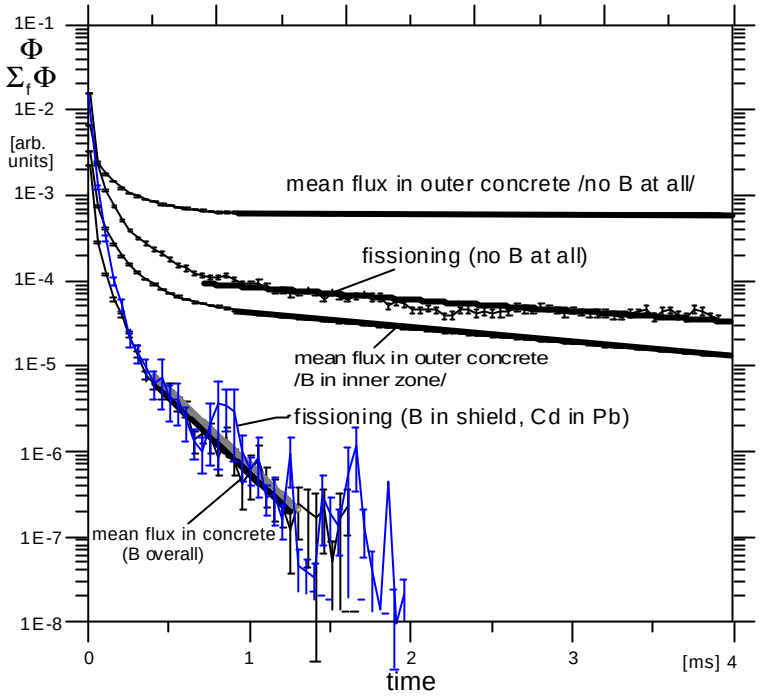

The picture presented in the Fig. 7.4 demonstrates the preponderant influence of shield on the shape of the neutron pulse at large neutron lifetimes in the system. It should be reminded here that the decay of neutron field in the concrete shield is a lengthy process with time constants well exceeding the ones regarding decay of the fission chain. Consequently, this has been an indication that the origin of neutrons in this time is just the shield. Thus, it has been concluded that the bulky shield and Pb reflector play the role of neutron storage, of quasi "a source" even determining the neutron field in such assembly. In addition to this, a validation of numerical tools in such conditions proves more difficult than it could be expected before. Namely, the exact parameters of the shield (e.g. its H and B content) must be known, and the pertinent experimental check /prior to inserting of fissile material/ rather necessary. In such circumstances, the shield influence on long lived neutrons will complicate the analysis of the PNS and hence the determination of the reactivity.

The performed calculations have confirmed that it is the shield that determines the behaviour of long lived neutrons in the system. The decisive proof was supplied by simulation of neutron pulse course without neutron multiplication in the system. It has indicated that the fission chain has no visible influence on the shape of the neutron decay for long lived neutrons. The neutrons entering the Pb reflector and the bulky concrete shield at the pulse beginning and preserved in there survive long enough to play the role of an additional delayed neutrons group. Thus, some experimental subcritical assemblies (i.e. SAD in these conditions) should be treated as two-region systems.

In Tab. 7.1 you can find the respective values of k_{eff} (prompt/total), k_s (prompt/total) and different characteristics tims for different shield materials.

Tab. 7.1: Parameters of the neutron field decay in the SAD model

Option	Prompt		Total		τ_s /decay slope, Fixed Source/ [μs]	τ /fission life span, KCODE/ [μs]	Pulse decay time [ms]	Pulse decay time /no fissions/ [ms]
	k_{eff}	k_s	k_{eff}	k_s				
Regular Shield	0.9445± .0005	0.9507	0.9480± .0005	0.9536	36.5	15.8	0.66	0.70
Regular* Shield	0.94597 ± .00008	^0.9544	0.94931 ± .00009	^0.9570				
No H_2O in* shield	0.9500± .0005	0.9563	0.9537± .0004	0.9588	23.5	5.6	0.47	0.44
No H_2O in*shield +Cd	0.9460± .0006	0.9523	0.9500± .0006	0.9541	4.5	1.5	0.098	0.05

*k_{eff} slightly adjusted with fuel content ^MCNPX calculated spectrum of source neutrons

The content of the Tab. 7.1 shows quite interesting simulation properties of subcritical systems with the MCNP code. One of the most significant is the discrepancy between the fission life span, evaluated directly in the KCODE mode and those ones deduced from the decay slope (Fixed Source). The scale of these inconsistencies has been so great that they cannot be accidental. The explanation of this effect lies in the different neutron distributions in the system in these two calculation modes corresponding to different physical states (KCODE – fundamental mode, Fixed Source – all harmonics plus the fundamental mode). In the KCODE all neutron histories always start from fissions i.e. in the fuel zone, whereas in any moment of the pulse decay many neutrons stay out of there, i.e. where the neutron life-times are much longer.

It seems purposeful to mention here a particularity of the MCNP regarding the values neutron lifetimes provided in its Fixed Source mode standard output. In that case, in contrast to the KCODE mode, neutron histories are not terminated by fissions (hold as non-terminating inelastic scattering events) and the first emerging neutron is further transported. Since neutrons are not killed by fission, the given lifetime actually does not concern an individual neutron but the chain of all subsequent generations.

The difference between the k_{eff} and k_s (Tab. 7.1) should not be a surprise, since the space-energy distributions of the source neutrons (generation 0) and in the first generation are well different from the distribution in the fundamental mode. The observed relation $k_s > k_{eff}$ is explainable in view of the high importance of the source neutrons characterised by harder spectrum. Besides, it is reflected also by the effective delayed neutron fraction in the system: $\hat{a}_{eff}$ and $\hat{a}_{s\ eff}$ approximated as $(k_{eff} - k_{effp})/k_{eff}$ and $(k_{st} - k_{sp})/ k_{st}$ respectively (Tab. 7.2.).

Tab. 7.2: *Effective â in the SAD model*

$\hat{a}_{eff}$ [pcm]	$\hat{a}_{s\ eff}$ [pcm]
393±30	252±70
^352±20	^292±40

^MCNPX spectrum of source neutrons

A lesser difference between the total and prompt equivalent neutron multiplication factor k_s as compared with the analogue difference between the k_{eff} values results nearly solely from higher contribution of prompt component in the fissions caused by the source neutrons of harder spectrum.

In this way it has been proved how the delayed component in the resultant source-driven field is lessened as compared with the one in fundamental mode. In view of all these remarks it seems also that a validation of numerical tools (by confrontation with the experiment) in such cases will be more difficult than it was expected before.

7.3 Source Jerk techniques

7.3.1 The Standard Source Jerk technique

The standard Source Jerk technique [7.1] is based on the fast removal of the source out of an initial stationary subcritical medium. Before the removal of the source the neutron- and precursor populations are given by:

$$n_0 = \frac{\Lambda S}{(-\rho)} \qquad \text{and} \qquad c_0 = \frac{\beta}{\Lambda \ell} n_0 \qquad (24)$$

When the source is ejected almost instantly, we can easily obtain the remaining neutron population if the precursor population has not changed meanwhile. Hence with $S=0$ and without time variation of the precursor population, the neutron population n_1 immediately after the removal after the source is given by:

$$n_1 = -\frac{\Lambda \ell}{\rho - \beta} c_0 = -\frac{\Lambda \ell}{\rho - \beta} \frac{\beta}{\Lambda \ell} n_0 \qquad (25)$$

From these two equations, one can now determine the reactivity in dollars by:

$$\rho_{\$} = \frac{n_0 - n_1}{n_1} \qquad (26)$$

In the MUSE experiments a Cf-252 source has been used for the Source Jerk technique by means of the SIRRANEAU measurement device.

7.3.2 Source modulation method

The Source Modulation technique [5.16, 7.8] is quite similar to the Source Jerk Method. For a given sub-critical level, the external neutron source rate is suddenly changed from a high count-rate level P_0 to a low count-rate level P_1. This can be obtained here by varying suddenly the frequency of the pulsed source resulting in a decrease of the average count-rate.

For the high count-rate level, the total count-rate averaged over the pulse period contains a prompt and a delayed contribution which are given by:

- Prompt averaged count-rate: $P_{0,p} = S \dfrac{\Lambda}{(-\rho + \beta) T_{high}}$ (27)

- Delayed averaged count-rate: $P_{0,d} = S\frac{\beta\Lambda}{(-\rho+\beta)(-\rho)T_{high}}$ (28)

- Total averaged count-rate: $P_0 = P_{0,p} + P_{0,d} = S\frac{\Lambda}{(-\rho)T_{high}}$ (29)

For the low count-rate level similar expressions are found:

- Prompt averaged count-rate: $P_{1,p} = S\frac{\Lambda}{(-\rho+\beta)T_{low}}$ (30)

- Delayed averaged count-rate: $P_{1,d} = S\frac{\beta\Lambda}{(-\rho+\beta)(-\rho)T_{low}}$ (31)

- Total averaged count-rate: $P_1 = P_{1,p} + P_{1,d} = S\frac{\Lambda}{(-\rho)T_{low}}$ (32)

Fig. 7.5: Schematic representation after the measured count-rate levels in the source modulation technique

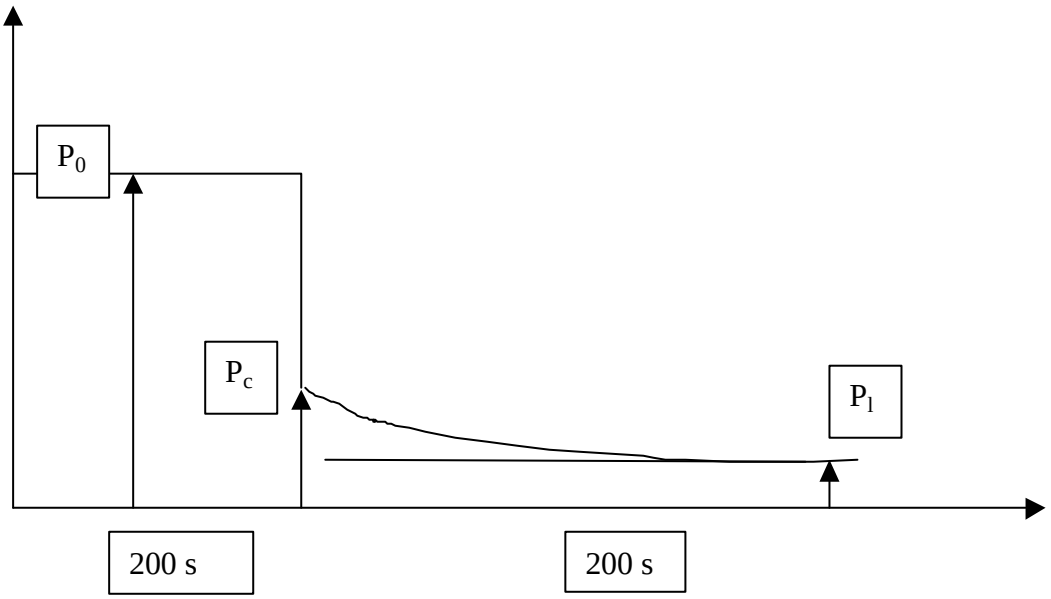

The average count-rate immediately after the change in frequency is characterized by:

- the presence of the delayed average count-rate during the high count-rate level
- the presence of the prompt average count-rate during the low count-rate level
- the absence of the delayed average count-rate during the low count-rate level

Hence, the average count-rate immediately after the change in frequency is given by:

$$P_p = P_{0,d} + P_{1,p} = S\frac{\beta\Lambda}{(-\rho+\beta)(-\rho)T_{low}} + S\frac{\Lambda}{(-\rho+\beta)T_{high}} \quad (33)$$

Based on these measured count-rates we can define the following quantity:

$$\frac{P_0 - P_c}{P_c - P_1} = \frac{P_{0,p} - P_{1,p}}{P_{0,d} - P_{1,d}} = \frac{(-\rho)}{\beta} \quad (34)$$

The measurement of the count-rate levels P_0, P_c and P_1 hence allows the determination of the reactivity expressed in dollars.

7.4 Noise methods

Noise methods are all based on the study of the neutron fluctuations in the reactor. Several analysis methods and variants can be applied:

- the Rossi-alpha method
- the Feynman-alpha method
- the Cross Power Spectral Density (CPSD).

These experiments can be performed with or without an external neutron source. First, the application of these noise methods with a stationary driving source is discussed, since these are well known techniques. When using a time-dependent driving source, new expressions were derived in the framework of this project.

7.4.1 Stationary source as the driving source for the noise methods

7.4.1.1 The Rossi-alpha method

The Rossi-á technique [7.11, 7.12] is based on the detection of neutrons which are correlated in time. Since with every fission on the average 2 to 3 neutrons are emitted at the same time, the neutron multiplication chains initiated by these neutrons are correlated in time. Neutrons from two separate fissions, belonging to the same multiplication chain will also be correlated in time, since they can be traced back to the same time origin, the fission event. The detection of these correlated neutrons will provide information about the die-away of the neutron multiplication chain as well as about the amplitude of the fission process.

The detection of neutron pairs will also contain uncorrelated neutron events, since most of the neutrons present in the reactor will not come from the same initial fission event. Therefore, the Rossi-alpha distribution will be the sum of an uncorrelated part and a correlated part. When point kinetics without delayed neutrons is used for the description of the neutron multiplication process, the Rossi-alpha distribution is represented by the following expression:

$$p_{Rossi}(t)\,dt = \mathrm{A}.dt + \mathrm{R}.\mathrm{e}^{-\alpha t}\,\alpha\,dt \quad (35)$$

with

á: the fundamental-mode decay constant: $\alpha = \frac{\beta_{eff} - \rho}{\Lambda} = \left(1 + \rho_{\$}\right) / \left(\frac{\Lambda}{\beta_{eff}}\right)$

A: the amplitude of the uncorrelated contribution

R: the amplitude of the correlated contribution

The fitting of the measured distribution to the above expression will yield the fundamental mode decay constant from which the reactivity can directly be derived.

In deep subcritical systems, the applicability of point-kinetics cannot be taken for granted and hence the validity of expression has to be investigated.

7.4.1.2 Feynman-alpha

The Feynman-alpha method [7.11, 7.12] is closely related to the Rossi-alpha technique. In this technique the number of counts in a certain time interval ÄT is measured. Hence the mean and standard deviation of the distribution of counts in this time interval is calculated.

The number of counts c in a time gate ÄT deviates from a Poisson distribution because of the fluctuations of the neutron population driven by the fission chain process. For a given time gate ÄT, the deviation is measured by the y-value defined as:

$$y = \frac{\text{variance}}{\text{mean}} - 1 = \frac{\langle c^2 \rangle - \langle c \rangle^2}{\langle c \rangle} - 1 \quad (36)$$

That expression can be generalized to the case of two different detectors k and l with detection efficiencies ϵ_k and ϵ_l, respectively:

$$y_{k,l}(\Delta T) = \frac{\langle c_k c_l \rangle - \langle c_k \rangle \langle c_l \rangle}{\sqrt{\langle c_k \rangle \langle c_l \rangle}} - \delta_{k,l} \quad (37)$$

where $\delta_{k,l}$ is the Kronecker symbol. For $k \neq l$, the numerator of the y-value is a covariance term.

The y-value is related to the Rossi-alpha distribution through the average number of pairs counted in a time gate ÄT :

$$\frac{c_k (c_l - \delta_{k,l})}{2} = \int_0^{\Delta T} dt_c \int_0^{t_c} dt_g \; p_{rossi}(t_c - t_g) \quad (38)$$

One thus obtains the following expression for the y-function assuming a point kinetic model and considering prompt neutrons only:

$$y_{k,l}(\Delta \mathrm{T}) = \frac{\sqrt{\varepsilon_k \varepsilon_l}\, D}{\alpha^2 \Lambda^2} \left(1 - \frac{1 - e^{-\alpha \Delta \mathrm{T}}}{\alpha \Delta \mathrm{T}} \right) \quad (39)$$

where D is the so-called Diven factor, defined as

$$D = \frac{\langle \nu(\nu - 1) \rangle}{\langle \nu \rangle^2} \quad (40)$$

By considering different time intervals ÄT, a Feynman-alpha distribution is obtained which can then be fitted to the expression to yield the fundamental mode decay constant.

Again for deep subcritical systems point kinetics might not be valid and a modified form for the Feynman-alpha expression needs to be introduced.

7.4.1.3 Power Spectral Density

The measurement of a Power Spectral Density [7.11, 7.12] essentially comes down to taking the Fourier transform of the time correlation between two signals. When the two signals are the same (1 detector), the Fourier transform of the autocorrelation will yield the following auto-power spectral density function:

$$APSD_{D_iD_i}(w) = \frac{e_i^2}{2a\left(\bar{u}\Lambda\right)^2}\left[\frac{F_I\bar{u}_I}{a\Lambda}\overline{u(u-1)} + F_I\overline{u_I(u_I-1)}\right]\frac{1}{\left(a^2+w^2\right)} + e_i^2\left(\frac{F_I\bar{u}_I}{a\Lambda}\right)^2 \quad (41)$$

When however two different detectors are used, the white-noise component will vanish and one obtains for the Fourier transform of the cross-correlation the following cross-power spectral density function:

$$CPSD_{D_1D_2}(w) = \frac{e_1e_2}{2a\left(\bar{u}\Lambda\right)^2}\left[\frac{F_I\bar{u}_I}{a\Lambda}\overline{u(u-1)} + F_I\overline{u_I(u_I-1)}\right]\frac{1}{\left(a^2+w^2\right)} \quad (42)$$

From the break frequency in the response of both spectral densities, the α-value of the system can be obtained. These expressions also rely on the point-kinetics assumption and neglect the low-frequency part due to delayed neutrons.

7.4.2 Pulsed neutron source as the driving source for the subcritical noise methods

Since in deep subcritical systems the correlated signal is strongly reduced due to the shortening of the neutron multiplication chain, one would like to increase the signal-to-noise ratio by increasing the correlated signal. One efficient way is to inject neutron pulses into the reactor and hence increase the correlated signal.

The expressions commonly used in neutron noise techniques needed however to be modified to include a time-dependent neutron source instead of a stationary one. In the following paragraphs the expressions for the different noise methods will be described and the deviations with the stationary case pointed out.

7.4.2.1 The Rossi-alpha method

When the accelerator is switched on, the correlation between neutrons will be enhanced. The Rossi-alpha expression for a periodically pulsed source basically comes down to a convolution of the reactor response with a train of Dirac pulses in the time domain (Fig. 7.6). When the pulsation period is not too small in comparison with the alpha decay constant, there is no overlap between the consecutive responses to a source Dirac pulse. Since in practice this decay constant is rather small in fast reactor cores, it is easy to find a pulsation frequency which satisfies this condition and is still high enough to obtain sufficient statistics in a reasonable measurement time.

Fig. 7.6: Rossi-alpha distribution for a pulsed neutron source

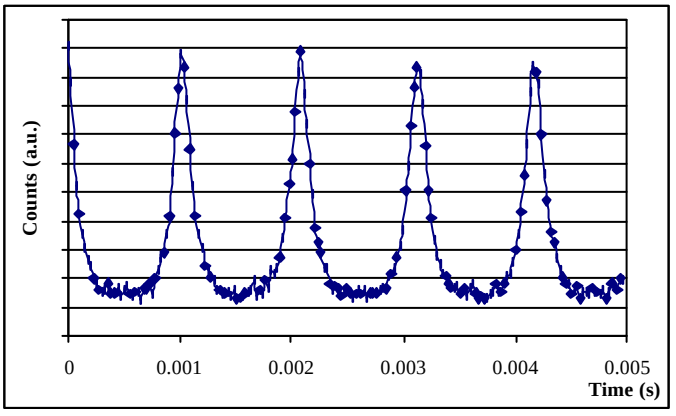

When such a pulsation frequency is chosen, the response to the first pulse can be isolated and can be described by [7.13]:

$$p(t) = A + Be^{-\alpha . t} \quad (43)$$

So, we obtain a similar expression as in the case of a stationary source with the same fundamental mode decay constant (when point kinetics is valid). The main difference of this expression compared to the one with a stationary source is the magnitude of the amplitudes. Here, the amplitude of the correlated signal is strongly increased. In this way, an increased signal-to-noise ratio is obtained for the determination of the correlated part and hence the fundamental mode decay constant.

Another particular feature of this measurement technique is related to the fact that the reactivity expressed in dollars can directly be determined from the uncorrelated amplitude signal A, the total average count-rate C_T and the average count-rate C_{IN} of the intrinsic source by means of the following expression:

$$A_V = \frac{A + C_{IN}^2 - 2C_{IN}C_T}{\left(C_T - C_{IN}\right)^2} = \frac{1}{\rho_\$ + 1}\left(\frac{2\rho_\$ + 1}{\rho_\$ + 1}\right) \quad (44)$$

This additional information is strongly related to the reactivity in dollars obtained with the PNS Area method.

7.4.2.2 Feynman-alpha

The theory of the Feynman-α method was originally elaborated for continuous, single emission sources, i.e. for traditional radioactive sources that emit one neutron at a time, and whose intensity is constant. Nevertheless, when the operating mode is time dependent, the corresponding Feynman-alpha formula will differ from the continuous one.

Actually, one can perform such pulsed measurements in two different ways. In the first one, we will consider each measurement gate time is synchronized with the start of a pulse. This alternative will be called deterministic pulsing. Another alternative is when the gate start time is not synchronized with the pulsing. This variant will be called stochastic pulsing. For both types of measurements analytical expressions were derived [7.14, 7.15] and we will only recall here the main results.

In stochastic triggering, the start of each time interval is chosen randomly with respect to the source pulses. Because of the temporal correlation between source neutrons, the variance-to-mean ratio as a function of the width of the time interval shows ripples that can be described by periodic functions as follows:

$$Y(t) = \frac{\sigma^2(t)}{m(t)} - 1 = \frac{\varepsilon l_f^2 \overline{(n(n-1))}}{a^2}\left(1 - \frac{1 - e^{-at}}{at}\right) + \frac{8\varepsilon l_f S_0 T_p a}{tWp^2}\sum_{n=0}^{\infty}\frac{1}{n^2 w_n^2 (a^2 + w_n^2)}\sin^2\left(\frac{w_n W}{2}\right)\sin^2\left(\frac{w_n t}{2}\right) \quad (45)$$

where σ^2 is the variance, m the mean value, T_p the period of the pulsed source, W is the pulse width, and the parameter w_n is defined as: $w_n = \frac{2n\pi}{T_p}$

Here the first term on the right hand side corresponds to the Feynman -curve with a continuous (constant) source, whereas the last term constitutes an oscillating deviation from it. This deviation is non-negative, and thus the curve of the continuous source constitutes a lower envelope of the stochastically pulsed system.

It is also worth mentioning that the oscillating part contains both the source S_0 and the prompt neutron time constant α. In the conventional Feynman alpha method both the mean and the variance are linear in the source term, and hence it disappears from the relative variance. In the stochastic pulsed method the variance has a term which is quadratic in the source, which hence does not disappear from the Feynman *Y*-function. The presence of S_0 and α in the expression means that the relative amplitude of the oscillating term (compared to the traditional smooth term) depends on the source strength and the subcritical reactivity. A strong source in a deep subcritical core can lead to very large oscillations in the Feynman *Y* curve. An illustration of such a Feynman Y-curve with stochastic pulsing is shown below (Fig. 7.7).

Fig. 7.7**:** Feynman Y-function for stochastic pulsing.

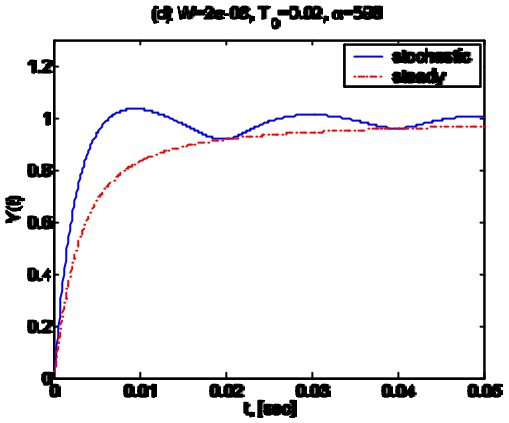

A second type of analysis is a Feynman-α technique using deterministic pulsing. In this case, the gates used in the analysis are synchronised with the accelerator pulses. The solution can be given as follows.

The following notations and parameters will be used:

T - measurement time length

W- pulse width

T_0 - the pulse repetition period

α - the prompt neutron time constant, $\alpha = \dfrac{\beta - \rho}{\Lambda}$

Z(T) = the expected value of detector counts during measurement time T;

$Y(T) = \dfrac{\sigma_Z^2(T)}{Z(T)} - 1 = \dfrac{m_Z(T)}{Z(T)}$ is the Feynman Y-function, where $\sigma_Z^2(T)$ is the variance of the

counts, and $m_Z(T) = \sigma_Z^2(T) - Z(T)$ is the modified variance.

The quantity $\omega_n = \frac{2\pi n}{T_0}$ is the same as before, i.e. the *n*-th harmonic of the pulse repetition frequency. $\lambda_d = \varepsilon\lambda_f$ and λ_f are the detection and fission probabilities per neutron per unit time.

By introducing the notations

$$a_n = \frac{\alpha(1-\cos\omega_n W) + \omega_n \sin\omega_n W}{n(\omega_n^2 + \alpha^2)}; \qquad b_n = \frac{\alpha\sin\omega_n W - \omega_n(1-\cos\omega_n W)}{n(\omega_n^2 + \alpha^2)} \tag{46}$$

then the expected number of detector counts is given as

$$Z(T) = \varepsilon\lambda_f S_0\left(\frac{WT}{T_0\alpha} + \frac{1}{\pi}\sum_n \frac{1}{\omega_n}\left\{a_n(1-\cos\omega_n T) + b_n \sin\omega_n T\right\}\right) \tag{47}$$

For the modified variance we introduce the following quantities:

$$p_n(\alpha,T) = \frac{\alpha\sin\omega_n T + \omega_n(e^{-\alpha T} - \cos\omega_n T)}{(\omega_n^2 + \alpha^2)} \tag{48}$$

$$A_n(T) = p_n(0,T) - 2p_n(\alpha,T) + p_n(2\alpha,T)$$

$$q_n(\alpha,T) = \frac{\alpha(\cos\omega_n T - e^{-\alpha T}) + \omega_n \sin\omega_n T}{(\omega_n^2 + \alpha^2)}$$

$$B_n(T) = q_n(0,T) - 2q_n(\alpha,T) + q_n(2\alpha,T)$$

Then the modified variance becomes

$$\begin{aligned} m_Z(T) = \frac{\lambda_d^2\lambda_f}{\alpha^2}\langle\nu(\nu-1)\rangle S_0\Big[\frac{WT}{T_0\alpha}\Big(1-\frac{1-e^{-\alpha T}}{\alpha T}\Big) + \frac{1}{\pi}\sum_n\frac{1}{\omega_n}\left\{a_n A_n(T) + b_n B_n(T)\right\} + \\ + (1-e^{-\alpha T})^2\frac{1}{\pi}\sum_n\frac{-a_n\omega_n + 2b_n\alpha}{\omega_n^2 + (2\alpha)^2}\Big] \end{aligned} \tag{49}$$

From these equations one then obtains the Y(T) function as

$$Y(T) = \frac{m_Z(T)}{Z(T)} \tag{50}$$

This second type of analysis has the advantage that the oscillating deviations from the smooth Feynman-α curve are much smaller, but the extraction of the correct alpha value is still quite difficult. A big disadvantage is that, because of the synchronization, much less data is actually used and that much longer measuring times are needed to arrive at well-converged results.

The effect of the pulse repetition frequency is illustrated in Fig. 7.8. As expected, for a high pulse repetition frequency the deviation from the continuous source is small. For low frequencites, or large pulse periods compared to $1/\alpha$, the deviations from the case with the continuous source become large. This is actually the case in the MUSE experiments, partly because in a fast core as MASURCA, the $1/\alpha$ value is small even for small subcriticalities.

Fig. 7.8: Feynman Y-curves for a low (left) and high (right) pulse repetition frequency, for two different pulse widths with deterministic pulsing

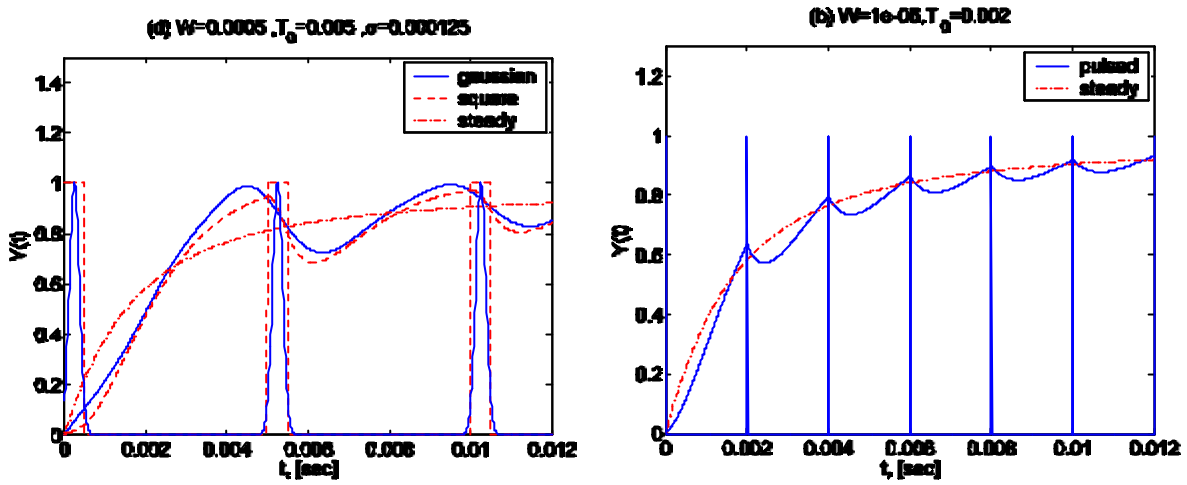

7.4.3 Monte Carlo investigations of the Feynman-á method

The main general question is what conditions should be fulfilled so that the simple formula (39) holds. There are several factors affecting the result of real experiments. The instruments are in principle nonlinear e.g. as a result of the dead time effect. In the source-driven neutron field the harmonics accompany the fundamental mode, i.e. the k proves generation dependent or k$_i$ k_{eff}, the Diven factor for the source (spallation) neutrons is different than in fission. Therefore, seeing difficulties in analytical expressing of the influence of such effects they have been numerically tested.

For the above purpose a simple FORTRAN code simulating the multiplication chain, confined to pertinent time-dependent phenomena has been written. In all the calculations discussed here k_{eff} = 0.95. The independence of the Feynman-á method of the reflector/shield influence has been demonstrated (Fig. 7.9). It has been assumed here, as usual, that the neutron source driving the subcritical system is a pulsed one with the period long as compared with decay of the prompt neutron chain but short, as compared with that of delayed neutrons.

Fig. 7.9: The effect of a reflected system on the Y-parameter

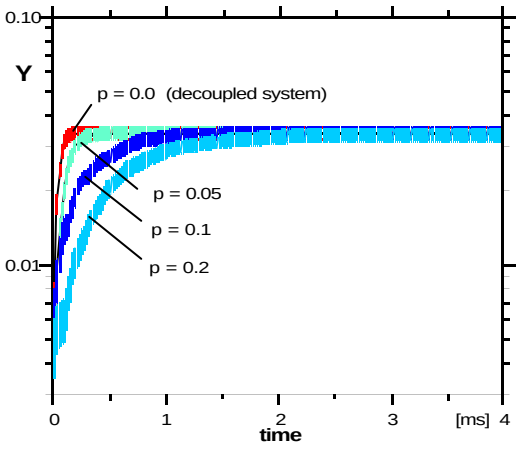

The "excursions" of neutrons to the zone surrounding the core, with probabilities p = 0.05, 0.1, 0.2 have been simulated with randomised neutron lifetime being there 100 times longer than in the core. The evident identity of the values of Y for sufficiently long times of collecting events confirm the insensitivity of the Feynman-á technique to the influence of the second region.

The next investigated effect has been the influence on the Feynman Y of harmonics in the neutron pulse making the effective multiplication of neutrons not to correspond to the sole k_{eff} but to another value named k-source i.e. k_s. These changes stem in general from two factors generation dependent: the number of neutrons per fission and the probability of fissioning, which both depend e.g. on the neutron energy. The formulae used for simulation of the dependency of multiplication factor on the generation number are:

- Type I: $k_i = 0.95(1+\exp(-2i))$
- Type II: $k_i = 0.95(1+1.5(1-\exp(-2i)))/2.5$

The results of calculations obtained by distorting the multiplication factor in initial neutron generations according to the Type I formula for detector with efficiency å are shown in the Tab. 7.3.

Tab. 7.3: Effect of the discrepancy k_s k_{eff} on the detector response for $(1-k_s) \approx 0.5(1-k_{eff})$

	å		
	10^{-2}	10^{-4}	10^{-5}
$Y(k_s \; k_{eff})/Y(k_s=k_{eff})$	1.23±0.03	1.13± 0.06	1.21 ±0.1

It can be seen that the significance of the k-source though not particularly strong, cannot be neglected: for the case when the number of neutrons i.e. power of the system is doubled the Y is changed by about 20% on the average.

The next tested effect was the fluctuation of the number $\acute{i}_{sp}$ of spallation neutrons [7.16]. The neutron multiplicity distribution modelled in simulations is shown in the Fig. 7.10 together with the experimental distributions. The spectrum of $\acute{i}_{sp}$ was obtained for fixed number of spallation neutrons $\acute{i}_{sp0} = \bar{\nu}_{sp}$ with the use of standard random generator of uniform distribution.

Fig. 7.10: The neutron multiplicity distribution for the spallation process

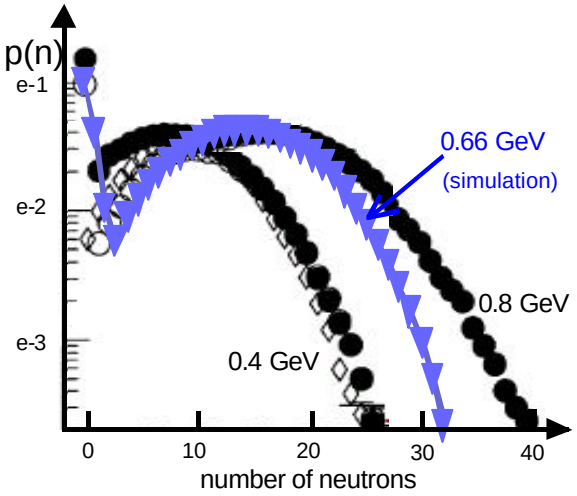

The spallation Diven factor, for such neutron multiplicity, amounts to 1.32. Its role has been checked by comparison of the respective Y value with that one obtained for a fixed number $\acute{\imath}_{sp} = \acute{\imath}_{sp0} = 12$ of spallation neutrons. i.e. the ratios of $Y(\acute{\imath}_{sp}$ rand$)/Y(\acute{\imath}_{sp0}$ const) have been calculated. The obtained results confirm a certain influence of source neutron multiplicity. Generally, the ratio $Y(\acute{\imath}_{sp})/ Y(\acute{\imath}_{spc})$ is > 1. However, since the observed increase in this ratio with decrease in the detection efficiency has not been satisfactorily proven (due to insufficient calculation statistics) further studies in this respect are required.

One of the most important distortions of measurements seems to be caused by the detector dead time. This effect has been simulated by registration of only one event of any if closer to each other than say, 100 ns. The calculations showed that solely in cases of few neutrons per burst and low detector efficiencies the influence of the detector dead time has proven negligible. To the contrary, for strong neutron pulses, even at relatively low detection efficiencies the dead time effect can extremely bias the results. Meanwhile, in exception of rare cases of extremely weak sources driving the system, usually the number of initial neutrons in a pulse is very high and the measurement results are distorted in dependence on the number of source neutrons per burst.

Then one may ask whether common dead-time correction techniques can be a remedy in this case. It seems, however, that a mere correction of the expected number of events (the first moment) is useless without knowledge of its variance. For adequate correction one would have to know the true number of events lost due to temporary detector overload in each neutron burst that seems to be a problem.

7.4.3.1 Power Spectral Density

To simplify the mathematical derivation of the CPSD for a pulsed neutron source, we assume that the time dependence of the source can be described by a train of Dirac delta pulses, as has been done for the other techniques like the Rossi-α and Feynman-α. Assuming that the number of pulses per time window in the analysis is N, then after some manipulation the CPSD is given by [4.11]:

$$CPSD_{D_1D_2}(w) = \frac{e_1 e_2}{2a(\bar{n}\Lambda)^2}\left[\frac{F_I\bar{n}_I + F_S\sum_{n=0}^{N}\exp(-iwnT_p)}{a\Lambda}\overline{n(n-1)} + F_I\overline{n_I(n_I-1)}\right]\frac{1}{(a^2+w^2)} \quad (51)$$

From this expression we can conclude that the $CPSD_{23}$ depends on the source frequency ($\Theta = 2p/T_p$) and the reactor break frequency α. Both the inherent source and the pulsed source have been included in the derivation of this equation. It is seen that the CPSD shows peaks corresponding to the source frequency and its harmonics (Fig. 7.11).

Fig. 7.11: Cross power spectral density for a pulsed neutron source

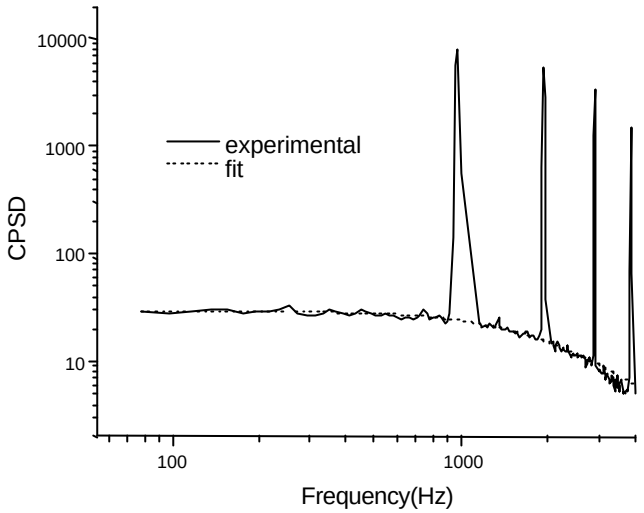

To avoid the peaks in the fitting, one can use a weight function proportional to the inverse of the variance function at each point, except in the peaks, where the weight function was taken zero (infinite variance). The second method we propose consists of removing the peaks before fitting. In this way, again a first order low-pass filter transfer function is obtained as was the case for a stationary source and the break frequency can be determined.

8 Experimental results from the MUSE-4 programme

In this paragraph, the main results of the different partners using different kind of techniques as laid out in the previous paragraphs are gathered. Only the four main configurations SC0, SC2 (1006 cells), SC2 (1004 cells) and SC3 with the pilot rod in bottom position are considered to allow a direct comparison between the different results. Tab. 8.1 gives an overview of the different reactivity's (in dollars) with their respected uncertainties (1ó between brackets) obtained.

Tab. 8.1: Reactivity levels with uncertainties for different configurations obtained with different measurement techniques

	Rod drop + MSA	**Rod drop + MSM**	**PNS fitting**			**k_p method**	**PNS Area** *		**Source Jerk**	**Source Mod.**	**Rossi-a (Area)**
			1 exp	*2 exp*	*3 exp*		*Direct value*	*Corrected value*			
SC0	-1.9 (0.09)	-1,86 (0.1)	-1,93 (0.03)	-1.921 (0.006)		-2,2 (0.3)	-2,00 (0.02)	-1.96 (0.09)	-1,92 (0.1)	-1,957 (0.004)	-2.04 (0.14)
SC2 1006 cells	-9.1 (0.5)	-8,7 (0.5)			-8.7 (0.7)		-8,9 (0.3)	-8.5 (0.4)			-8.8 (0.2)
SC2 1004 cells	-9.7 (0.5)	-9,1 (0.6)				-9,7 (0.3)				-9,23 (0.12)	
SC3	-14.1 (0.8)	-13,6 (0.8)		-15.6 (0.6)	-11,7 (0.9)	-14,1 (0.3)	-13,7 (0.5)	-12,3 (1.0)	-14.6 (0.9)		-13,4 (0.5)

* The direct value is obtained by applying equation (23). The corrected value was obtained by applying a correction factor based on calculations [5.15] to take into account spatial effects

The results from Tab. 8.1 are also depicted separately for every configuration in Fig. 8.1, 8.2, 8.3, 8.4 and 8.5 respectively for the configurations SC0, SC2 (1006 cells), SC2 (1004 cells) and SC3.

Fig. 8.1: Reactivity ($) of the SC0 configuration obtained with different measurement techniques

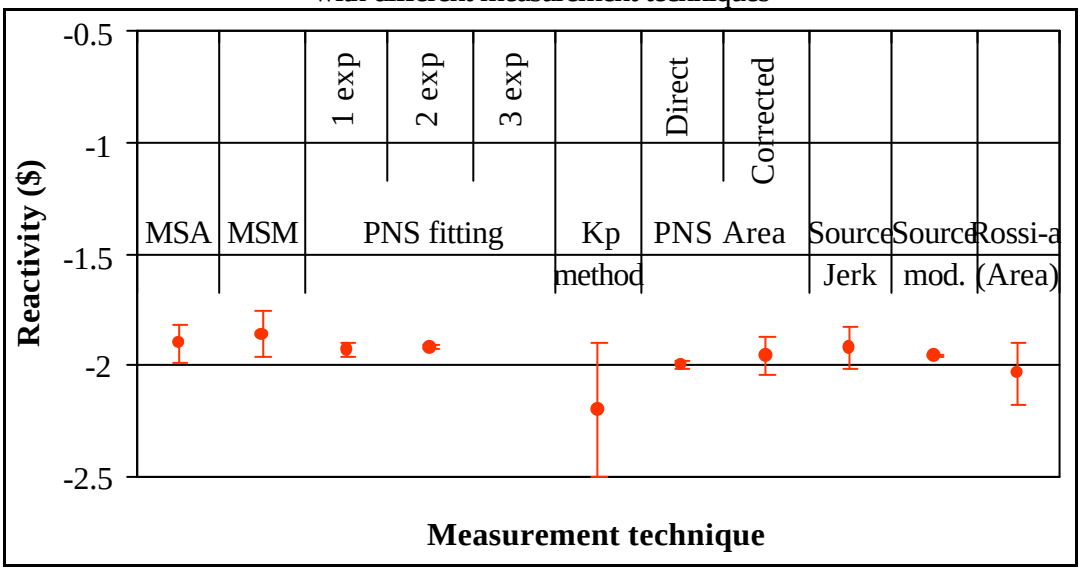

Fig. 8.2: Reactivity ($) of the SC2 configuration (1006 cells)
obtained with different measurement techniques

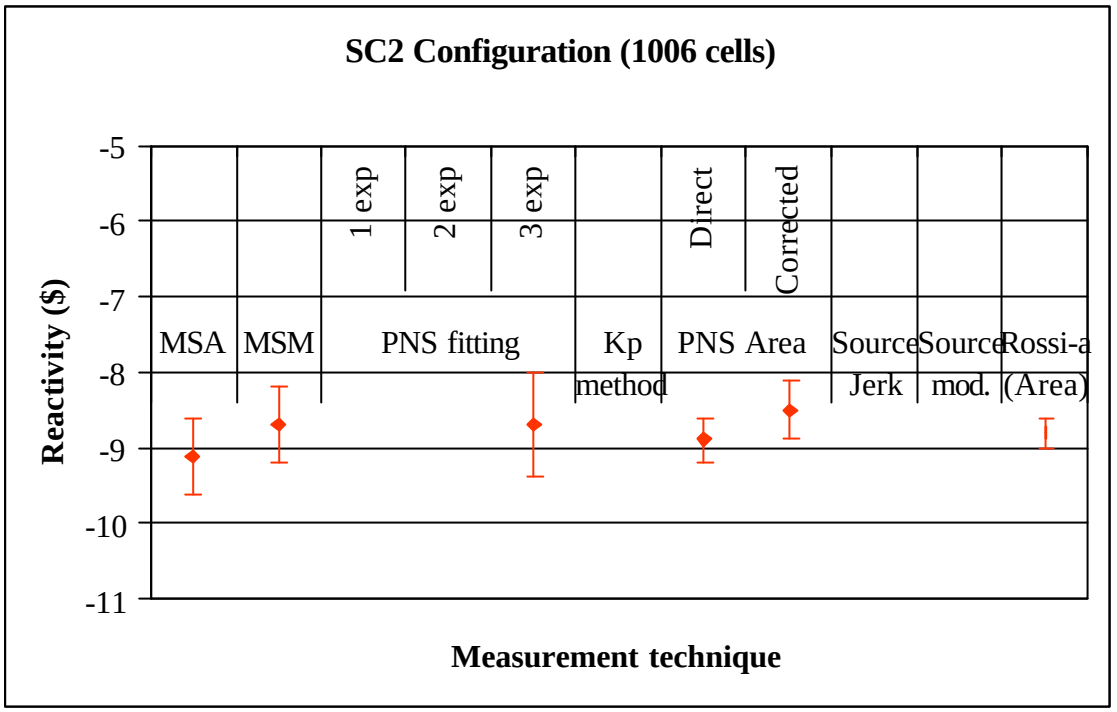

Fig. 8.3: Reactivity ($) of the SC2 configuration (1004 cells)
obtained with different measurement techniques

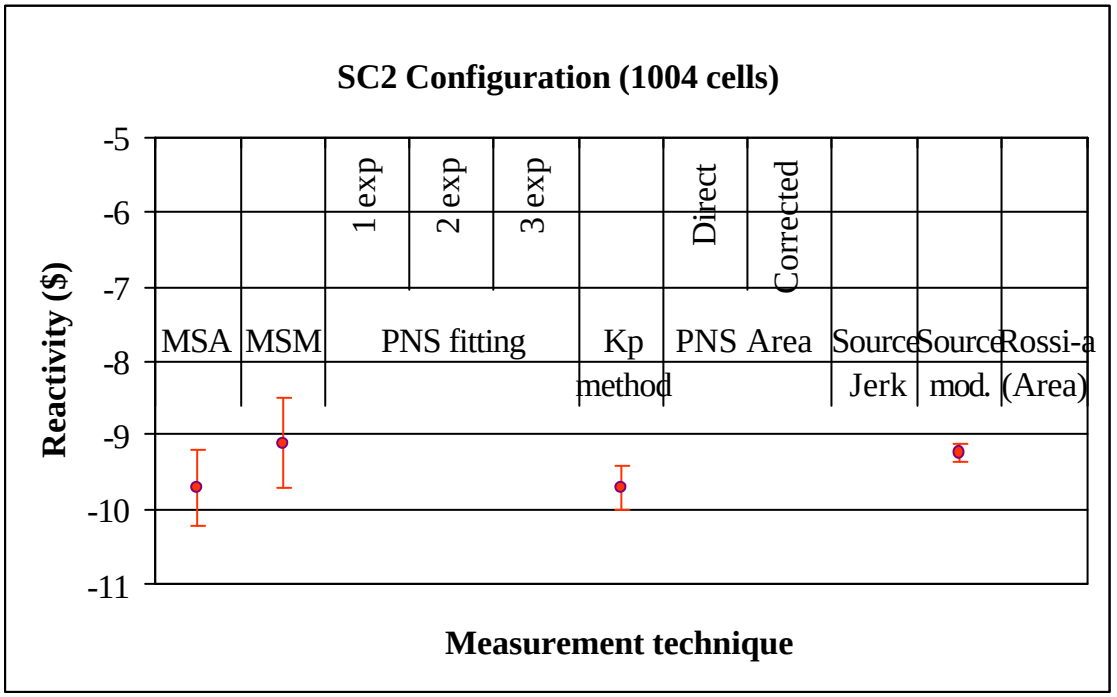

Fig. 8.5: Reactivity ($) of the SC3 configuration obtained with different measurement techniques

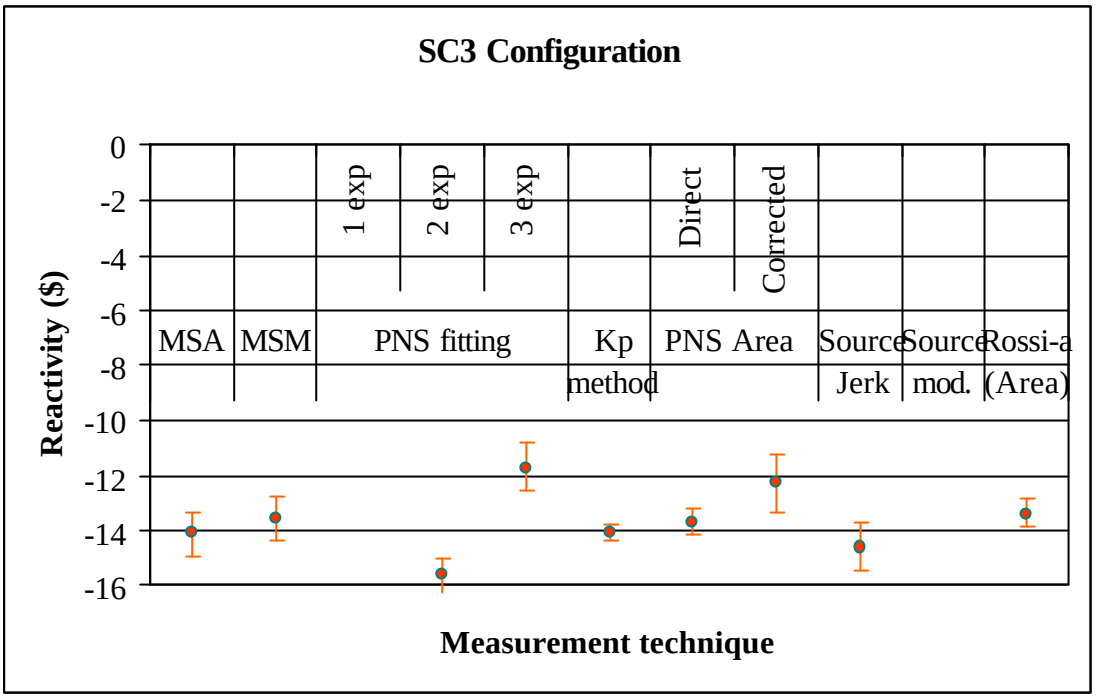

From the table and the figures, it can be concluded that the reactivity level can be obtained with different kind of techniques with an accuracy in the order of 10%. The correction induced by the MSM-factor with regard to the simple MSA method remains very small, in the order of -5% in the core and less of –20% in the shielding (table 8.1).

Table 8.1 : MSM factors (reference configuration= 1125 fuel cell configuration)

		Perturbed configuration				
Detector positions	Zone	SC0 1108 cells	SC2 1006 cells	SC2 1004 cells	SC3 Na 972 cells	SC3 Na/Lead 972 cells
W16-17	Core	0,99	0,97	0,96	0,94	0,94
W19-17	Core	0,98	0,96	0,95	0,94	0,94
E22-17	Core	0,97	0,96	0,92	0,98	0,97
E22-16	Core	0,97	0,97	0,94	0,97	0,96
W14-14	Reflector	0,99	0,93	0,93	0,88	0,88
E14-13	Reflector	0,99	0,95	0,94	0,89	0,88
W22-14	Reflector	0,96	0,94	0,92	0,93	0,92
E22-13	Reflector	0,97	0,94	0,91	0,93	0,92
W11-11	Shielding	0,99	0,87	0,87	0,83	0,82
E11-11	Shielding	0,99	0,88	0,87	0,83	0,82
W26-12	Shielding	0,95	0,87	0,85	0,89	0,88
E26-11	Shielding	0,96	0,87	0,85	0,90	0,89

Among the different measurement techniques PNS fitting techniques show the largest deviations from the reference MSM value. One also notices that the correction for spatial effects in the PNS Area method by means of calculated correction factors remains in the order of 10% for the most penalizing configuration SC3.

9 Applicability of the different measurement techniques for reactivity monitoring in ADS

9.1 Current-to-flux reactivity indicator

By monitoring the ratio of the beam current and the flux level of an ADS providing a continuous accelerator current, one can evaluate the deviation of the actual reactivity from the reference reactivity and take appropriate actions, when pre-set limits are being attained. Since both parameters, flux level and beam current, can be followed on-line, the current-to-flux ratio provides an on-line indicator for the subcriticality level.

The strong advantage of this on-line subcriticality indicator is its simplicity. The measurement of a beam current and a flux level (with e.g. fission chambers) are well established techniques which don't require any sophisticated electronics or data treatment. Since the measurement of the beam current and the flux can be performed with an expected uncertainty of 1%, the precision on the current-to-flux reactivity indicator will be in the order of 1%. The bias of this reactivity indicator will depend on the calibration technique which has been used and the stability of the current-to-flux indicator. Based on the measurement performed in the MUSE project, it is felt that an absolute determination of the reactivity level by means of a dedicated calibration technique will yield the exact reactivity value with a maximum uncertainty of 10%. In practice, the on-line reactivity indicator will only be used to monitor the deviations of the reactivity level from a preset-value value and hence the expected uncertainty on the measurement of the reactivity level will be in the order of 1 %. Since no additional time constants are introduced in these measurements, an on-line, delay-free measurement of the subcriticality is feasible.

However, some precautions should be taken to guarantee an accurate determination of the subcriticality level:

- The proportionality constant should be determined in advance by means of calculation tools or even better by **absolute measurement techniques**.
- Since this proportionality constant depends on the forward and adjoint flux distributions and on the source distribution, this constant should be verified regularly by independent measurement techniques. Hence, the need for **reactivity cross-checking techniques**.
- The **stability** of the current-to-beam indicator due to changes in source characteristics and detection efficiency has to be guaranteed in between cross-checking calibrations:
    - The impact of variations of the source importance can be limited by **monitoring** operational parameters that are in strong relation with the different **source characteristics** influencing the source importance, e.g. the horizontal and vertical beam position, the proton energy,..
    - For a solid target, the burn-up of the target can also have an influence on the proportionality factor. However, since a circulating fluid Pb(-Bi) spallation target is considered in most ADS designs, this aspect can be neglected.
    - The variations of the detector efficiency due to a different flux profile and the burn-up of the fissile deposit of the detector are slow processes which can be accounted for by cross-calibration of in-core and ex-core detectors and by calculation input.

Based on these theoretical considerations, we can consider the current-to-flux measurement to be a simple and robust on-line reactivity indicator. However, we have to be clear that this statement still has to be verified by extensive measurement campaigns in future programmes,

since we did not have the opportunity in MUSE to investigate it due to the pulsed nature of the GENEPI source.

When the external source of an ADS is not continuous, but for instance pulsed, it is not yet clear under which experimental conditions the current-to-flux indicator could be used as an on-line indicator. Future programmes will have to point this out.

9.2 Reference Techniques

9.2.1 The Rod-drop technique

The rod-drop technique has been a standard method of reactivity measurement from the beginning, and many consider it the most accurate and reliable. It also is used to determine sub-critical reference reactivity for other techniques such as source multiplication. However, it is very unlikely that the classic rod-drop technique will be used as a reference measure of sub-critical reactivity for an ADS. In this technique one begins from the known critical state (k=1) and then performs the drop. Through inverse kinetics, the sub-critical reactivity after the drop is obtained in a straightforward manner. But, it is not envisioned that a power ADS will be able to achieve criticality, as that would defeat much of the safety basis. Without starting from that known state (k=1) one cannot infer the absolute reactivity level after the drop.

On the other hand, it is still an open question as to whether an ADS will have some form of control rods. If there are control rods, these could be used to provide some sort of monitoring of the operation provided the initial sub-critical state was determined via other means. A well-characterized absorber could also play a role in a similar manner.

9.2.2 The MSA/MSM Source Multiplication technique

Some form of source multiplication technique will almost certainly be required in an ADS. The fact is that an ADS is essentially a sub-critical multiplier, and all aspects of the behavior (power history, for example) are driven by the level of sub-criticality. These techniques will likely be used to infer initial reactivity's as well as provide monitoring in operation. It must be noted that to obtain an absolute reactivity level, as in the rod-drop, it is required to have some reference level determined by other means. Not being able to achieve criticality will put additional uncertainties on these methods.

The MSM/MSA technique is closely related to the current-to-flux power indicator and will hence be characterized by the same properties as described in the previous paragraph.

The rod-drop and MSM methods have been the staple of sub-critical measurements for years, and most people feel that measurements with uncertainties of less than 5% could be feasible at levels of 5000 pcm if uncertainties on neutron delayed data could be reduced. However, our experience in the MUSE programme was not very satisfactory. Several changes of the reference reactiviy, due to monitor movings and electronic changes, lead to higher uncertainties. We must emphasize that for future experiments more attention must be paid to ensure high quality measurements.

9.3 Pulsed Neutron Techniques

9.3.1 PNS Area method

Since in the PNS method a pulsed neutron source is required such a technique is not suitable as an on-line reactivity indicator. Even as a cross-checking of the on-line reactivity indicator during operation the PNS Area Method cannot be used, since during power operation the accelerator source will not be operated in pulsed mode. However, during the start-up phase or at low power this method could be used for absolute calibration purposes if the accelerator could operate in pulsed mode or a separate pulsed neutron source is available. Using the accelerator in pulsed mode would have the advantage of generating the same source characteristics as at nominal power level.

One of the main advantages of the PNS Area method lies in its relatively simple analysis. The experimental results have also pointed out that this is a quite robust technique, since the different partners (with different hardware and software) obtained the same experimental results. Moreover, this technique does not seem to be very sensitive to the detector position when the detector is placed in the reflector region or far from very absorbent special regions as safety rods. In addition, the corrections necessary to obtain the standard reactivity are smaller than 10% according to Monte Carlo simulations.

It is obvious that this technique can be used in fast as well as in thermal reactors. The only difference will be the time scale that will have to be looked at.

9.3.2 PNS Fitting technique

Since the PNS fitting is also based on the presence of a pulsed neutron source, this technique cannot be used as an on-line reactivity indicator. The PNS Fitting technique as it was studied in the MUSE experiments cannot be applied as such, since no pulsed source is present. One can however impose during power operation repetitive beam trips (or make use of accidental beam trips). After every beam trip the decaying neutron population can be measured. In such a way the PNS fitting technique can be used as a cross-checking technique for the on-line reactivity indicator.

The time structure of this response will essentially be the same as the one studied in the MUSE experiments. Therefore, the results from the MUSE experiments can easily be extrapolated to application of this PNS Fitting technique in a real ADS in power operation. The fact that during the MUSE experiments the system was operated at low power compared to the high power in a real ADS will result in an adapted choice of the neutron detector sensibility and detector operation mode (pulse or current mode).

Based on the MUSE experiments certain recommendations can be given with regard to the beam trip structure for real ADS systems. For a system with a mean neutron lifetime of 0.56 µs (as in MUSE), the trip period should be in the order of about 300 µs to allow the recording of the relevant part of the decay of the neutron population from which the reactivity indicator can be determined. Hence, a maximum repetition frequency of 1 kHz has to be used. Of course, a lower repetition frequency can be used, but this will increase the overall measurement time. The measurement time which was needed to obtain sufficient statistics was in the order of several minutes for an average count-rate of about 1000 cps and a repetition frequency of 1 kHz. When

in the considered real ADS system the mean neutron lifetime is different from the one in MUSE, this proposed trip period and maximum repetition frequency will have to rescaled accordingly. The measurement time in a real ADS system to obtain sufficient statistics will strongly depend on the sensibility of the detector and system power. Anyway, the detectors can be chosen in such a way to minimise the measurement time in the considered operating conditions.

One of the main issues with regard to the applicability of the PNS Fitting method is the analysis (or fitting) procedure which is used and subsequently which kind of interpretation model is applied. In the framework of the MUSE experiments four different kind of analysis techniques and associated interpretation models were used:

- Mono-exponential fitting
- Two exponential fitting
- Three exponential fitting
- k_p-method

9.3.3 Mono-exponential fitting

The mono-exponential fitting of the recorded decaying neutron population is the standard technique used in (near-) critical reactors to obtain the fundamental mode decay constant from which the effective neutron multiplication can be inferred. The measurements performed in MUSE have however pointed out that in deep subcritical systems representative for a real ADS (k_{eff} = 0.95 ➔ 0.97) the measured neutron population decay cannot adequately be fitted with a mono-exponential function, even after elimination of the first part. The first part of the measured decay function is strongly perturbed by the presence of harmonics introduced by the large subcriticality level and non-fundamental mode distribution of the flux in presence of the external source.

The fact that the measured decay function cannot be fitted by a mono-exponential is for a large part due to the reflector effect which perturbs the mono-exponential behaviour. If one nevertheless infers a reactivity from the decay constant, one obtains a large bias with respect to the reference reactivity value. As a result we will not retain the mono-exponential fitting as a potential way to exploit the PNS data in a real ADS system. It might still be useful for detecting and probably estimating very small reactivity changes [5.15], but still has to be confirmed by further measurements.

9.3.4 Two-exponential fitting

In the two-exponential fitting procedure, the measured decay curve is fitted with two exponentials after elimination of the first part (due to higher harmonics). Generally this fitted curve fits very well with the measured curve and two decay constants can be obtained. The value of these two decay constants however depends to a non-negligible degree on the fitting parameters, especially the starting point of the analysed region. This is due to the fact that the proposed two-exponential model is not perfect. The interpretation of these decay constants is based on the so-called two region kinetic model where the core and the reflector are considered as two separate regions. Based on this model one can deduce that in the case of fast cores it is not always guaranteed that one of the two decay constants can directly be related to the effective multiplication constant. This will depend on the time constant of the reflector, the subcriticality level and the core mean neutron lifetime.

In the MUSE experiments, it was demonstrated that for large subcriticality levels (k_{eff} = 0.95), the smallest decay time could be related to the core fundamental mode decay constant which is different from the system fundamental mode decay constant (k_{eff}). By means of some additional calculated parameters the core fundamental mode decay constant can be linked to the effective neutron multiplication factor. Hence, it is easily understood that the obtained reactivity is closely related to k_{eff} and not to the source multiplication constant k_s. Since the applicability of the two exponential fitting strongly depends on the characteristics of the system (core – reflector), its applicability in a real ADS cannot be completely evaluated based on the MUSE experiments.

9.3.5 Three-exponential fitting

Since the fitting of the measured curve with two exponentials revealed that no perfect fitting is obtained, an interpretation model based on the sum of three exponentials was proposed. This model is based on two systems (core and reflector-shield – 3 regions) and three energy groups (fast, epithermal and thermal) with strong coupling. When physical conditions are imposed, this leads to a description of the flux response with three decay constants that must be the same for the two systems.

This method relies on the simultaneous fitting of all detector responses in the core and the reflector/shield to this sum of three exponentials. In this way, a complex fitting procedure is required to extract a reliable value for the á eigenvalue parameter and the associated reactivity. This more complicated data treatment makes the application of this analysis procedure less suited to a real ADS where a robust and "simple" technique is preferred.

The analysis of the measurements has also demonstrated that the contribution of the third exponential is negligible in core detectors but necessary to understand the behavior of reflector detectors. Within the interpretation model and under the conditions described at [5.15], fulfilled by MUSE-4, the decay constant with the highest absolute value is very closely related to the prompt decay constant of the coupled reactor, and can in a first approximation be considered as the equivalent of the á eigenvalue in the point kinetic model for a simple reactor. The lowest decay constant, in absolute value, is related to the low energy neutron lifetime in the second system, which is not multiplicative, so it is independent of the reactivity of the system. Further experiments will have to be point out whether the interpretation model is sufficiently robust for different experimental configurations and different ADS systems.

The results about the applicability of all the above mentioned fitting techniques in thermal systems cannot be extrapolated in a straightforward manner from the MUSE experiments, since the time characteristics and decay behaviour of the neutron population will strongly depend on the core (moderator) characteristics.

9.3.6 k_p-method

The last method which was used in the course of the MUSE experiments to obtain a reactivity indicator from the decay of the neutron population after a Dirac pulse or a beam trip is the kp-method. The k_p-method is based on the calculation of the detailed time response via a MCNP KCODE run which means that in fact the fundamental mode decay of the prompt neutron population is obtained.

In a subcritical medium not all the neutron generations have exactly the same P(ô) behaviour. In fact, the first generations are still strongly influenced by the source characteristics. The older neutron generations (n>5 is a good approximation) have approximately the same distribution since at that time a stabilised "fundamental mode" fission source distribution exists. Since the first generations have only an important influence in the first part of the measured response (some µs), an analysis which only takes the remaining part into consideration will not biased. Therefore, in practice these contributions can be neglected and a calculation of P(ô) for the stabilised "fundamental mode" fission source distribution via an MCNP KCODE calculation will be sufficient.

When moreover the detector deposit does not have the same composition as the average fuel in the reactor, the measured response will not be completely described by the proposed k_p-formalism. In order to take this detector effect into account, the response of a detector to a fundamental mode fission source distribution can be calculated and incorporated into the overall formalism as described in the introduction.

One of the apparent concerns in the robustness of this technique is the sensitivity of the obtained k_p to the geometrical modeling and data libraries in Monte Carlo codes. The MUSE calculations (experiments) have pointed out that the method is not very sensitive to these kinds of effects [Vollaire].

As the other PNS fitting techniques, the k_p-method will yield a reactivity indicator which is related to the effective multiplication constant k_{eff}, rather than to the source multiplication constant k_s. The k_p-method needs the value of the effective delayed neutron fraction to finally arrive at the reactivity, but this is the same for the other PNS techniques. One of the major advantages of the k_p-method is that no multi-exponential fitting is used which is a source of uncertainty and a detailed time structure can be used.

With respect to application in a real ADS, the possibility to apply this technique with reflector detectors is important. In MUSE, the main focus was directed to core detectors since the cleanest response is observed in the core. Another issue important for its implementation in a real ADS is the measurement time needed to obtain adequate statistics to derive the reactivity indicator.

9.4 Source Jerk Techniques

9.4.1 Standard Source Jerk Technique

The standard Source Jerk technique is a well-known technique in reactor physics. To accurately determine the prompt jump fraction appropriate fitting routines are required. Generally, the most accurate results are obtained with fitting routines based on inverse kinetics. The drawback of such fitting techniques is of course the obligatory knowledge of other kinetic parameters which have to be provided by calculations.

To obtain sufficient statistics with the standard Source Jerk technique, a sequence of repeated experiments has to be performed. In this way, the individual responses can be summed up to obtain one averaged response with sufficient statistics. In the MUSE experiments significant problems were encountered to obtain a sufficient stable repetition level to enable to an easy and unbiased summing up of the different contributions.

It is clear that the standard source jerk technique can only be used during start-up or loading/unloading or specific calibration procedures when the accelerator is turned off. In order to limit in these circumstances the measurement time a very high source strength and high efficient detectors are needed which both are difficult for real ADS systems. It will be difficult to install an isotopic Cf-252 source with a source strength which will be sufficiently large compared to the intrinsic source of the spent fuel in the core. The possibility of obtaining high efficient detectors in fast ADS cores which are not designed for having large volume detectors is rather limited. Hence, large measurement time will be needed. Therefore, the standard source jerk technique will probably not be applied for reactivity determination in an ADS.

9.4.2 ADS source jerk technique

The ADS source jerk technique is based on the determination of the removal of the prompt neutron part as in the rod-drop technique. Since the beam trip is practically instantaneous and there is no need to wait for the delayed neutrons to decay, the levels before and after the beam trip will be measured. By averaging the level after the beam trip over a certain time period (in the order of some hundreds of microseconds), the uncertainty will be strongly decreased, but a possible small bias may arise due to the decay of the delayed neutron population. Measurements will have to point how the investigated period can be optimized in terms of uncertainty and bias, but also with respect to operational conditions of the ADS. The main advantage of this technique is related to the fact no fitting based on an interpretation model has to be performed.

9.4.3 Source Modulation Technique

The source modulation technique (SMT) allows the determination of the reactivity expressed in dollars. The SMT as used in the MUSE experiments will not be easy to implement for real ADS, since the rapid variation of the pulse frequency from a high frequency to a low frequency will not be envisaged. Moreover, other measurement techniques such as the PNS Area Method are able to provide the same information with a much simpler time structure of the beam. Therefore, this technique will not have a direct application for reactivity monitoring in a real ADS.

9.5 Noise methods

9.5.1 Noise methods without an external neutron source (only intrinsic source)

It is obvious that noise techniques without an external source cannot be used as an on-line technique or cross-checking technique, since in these cases one supposes that an external source is present. Hence, noise methods with the intrinsic source can only be used in the exploitation of an ADS as a calibration method. They can be applied during start-up or in a calibration phase, when the external beam current is switched off and dedicated experimental conditions can be met.

When one uses such noise techniques at deep subcritical levels, very long measurement times are encountered, even with very efficient detectors. From a practical point of view long measurements are always to be avoided. High efficient detectors in fast cores moreover cause the problem of strong local reactivity perturbations which is not desirable.

Since as in PNS methods the reactor response cannot be described by simple point-kinetics due to the break-down of the fundamental-mode approximation, the measured distribution cannot adequately be fitted to a mono-exponential. Due to the fact that noise methods rely on the convolution of the reactor response function in the time domain (and the quadrate of the response function in the spectral domain), this effect will be even more pronounced and more difficult to fit and interpret.

One of the points which make the noise methods attractive to apply for the determination of the reactivity is the fact that in general three different measurement quantities can be obtained from the distribution: decay constant, amplitude of the correlated signal and the amplitude of the uncorrelated signal. This makes it easier to determine the reactivity in an absolute way independent from calculated parameters. The following points make it however difficult to extract this supplementary information in ADS:

- Difficult to obtain sufficient statistics on all of the measurement quantities
  - High efficient detectors are needed
- No fundamental mode
- Knowledge of detector efficiency or source strength is essential
  - Large uncertainty on the inherent source strength (spent fuel)
  - Calibration of detector in representative conditions is difficult

Hence, noise methods without a pulsed neutron source are not very suited for the determination of the reactivity level in an ADS.

9.5.2 Noise methods with a pulsed neutron source

Due to the limited interest in using noise methods without a pulsed neutron source it was considered more useful to investigate the possibility of using noise methods in combination with a pulsed neutron source. It is however also clear that such a technique is not suited as an on-line monitoring technique due to the imposed pulsed beam structure and long measurement time. Whether it can be used as a cross-checking technique is not completely ruled out, but will depend on the beam structure one can obtain and on the measurement time one can allocate to the cross-checking procedure. Probably noise methods with a pulsed neutron source will have more success in ADS reactivity determination as a calibration technique, since in that case the measurement conditions can be optimized.

9.5.2.1 Rossi-alpha method with a pulsed neutron source

The use of a pulsed source makes it possible to apply noise methods such as the Rossi-alpha method in deep subcritical systems due to the increased correlation. As a consequence sufficient statistics are obtained in an acceptable measurement time, something which cannot be achieved without a pulsed neutron source.

The fact that point-kinetics is no longer valid is not changed, because it is inherent to deep subcritical systems. Hence, the fitting of the measured distribution to obtain the fundamental mode decay constant will suffer at least the same degree of difficulty as in the PNS fitting methods due to the fact the Rossi-alpha method relies on the correlation of the reactor response function.

Based on the experiments it was also shown that the reactivity in dollars could easily be derived from integral parameters obtained from the measured distribution. This measurement quantity cannot be derived from a Rossi-alpha distribution recorded without the presence of a pulsed neutron source. This determination of the reactivity in dollars has in fact the same characteristics as the PNS Area method.

This additional measurement quantity, the reactivity in dollars, could then be used in combination with the standard three measurement quantities obtained from a Rossi-alpha method to derive the reactivity in absolute way. The practical feasibility of this procedure still has to be checked.

9.5.2.2 Feynman-alpha method with a pulsed neutron source

As it was outlined in the description of the Feynman-alpha method with a pulsed neutron source, two different implementations can be distinguished: deterministic pulsing and stochastic pulsing. Since for both types analytical formulae were derived and they were confirmed by experiments, it is in principle possible to use this technique in an ADS. However, the analytical formulae and hence the subsequent fitting procedure is much more complicated in the Feynman-alpha method compared to the Rossi-alpha technique. Nevertheless, the stochastic pulsed Feynman method was applied successfully for the determination of reactivity with high accuracy in recent measurements in a thermal system [7.15].

Both techniques applied in a deep subcritical system suffer from the break-down of point-kinetics, but the way the Rossi-alpha technique can deal with it is more straightforward due to the simpler analytical expressions.

Since no additional information can be obtained from the Feynman-alpha technique compared to the Rossi-alpha technique, the Feynman-alpha technique with a pulsed source is less attractive than the Rossi-alpha technique for the determination of the reactivity in an ADS.

9.5.2.3 CPSD with a pulsed neutron source

As already mentioned the use of a pulsed source will result in an increased correlation. As a consequence sufficient statistics are obtained with CPSD in an acceptable measurement time, something which cannot be achieved without a pulsed neutron source.

The fact that point-kinetics is no longer valid is also true in this case, since it is a characteristic of deep subcritical systems. Hence, the fitting of the measured distribution to obtain the fundamental mode break frequency will suffer at least the same degree of difficulty as in the PNS fitting methods. The fitting is made even more difficult by the presence of harmonics of the pulse frequency.

The possibility to derive from the CPSD other measurement quantities besides the break frequency in order to obtain a more absolute determination of the reactivity still has to be investigated for various measurement conditions.

Compared to the Rossi-alpha technique, which is based on pulse detection, the CPSD method, which is based on current measurement, has the advantage that it can be applied at

higher power levels but has at the same time the disadvantage that at low ("zero") power the technique has more difficulty to obtain sufficient statistics.

9.6 General methodology for reactivity measurement in ADS

Based on the results of the different measurement performed in the different configurations with various methods it is clear that no unique measurement technique can be proposed to measure the different kinetic parameters and especially the reactivity.

As the final goal is to provide an accurate and robust on-line measurement of the reactivity during power operation and during loading operations no single experimental technique can accomplish this task. Since only few techniques can act as an on-line indicator for reactivity and these techniques require additional information to extract the reactivity, additional measurement techniques are needed. Therefore only a combination of techniques will be able to solve the task and a step-wise and in-depth approach of reactivity determination is proposed.

For on-line reactivity monitoring, the current-to-power indicator seems the most appropriate choice since as outlined in paragraph 3.1 it is simple, robust indicator with a small relative uncertainty. This reactivity prerequisites the knowledge of a proportionality factor containing the detector efficiency and the source importance. Since both parameters can change during reactor operation and loading, it is important to check this proportionality constant on a regular basis. In between checks, one should then be able to guarantee that the proportionality constant remains constant over the considered period. This can be accomplished by monitoring signals which together determine the source characteristics such as the beam position, proton energy,.. By calculating the reactivity sensitivity coefficients for these source signals, the overall bias due to an unknown variation in the proportionality constant can be limited by bounding the acceptance range of the source signals. In this way, the current-to-power reactivity indicator can serve as a reliable and accurate on-line reactivity monitoring technique.

The verification of the proportionality constant of the current-to-power indicator will have to be accomplished by independent measurement techniques. To limit the perturbation to the power operation of the ADS, benefit would be taken from the unavoidable occurrence of beam trips. At every beam trip the response of the reactor could be recorded. Since the repetition-rate of these beam trips is unpredictable and probably not sufficient to obtain desired statistics on the measured parameters, an imposed repetition of induced beam trips will have to be foreseen.

The candidate measurement techniques to be used in these experimental conditions are either a PNS fitting technique or the ADS source jerk technique. The ADS source jerk technique is based on the determination of the removal of the prompt neutron part as in the rod-drop technique. In practice, the levels before and after the beam trip will be measured. By averaging the level after the beam trip over a certain time period (in the order of some hundreds of microseconds), the uncertainty will be strongly decreased, but a possible small bias may arise due to the decay of the delayed neutron population. Measurements will have to point how the investigated period can be optimized in terms of uncertainty and bias, but also with respect to operational conditions of the ADS. The main advantage of this technique is related to the fact no fitting based on an interpretation model has to be performed.

In the PNS fitting technique, the investigated period after a beam trip can be much shorter, since only the die-away of the prompt neutron population is recorded. From the measurements in MUSE it was demonstrated that he decay of the prompt neutron population cannot adequately

be represented by a mono exponential. Therefore more complex interpretation models are needed among which the kp-method seems to be the most robust and promising one. The kp-method however heavily depends on calculation input which could be considered as a drawback. One still has to be cautious in extrapolating the results obtained in MUSE for the PNS fitting techniques to a real ADS, since the beam structure in both situations is different. For a real ADS the decay after the interruption of a continuous beam will be investigated instead of the response to an impulse as in MUSE. Since the prompt neutron decay in both situations is different, the extrapolation of the results with regard to the applicability has to be confirmed by future experiments.

In order to calibrate the above mentioned techniques, additional independent and robust measurement techniques have to be applied. The standard approach followed in critical reactors by using a rod-drop and in combination with the MSM-technique is not feasible in ADS, since the critical state of the system is not intended to be reached. For the purpose of calibration dedicated experimental conditions can be envisaged, such as zero-power conditions. These calibrations could be incorporated in the loading and start-up procedures of the ADS. In these circumstances, dedicated external sources could be used to solicit the system. One possibility could be to use a pulsed neutron source as in MUSE and apply the PNS Area method which has been shown to be a very simple and robust measurement technique. The use of an external isotopic source in a standard source jerk measurement was seen to be less attractive for reasons of radioprotection, practical implementation and measurement accuracy. The possibility of using the Cf source driven technique was not investigated in the framework of the MUSE project. This technique cannot be excluded from consideration, but the need for a high measurement precision might lead to an unpractical source-strength of the Cf source.

9.7 Conclusions

Different measurement techniques for the determination of kinetic parameters and more in particular the reactivity were investigated in the framework of the MUSE project.

The main experimental results obtained by the different partners showed that the reactivity level for an ADS (with k_{eff}=0.95) can be calibrated with an accuracy in the order of 10%. In MUSE, the correction induced by the MSM-factor with regard to the simple MSA method remains very small, in the order of 5%. This small correction is probably due to the quite homogeneous MUSE core and the averaging over a lot of different core detectors in the MSA method which reduces the overall spatial effect.

Based on the measurements performed in the MUSE project and the envisaged conditions of a future ADS the applicability of the different methods towards future application in an ADS were investigated. It was concluded that a combination of techniques will be needed to provide an accurate and robust monitoring of the reactivity.

The monitoring of the reactivity is achieved through an in-depth philosophy of calibration and validation. The current-to-power indicator provides a simple and on-line reactivity indicator, which is regularly checked. A cross-check can be performed at beam trips (imposed or not) with an ADS source jerk technique or a PNS fitting technique such as the kp-method. An absolute determination of the reactivity level can be obtained by use of PNS based techniques.

10 General Conclusions

Two major objectives of the MUSE programme were: (1) the characterization of a typical ADS type core, e.g., core parameters, source importance, spectral indices, reaction rate traverses, by means of experiments and calculations, thereby establishing a reference calculational route, and (2) the investigation of techniques for sub-critical measurement and monitoring. Particularly towards the latter, it is well recognised by the community that MUSE was an essential step in the qualification of a future ADS. With MUSE, we were able to investigate in depth methods of reactivity measurements in cold conditions with four sources: intrinsic, Cf, DD neutrons, and DT neutrons. A part of these measurements has been repeated in TRADE phase I in 2004 and should be continued in 2005 providing thereby a sort of "generic validation". In the immediate future, experiments should be carried out in the IP-Eurotrans DM2 to include thermal feedback properties, since this effect was out of scope due to the zero-power nature of the MASURCA facility.

In addition to the MUSE-4 project, activities performed in the frame of the SAD project were aimed (1) to test and develop calculation tools for the characterization of spallation targets bombarded by a high energy proton beam, by means of measurements performed at Dubna and (2) to study the influence of the SAD core characteristics on the applicability of different methods of subcriticality determination, providing thereby complementary information to the analyses performed in MUSE.

With regard to the core characterization effort, it is recognised that some of the measurements in subcritical states are very time-consuming. This lead to a reduction of the number of measurements that could be done within the frame of the project. Certain aspects of the MUSE core were very attractive to the consortium of the project. This includes the behaviour of the lead buffer, reflector effects, source spectrum effects, and the last configuration studied, SC3 with a lead central zone. The investigation of different calculation routes for these parameters yielded some interesting conclusions. The C/E value for the determination of k-eff was found to be very satisfactory for both deterministic and Monte Carlo codes. The simulation of the experiments in the lead phase, in particular, did not bring out any specific problem. The comparison between experiment and deterministic codes for the kinetic parameters $\hat{a}_{eff}$ and Ë measured in near-critical conditions was very satisfactory. With regard to Monte Carlo methods, a new and fast technique was developed for the calculation of $\hat{a}_{eff}$ which also yielded a very good C/E value in near-critical conditions. Nevertheless, the interpretation of the mean neutron lifetime Ë is still an open issue within the Monte Carlo calculation route. What concerns fission rate distribution, an overall good agreement was found for measurements at delayed critical. In subcritical configurations, we found good agreement (with predictions) for U-235, and less for isotopes with threshold reactions. The U-238 flux traverse in the centre of the configuration was shown to be very sensitive to the exact level of subcriticality in the calculation. Spectral indices with fission chambers exhibited some problems that are still to be resolved where as foil activation technique lead to very interesting conclusions. In spite of some discrepancies that need further studies, the MUSE-4 programme has produced an impressive amount of data which helped the analysts in their understanding of the behaviour of a sub-critical fast assembly. Finally, Monte Carlo-based representativity studies showed that the buffer-leakage neutrons coming from the (D,T)-source has an energy spectrum similar to that of the spallation source and from that point view can be considered representative of an ADS. Moreover, the energy spectra in the core were found to be completely dominated by the fission multiplication in the fuel and therefore are independent of the distribution of the external source. Hence, considering the study of spectrum-weighted quantities, the MUSE-4 experiments can be assumed to be representative of an ADS.

In addition to the above, the experiments conducted at Dubna concentrated on the measurements with the bare lead target exposed to 660 MeV proton beam, hadron distributions around the target and assessment of its activation. Analyses of results of experiments and calculations demonstrated that angular distribution of hadrons around the target shows an agreement within 6 - 15 % when much larger discrepancies, at the worst within one order of magnitude, were observed for the axial distributions of activity. Almost always the C/E ratio was between 3 and 1/3. From these results, it was concluded that one cannot point out a single code and/or nuclear reaction model yielding good results simultaneously for all examined nuclides. In definitive, the model of Cugnon gave the best agreement with experimental values - about 70 % of results remain within 30 % difference.

Turning to the reactivity measurement aspect of the MUSE programme, there were five teams that devoted a great deal of time and effort in trying to understand the physics of sub-critical systems. We studied the traditional rod drop/MSM method, source jerk methods, variations of the PNS methods, and variations of noise methods. There were problems with the MSA/MSM measurement (which is normally the reference method) owing to essential modifications that had to be realized on several detectors during the programme. These modifications lead to uncertainties on the reactivity measurements, in the range 6-8% (1σ), that unfortunately limited the conclusions of our analyses. There has been a valuable lesson learned from this experience, and it will be carried forward to IP-Eurotrans DM2 and hopefully beyond; that is, more attention must be given to the base-line measurements, whatever they may be in an ADS.

Much effort was devoted to dynamic methods. We had some difficulties with the standard source jerk method that demonstrated that this technique could only be used during start-up or loading/unloading phases. Nevertheless, in that case, the source strength should be sufficiently large compared to the intrinsic source of the spent fuel in the core. The source modulation technique gave better results but cannot be seriously envisaged for the reactivity monitoring of a real ADS. A rapid variation of the pulse frequency from a high frequency to a low frequency seems indeed difficult to set-up in a power reactor. We found that traditional noise methods (driven by the intrinsic or Cf source) such as the CPSD, Rossi- and Feynman-á were usable only in the case where the reactivity was close to critical. A Rossi type technique driven by the neutron generator is more promising, but it remains to be seen if these kinds of methods will have a role in the reactivity monitoring of an ADS. At this point, it appears that some form of the PNS method will be the most useful. Several PNS models based on the interpretation of the slope of the signal (2-region, 3-region, kp-method) were investigated. Analyses based on the fitting of the prompt neutron population was shown very sensitive to the kinetics model and fitting parameters, but seems promising for detecting small reactivity changes. On the other hand, the so-called kp-method has the advantage of a simple and robust interpretation algorithm but needs extensive Monte Carlo simulations. In definitive, studies in MUSE have shown that the so-called PNS “area method” is quite forgiving in relation to other PNS models based on the study of the slope of the signal. It seems that this method could be used in a cold start-up configuration of an ADS, particularly since small neutron generators are easily obtained. Last, studies carried out on some versions of the SAD, PDS-XADS and MYRRHA cores demonstrated that the reflector and the shielding properties could affect the possibility of measuring the reactivity. This aspect should be considered in future core design projects.

For the day-to-day monitoring however, it appears that some form of a proton current/power/reactivity relation will be used. In general, under stable conditions when everything remains constant, the ratio of the flux and proton current are proportional to a simple function of the reactivity, and simple real time monitoring (as in a typical power reactor) will

yield sufficient information for control in normal operations. The potential problem occurs if there is an unknown configuration change, leading to change in source importance or a change in local reactivity values. In order to provide a simple means to study the stability of the current-to-flux method to unexpected changes in the target-core properties, the proton source efficiency parameter (Ψ^*) was defined. Since Ψ^* constitutes the proportionality factor between the monitored neutron flux and the proton beam current, its dependence on those factors, which potentially is able to change the current-to-flux ratio, will give an estimation of the sensitivity of the reactivity indicator.

Simply monitoring the flux and current will not provide any information for such a change. Thus, some form of independent, periodic, absolute determination will be required that can yield an independent measure of the reactivity. At the present time, it is envisioned that some sort of beam chop will be used, but it was not possible to test such a technique in MUSE-4. This, together with the continuous on-line monitoring will be a major task for the IP-Eurotrans DM2 in the future.

In summary, despite some technical problems, overall the MUSE-4 project was a great success. It brought together some of the best experimental reactor physicists in the world, and produced many data for subsequent analysis. Numerous advances were made in the understanding of the behaviour of sub-critical systems and the viability of various methods of reactivity monitoring although the uncertainty assessment related to the analyses still needs to be completed. Moreover, it is clear hat we do not understand (or at least cannot fully predict) some effects, and this leaves the door open for future lines of research. It is also clear that the fully coupled space-time problem has yet to be solved in its entirety.

Last, but not least, the programme produced some of the best collaborations seen in recent years, certainly in the reactor physics world. It produced eight Ph.D. theses since the year 2000, and a great many publications in conferences and journals. It can safely be said that the MUSE programme has made a truly significant contribution to experimental reactor physics in the last four years.

References

[2.1] R. Soule & al , *"Neutronic Studies in Support to ADS: The Muse Experiments in the MASURCA Facility*"
Nuclear Science and Engineering, Vol. 148 (2004) 124-152

[2.2] J. Janczyszyn, W.Pohorecki, S. Taczanowski, G. Domañska V.N. Shvetsov, G. Gerbish *"Experimental Assessment of Radionuclide Production in Materials Near to the Spallation Target*", Proc. of International Conference on Accelerator Applications/Accelerator Driven Transmutation Technology and Applications (AccApp/ADTTA'01), Reno, USA, November 12-15, 2001, CD-ROM, ISBN: 0-89448-666-7, 2002

[3.1] M. Salvatores et al., *"MUSE-1 : A first experiment at MASURCA to validate the physics of sub-critical multiplying systems relevant to ADS*", Proc. Of Second International Conference on Accelerator-Driven Transmutation Technologies and Applications (ADTTA'96), Kalmar, Sweden, June 3-7, 1996.

[3.2] R. Soule et al., "*Validation of neutronic methods applied to the analysis of fast subcritical systems: The MUSE-2 experiments*", GLOBAL'97, Yokohama; Japan, October 5-10, 1997.

[3.3] J.F. Lebrat et al., "*Experimental Investigation of Multiplying Subcritical Media in presence of an External Source : the MUSE-3 Experiment* ", ADTTA'99, Prague, May 1999.

[3.4] C. Destouches & al, *"The GENEPI accelerator operation feedback at the MASURCA reactor facility*", Submitted to AccApp'05 - International Topical Meeting on Nuclear Applications of Accelerator Technology, Venise, Italy, August 28/September 1, 2005

[3.5] V.S Barashenkov, I.V. Puzynin, A. Polanski , "*ADS's based on the 660 Mev proton Phasotron of JINR for research on utilization of Plutonium*", Proc. of the 10th International Conference on Emerging Nuclear Energy Systems (ICENES,), Petten, September 24-28, 2000, p. 429

[4.1] 5th EURATOM FP – Contract n°FIKW-CT2000-00063
Deliverables n°4 & 5
MUSE experiments : Experimental data set description and Physical experimental data set

Three separated reports :
Part one : Reference and SC0 configurations
Part two : SC2 and SC3 configurations
Part three : SC3 Sodium/Lead configuration

[4.2] 5th EURATOM FP – Contract n°FIKW-CT2000-00063
Deliverable n°7
SAD experiments : Reference route and final report

[4.3] 5th EURATOM FP – Contract n°FIKW-CT2000-00063
Deliverable n°6
MUSE experiments : Reference route and final report

[4.4] F. Gabrielli, M. Carta, A. D'Angelo, V. Peluso, "*Interpretation of the MUSE-4 kinetics experiments: Analysis of a selected configuration*", ENEA Technical Report, RT/2004/28/FIS (June 2004).

[4.5] J.F. Lebrat, C. Broeders, A. Courcelle, A. Hogenbirk, N. Messaoudi, M. Plaschy, P. Seltborg, R. Soule, D. Villamarín and P. Wachtarczyk, "*Intercomparison of JEF-2 based deterministic and Monte Carlo reactivity calculations of a simple subcritical benchmark*"
Report NT DER/SPRC/LEPH 01-214, CEA Cadarache (21 December 2001).

[4.6] D. Villamarín, R. Soule, and E. González. "*Benchmark on computer simulation of MASURCA critical and subcritical experiments (MUSE-4 benchmark)*"
Technical Report NEA/SEN/NSC/WPPT(2001)5, OECD/NEA report, December 2001.

[4.7] R. Klein Meulekamp, S.C. van der Marck
Delayed neutrons
Report 20571/04.57372/P, NRG/Petten

[4.8] M. Szieberth and J.L. Kloosterman, "*New Methods for the Monte Carlo Simulation of Neutron Noise Experiments*", Proc. of International Conference on Nuclear Mathematical and Computational Sciences: A Century in Review, A Century Anew (M&C 2003), Gatlinburg, Tennessee, April 6-11, 2003, on CD-ROM

[4.9] P. Baeten, "*Heuristic derivation of the Rossi-alpha formula for a pulsed neutron source"*, Annals of Nuclear Energy, volume 31/1, 43-53 (2003)

[4.10] I. Pázsit, M. Ceder and Z. F. Kuang , *"Theory and Analysis of the Feynman-a Method for Deterministically and Randomly Pulsed Neutron Sources"*
Nuclear Science and Engineering, Vol. 148 (2004) 67-78

[4.11] Y. Rugama, J.L. Kloosterman, J.L. Munoz-Cobo, "Application of the stochastic transport theory to reactivity measurements in a subcritical assembly driven by a pulsed source", Nuclear Mathematical and Computational Sciences, Tennessee, USA, April 6-11, 2003

[4.12] M. Plaschy, S. Pelloni, P. Coddington, G. Rimpault, R. Chawla, "*Importance of the MUSE experiments for emerging ADS concepts from the nuclear data viewpoint*"
Annals of Nuclear Energy, Volume 32, Issue 8, May 2005, pages 843-856

[4.13] 5th EURATOM FP – Contract n°FIKW-CT2000-00063
Deliverable n°3
Physical data set description

This deliverable is composed of five separated reports :

Geometrical and physical data associated to the MUSE-4 reference configuration

Technical report CEA/DEN/CAD/DER/SPEx/LPE/01/015 indice 1
R. Soule, W. Assal, D. Villamarin

Geometrical and physical description of the MASURCA pilot rod during the MUSE-4 experiments
Technical report CEA/DEN/CAD/DER/SPEx/LPE/02/053
R. Soule, W. Assal

Geometrical and physical description of the MASURCA instrumental assemblies used by the CNRS/ISN during the MUSE-4 experiments
Technical report CEA/DEN/CAD/DER/SPEx/LPE/02/067
W. Assal, R. Soule

Geometrical and physical description of the MASURCA safety rods during the MUSE-4 experiments
Technical report CEA/DEN/CAD/DER/SPEx/LPE/02/063
W. Assal

Geometrical and physical description of the MASURCA instrumental assemblies used for the beff measurements during the MUSE-4 experiments
Technical report CEA/DEN/CAD/DER/SPEx/LPE/03/046
W. Assal

[4.14] "*L'accélérateur GENEPI : Conception, technologie, caractéristiques*"
Technical report CNRS/IN2P3/ISN-GENEPI -NT-4031 index 0,13/10/99

[5.1] J. Vollaire, A. Billebaud, R. Brissot, C. Le Brun, E. Liatard, "*Calibration and monitoring of the GENEPI Neutron Source for the MUSE IV Experiment*"
Report LPSC-03 26, IN2P3-CNRS/UJF/INPG, 6 June 2003

[5.2] *The JEF-2.2 Nuclear Data Library*, JEFF Report 17, NEA Paris (April 2000).

[5.3] *ENDF-201, ENDF/B-VI Summary Documentation*, Report BNL-NCS 17541, P.F. Rose (Ed.) 4th Edition (1996).

[5.4] T. Nakagawa, K. Shibata, S. Chiba, T. Fukahori, Y. Nakajima, Y. Kikuchi, T. Kawano, Y. Kanda, T. Ohsawa, H. Matsunobu, M. Kawai, A. Zukeran, T. Watanabe, S. Igarasi, K. Kosako and T. Asami, "*Japanese Evaluated Nuclear Data Library Version 3 Revion-2: JENDL-3.2"*, J. Nucl. Sci. Technol. 32 (1992) 1259.

[5.5] G. Rimpault et al., "*The ERANOS code and data system for fast Reactor Neutronic Analysis*", Proc. International Conference on the New Frontiers of Nuclear Technology: Reactor Physics, Safety and High-Performance Computing (PHYSOR 2002), Seoul, Korea, (7-10 October 2002).

[5.6] *MCNP - A General Monte Carlo N-Particle Transport Code*, Version 4C, Report LA-13709-M, Los Alamos National Laboratory, J. F. Briesmeister (Ed.) April 2000.

[5.7] J.F. Lebrat et al., "*Fast reactor core-reflector interface effects revisited*", Proc. International Conference on the New Frontiers of Nuclear Technology: Reactor Physics, Safety and High-Performance Computing (PHYSOR 2002), Seoul, Korea, (7-10 October 2002).

[5.8] M. Carta, A. D'Angelo, V. Peluso, G. Aliberti, G. Imel, V. Kulik, G. Palmiotti, J.F. Lebrat, Y. Rugama, C. Destouches, E. Gonzalez-Romero, D. Villamarín, S. Dulla, F. Gabrielli, P. Ravetto and M. Salvatores, "*Reactivity assessment and spatial time-effects from the MUSE kinetics experiments*", Proc. International Conference on the Physics of Fuel Cycles and Advanced Nuclear Systems (PHYSOR 2004), Chicago, Illinois, (25-29 April 2004)

[5.9] *MCNPX User's Manual*, Version 2.3.0, Report LA-UR-02-2607, Los Alamos National Laboratory, L.S. Waters (Ed.) April 2002.

[5.10] H. Bachmann, G. Buckel, W. Hoebel, S. Kleinheins, The Modular System KAPROS for Efficient Management of Complex Reactor Calculations, Proceedings Conference Computational Methods in Nuclear Energy, Charleston, CONF-750413, 1975

[5.11] P. Seltborg and R. Jacqmin, "*Investigation of neutron source effects in subcritical media and application to a model of the MUSE-4 experiments*", Proc. Int. Conference on Mathematical Methods for Nuclear Applications, Mathematics and Computation, Salt-Lake City, USA, September, 2001.

[5.12] A.J. Koning, S. Hilaire, M. Duijvestijn, Proc. of the 2002 Frederic Joliot/Otto Hahn summer school in reactor physics: Modern reactor physics and the modelling of complex systems, Aug. 21-30, 2002, Cadarache, France.

[5.13] S.C. van der Marck and R. Klein Meulekamp, "*Benchmark results for the effective delayed neutron fraction*", Report JEF/Doc-973 (October 2003).

[5.14] T.E. Valentine and J.T. Mihalczo, "*MCNP-DSP: a neutron and gamma ray Monte Carlo calculation of source-driven noise-measured parameters*", Annals of Nuclear Energy 23 (1996) 1271-1287.

[5.15] D. Villamarín, *"Análisis dinámico del reactor experimental de fisión nuclear MUSE-4"* PhD Thesis, Universidad Complutense de Madrid, 2004.

[5.16] A. Billebaud, J. Vollaire, R. Brissot, D. Heuer, C. Le Brun, E. Liatard, J.-M. Loiseaux, O. Méplan, E. Merle-Lucotte and F. Perdu, "*The MUSE-4 Experiment : Prompt Reactivity and Delayed Neutron Measurements*", Proc. GLOBAL 2003, Atoms for Prosperity: Updating Eisenhower's Global Vision for Nuclear Energy, New Orleans, Louisiana, November 16-20, 2003.

[5.17] M. Plaschy, "*Etudes Numériques et Expérimentales de Caractéristiques d'un Système Rapide Sous-Critique Alimenté par une Source Externe*", Thèse de Docteur es Sciences n°2953 (2004), Ecole Polytechnique Fédérale de Lausanne

[5.18] M. Plaschy , R. Chawla, C. Destouches, C. Domergue, H. Servière, P. Chaussonnet, J.M. Laurens, R. Soule, G. Rimpault , "*Foil activation studies of spectral variations in the MUSE 4 critical configuration*", Proc. International Conference on the New Frontiers of Nuclear Technology: Reactor Physics, Safety and High-Performance Computing (PHYSOR 2002), Seoul, Korea, (7-10 October 2002).

[5.19] R. Klein Meulekamp, A.J. Koning, A. Hogenbirk, *'Sensitivity for Pb cross section and influence of (n,2n) reaction in MUSE-4 experiments*"
Report 20571/02.50737/P, NRG/Petten

[5.20] P. Seltborg et al., "*Definition and Application of Proton Source Efficiency in Accelerator Driven Systems*"
Nuclear Science Engineering, Vol. 145, 390-399 (2003).

[5.21] P. Seltborg and J. Wallenius, *'Proton Source Efficiency for different Inert Matrix Fuels in Accelerator Driven Systems*", Proc. of International Conference AccAPP'03, June 1-5, 2003, San Diego, California, USA (2003).

[5.22] P. Seltborg et al., "*Impact of Heterogeneous Cm-distribution on Proton Source Efficiency on Accelerator-driven Systems*", Proc. of International Conference PHYSOR 2004, April 25-29, 2004, Chicago, Illinois, USA (2004).

[6.1] V.P. Bamblevski et all., "The Investigation of the Radiation Field Around the Thick Lead Target Irradiated by the 650 MeV Protons", Report E1-2000-307 JINR Dubna, 2000

[6.2] V.P. Bamblevski et all., "Comparison of Evaluation and Experiment for Nuclear Cascade Induced by 650 MeV Protons in Thick Lead Target of a Subcritical Assembly", Report E3-2002-273 JINR Dubna, 2002

[6.3] J. Janczyszyn, W. Pohorecki, S. Taczanowski, V. Shvetsov, G. Gerbish, G. Domañska *"Experimental Validation of Calculations of Radionuclide Production in the Vicinity of a Spallation Neutron Source"*, in Materials of round table and co-ordination seminar „Poland in JINR", V.G. Kadyshewskiy, A.N. Sisakian i A. Hrynkiewicz (editors), JINR, Dubna, 2001, pp. 25-35;

[6.4] W. Pohorecki, J. Janczyszyn, S. Taczanowski, G. Domañska, *"Badania produkcji nuklidów w otoczeniu spalacyjnego Ÿród³a neutronów"* , Raport IChTJ Seria A nr 1/2002, Instytut Chemii i Techniki J¹drowej, Warszawa 2002, s. 156-164,

[6.5] J. Janczyszyn, W. Pohorecki, S. Taczanowski, V. Shvetsov, O. Kaczmarek, "*Measurement of cross section for (p,x) reactions on natural Fe for 650 MeV protons"*, Semi-annual topical MUSE Meeting, 5th Framework Programme MUSE, ISN Grenoble, 18-19.10.2001, CD-ROM (2002)

[6.6] J. Janczyszyn, W. Pohorecki, S. Taczanowski, G. Domañska V. Shvetsov, G. Gerbysh *"Experimental Assessment of Radionuclide Production in Materials Near to the Spallation Target"*, Proceedings of the ANS Topical Meeting on Accelerator Applications/Accelerator Driven Transmutation Technology and Applications - AccApp/ADTTA'01 - Reno November 11-15, 2001, CD-ROM, ISBN: 0-89448-666-7, 2002,

[6.7] W. Pohorecki, J. Janczyszyn, S. Taczanowski, A. Polañski, *"Measurements of production and distribution of radionuclides in the spallation target"*, PHYSOR 2002 Int. Conference on the New Frontiers of Nuclear Technology: Reactor Physics, Safety and High-Performance Computing, Seoul, Korea, October 7-10, 2002, CD-ROM;

[6.8] W. Pohorecki, T. Horwacik, J. Janczyszyn, S. Taczanowski, I. V. Mirokhin, A. G. Molokanov, A. Polanski, *Spatial distributions of reaction rates inside and next the spallation neutron source*, Proceedings of the International Workshop on P&T AND ADS DEVELOPMENT 2003, W. Haeck, G. Van den Eynde, Th. Aoust, H. Aï t Abderrahim, P. D'hondt (Editors), SCK•CEN Club-House, Belgium, October 6-8, 2003, CD-ROM, ISBN 9076971072, BLG-959, 2003].

[6.9] G. Domañska, S. Taczanowski, J. Janczyszyn, W. Pohorecki V.S. Shvetsov, "*Investigations of the SAD design parameters for optimum experimental performance"*, Annals of Nuclear Energy **31** (No 18) 2004, pp 2127-2138

[6.10] R.E. Prael, H. Lichtenstein, *"User guide to LCS: The LAHET code system"*, LANL Report LA-UR-89-3014, 1989

[6.11] Briesmeister J.F. (Ed.), MCNP – A General Monte Carlo N-Particle Transport Code, LANL Report LA-12625-M, Version 4A, 1997

[6.12] A.K. Lavrukhina, L.D. Revina, V.V. Malyshev, L.M. Satarova, Su Hun-Guy, I.S. Kalicheva, L.D. Firsova, *"The Later Investigation Spallation of Fe Nuclei Induced By 660 MeV Protons"*, Radiokhimia 5, 721 (63) (in Russian),

[6.13] J.S. Hendricks with MCNPX Team,
MCNPX, version 2.5.d, LA-UR-03-5916, 2003

[6.14] W. Pohorecki J. Janczyszyn, S. Taczanowski, I.V. Mirokhin, A.G. Molokanov, T. Horwacik, A. Polanski, "*Investigations of Radionuclide Production in a Spallation Target carried out in the frame of MUSE and SAD projects*", to be published in Proceedings of the Euradwaste-2004 Conference, Luxembourg, March 29-31, 2003

[6.15] A. Fasso, A. Ferrari, J. Ranft, P.R. Sala,, *"FLUKA: Status and Prospective for Hadronic Applications"*, Proceedings of the Monte Carlo 2000 Conference, Lisbon, October 2000

[6.16] V. Baylac-Domengetroy, "*Investigations Related to the Generation of Reaction Products in the Target of Accelerator Driven Systems for Nuclear Waste Incineration*", FZKA6908 (2003). This reference is as pdf-file on the website: http://inrwww.fzk.de/fzka6908.pdf.

[6.17] M. C. Lagunas-Solar et al., *"Cyclotron Production of No-Carrier-Added 206Bi (6.24 d) and 205Bi (15.31 d) as Tracers for Biological Studies and for the Development of Alpha-Emitting Radiotherapeutic Agents*", J. App. Rad. Isot. 38, 129 (1987).

[7.1] K.O. Ott and R.J. Neuhold, *"Introductory Nuclear Reactor Dynamics"*, American Nuclear Society, (1985)

[7.2] J.L. Kloosterman, Y. Rugama, M.Szieberth, C. Destouches, *"Measurement and calculation of control rod worths in Masurca"*, PHYSOR 2002, International Conference on the New Frontiers of Nuclear Technology: Reactor Physics, Safety and High-performance Computing, Seoul, Korea, October 7-10, 2002

[7.3] G.D. Spriggs, R. D. Bush, T. Sakurai and S. Okajima, *"The equivalent Fundamental-Mode Source"*, Annals of Nuclear Energy 26, p 237-264, 1999

[7.4] P. Baeten, H. Aït Abderrahim, *"Reactivity monitoring in ADS. Application to the MYRRHA ADS project"*, Progress in Nuclear Energy, volume 43, No. 1-4, 413-419 (2003)

[7.5] A. Garelis, *"Survey of pulsed neutron source methods for multiplying media"*, Proceedings of the Symposium on Pulsed Neutron Research, AIEA, Karlsruhe, May 10-14, 1965.

[7.6] G.D. Spriggs, R.D. Bush, J.G. Williams, "*Two-Region Kinetic Model for Reflected Reactors"*, Annals of Nuclear Energy Vol. 24, pp 205-250, 1997

[7.7] F. Perdu, *"Contributions aux études de sûreté pour des filières innovantes de réacteurs nucléaires*", Thèse de Docteur de l'Université Joseph Fourier de Grenoble, 2003

[7.8] J. Vollaire, *"L'expérience MUSE-4: Mesure en ligne des paramètres dynamiques d'un système sous-critique"*, Thèse de doctorat, Institut National Polytechnique de Grenoble, le 8 octobre 2004

[7.9] S.Taczanowski, M.Kopeæ, "*Monte-Carlo Simulation of Time-dependent Processes in External-driven Subcritical Systems"*, PHYSOR 2002, Int. Conf. on the New Frontiers of Nuclear Technology: Reactor Physics, Safety and High-Performance Computing, Seoul, Korea, October 7-10, 2002, CD-ROM, 9E-07

[7.10] S.Taczanowski, M. Kopeæ and J. Janczyszyn, "*Simulation of Time-dependent Processes of Subcritical Systems with the MCNP Code*", Accelerator Applications/Accelerator Driven Transmutation Technology and Applications (AccApp/ADTTA'01), November 12-15, 2001, Reno, Nevada CD ROM, ISBN: 0-89448-666-7.

[7.11] R.E. Uhrig, *"Random Noise Techniques in Nuclear Reactor Systems"*, Ronald Press, New York (1956).

[7.12] J. A. Thie, *"Reactor Noise"*, Rowman and Littlefield, Inc. New York, 1963

[7.13] P. Baeten, *"Heuristic derivation of the Rossi-alpha formula for a pulsed neutron source"*, Annals of Nuclear Energy, volume 31/1, 43-53 (2003)

[7.14] I. Pázsit, M. Ceder M. and Z. Kuang Z, "*Theory and analysis of the Feynman-alpha method for deterministically and randomly pulsed neutron sources*", Nucl. Sci. Eng. 148, 67-78 (2004)

[7.15] I. Pázsit, Y. Kitamura, J. Wright and T. Misawa, "*Calculation of the pulsed Feynman-alpha formulae and their experimental verification*", Submitted to Ann. nucl. Energy (2004)

[7.16] Taczanowski et al., *"Properties of the Feynman-á method applied to Accelerator-Driven Subcritical Systems"*, Proc. of the ICRS –10, 9-14.05. 2004, Madeira, (in the press in Radiation Protection Dosimetry)

Annex 1: List of Publications, Papers in Int. Conf., Meetings, Workshops

Publications

Reactivity Determination for Subcritical Systems by Source-Pulsed Experiments
S. Dulla, P. Ravetto, M.M. Rostagno, P. Vinai
Kerntechnik, 67 (5-6), 256-260 (2002)

Definition and Application of Proton Source Efficiency in Accelerator-Driven Systems
Per Seltborg, Jan Wallenius, Kamil Tucek, and Waclw Gudowski
Nuclear Science and Engineering, Vol 145 (2003) 390-399

Prompt reactivity determination in a subcritical assembly through the response to a Dirac pulse
F. Perdu, J.M. Loiseaux, A. Billebaud, R. Brissot, D. Heuer, C. Le Brun, E. Liatard, O. Meplan, E. Merle, H. Nifenecker,J. Vollaire
Progress in Nuclear Energy, Vol. 42 (2003) 107-120.

Heuristic derivation of the Rossi-alpha formula for a pulsed neutron source
P. Baeten
Annals of Nuclear Energy, Vol. 31/1(2003), p. 43-53

Investigations of Neutronics of Subcritical Systems with the Use of MCNP Code
S. Taczanowski and M. Kopec
Emerging nuclear energy and transmutation systems: Core physics and engineering aspects, IAEA-TECDOC-1356, pp. 228-239, IAEA Vienna 2003

Preliminary measurements of the prompt decay constant in MASURCA
Y. Rugama, J.L. Kloosterman, A. Winkelman
Progress in Nuclear Energy, Vol. 43 (2004) 421-428

Analytical solution for the Feynman-alpha formula for ADS with pulse neutron sources
M. Ceder, I. Pázsit
Progress in Nuclear Energy, Vol. 43 (2004) 429-436

Experimental results from noise measurements in a source driven sunbcritical fast reactor
Y. Rugama, J.L. Kloosterman, A. Winkelman
Progress in Nuclear Energy, Vol. 44 (2004) 1-12.

Theory and Analysis of the Feynman-a Method for Deterministically and Randomly Pulsed Neutron Sources
I. Pázsit, M. Ceder and Z. F. Kuang
Nuclear Science and Engineering, Vol. 148 (2004) 67-78

Application of the multipoint method to the kinetics of Accelerator-Driven Systems
P. Ravetto, M.M. Rostagno, G. Bianchini, M. Carta, A. D'Angelo
Nuclear Science and Engineering, Vol. 148, 79-88 (2004)

Transport Effects for Source-Oscillated Problems in Subcritical Systems
S. Dulla, P. Ravetto, M.M. Rostagno
Nuclear Science and Engineering, Vol. 148 (1), 89-102 (2004)

Neutronic Studies in Support to ADS: The Muse Experiments in the MASURCA Facility
R. Soule & al
Nuclear Science and Engineering, Vol. 148 (2004) 124-152

Investigations of the SAD Design Parameters for Optimum Experimental Performance
G. Domañska, S. Taczanowski, J. Janczyszyn, W. Pohorecki, V.S. Shvetsov
Annals of Nuclear Energy, 31 (No 18) 2004, pp 2127-2138

Feynman-α measurements on the fast critical zero-power reactor MASURCA
J.L. Kloosterman, Y. Rugama,
Progress in Nuclear Energy, Vol. 46, n°2, pp. 111-125, 2005

On some features of neutron space kinetics for multiplying systems
S. Dulla, P. Ravetto, M.M. Rostagno, G. Bianchini, M. Carta, A. D'Angelo
Submitted to Nuclear Science and Engineering

Calculation of the pulsed Feynman-alpha formulas and their experimental verification
I. Pázsit, Y. Kitamura, J. Wright and T. Misawa
Accepted in Annals of Nuclear Energy (October 2004)

Theory and Analysis of the Transfer Function Method in a Subcritical Fast Reactor Driven by a Pulsed Source
Y. Rugama and J.L. Munoz-Cobo
Accepted in Nuclear Science and Engineering (2005)

Importance of the MUSE experiments for emerging ADS concepts from the nuclear data viewpoint
M. Plaschy, S. Pelloni, P. Coddington, G. Rimpault, R. Chawla
Annals of Nuclear Energy, Volume 32, Issue 8, May 2005, pages 843-856

International conferences, meetings or workshops

Proceedings of the Tenth ICENES, Petten, 24-28 September 2000, p.429

ADS's based on the 660 MeV proton Phasotron of JINR for Research on utilization of Plutonium
V.S.Barashenkov, I.V.Puzynin i A.Polanski,

Co-operation of JINR with Polish Institutes and Universities, Proc. JINR Dubna, 2001, ISBN 5-85165-668-9

Experimental Validation of Calculations of Radionuclide Production in the Vicinity of a Spallation Neutron Source
J. Janczyszyn, W. Pohorecki, S. Taczanowski, V. Shvetsov, G. Gerbysh, G. Domañska

Theoretical and Experimental Studies of Accelerator-driven Systems for Nuclear Waste Transmutation
S. Taczanowski

Accelerator Applications/Accelerator Driven Transmutation Technology and Applications (AccApp/ADTTA'01), Reno, November 12-15, 2001, CD-ROM, ISBN: 0-89448-666-7, 2002

Simulation of Time-dependent Processes of Subcritical Systems with the MCNP Code,
S. Taczanowski, M. Kopec and J. Janczyszyn,

Experimental Assessment of Radionuclide Production in Materials Near to the Spallation Target,
J. Janczyszyn, W.Pohorecki, S. Taczanowski, G. Domañska V.N. Shvetsov, G. Gerbish

Monte Carlo Modelling of a Subcritical Assembly Driven With The Existing 660 MeV JINR Protons Accelerator
W.Gudowski, A.Polañski, I.Puzynin i V.Shvecov,

Reactivity monitoring in ADS with neutron fluctuation analysis
I. Pázsit, Z.F. Kuang

SMORN VIII – Göteborg – Sweden – 27/31 May 2002

Preliminary measurements of the prompt neutron decay constant in MASURCA
Y. Rugama, J.L. Kloosterman, A. Winkelman

Analytical solution of the Feynman-alpha formula for A.D.S. with pulsed neutrons source.
M. Ceder, I. Pázsit

Reactivity monitoring in ADS. Application to the MYRRHA ADS project
P. Baeten, H. Aï t Abderrahim

PHYSOR 2002, International Conference on the New Frontiers of Nuclear Technology: Reactor Physics, Safety and High-Performance Computing, ANS 2002 RPD Topical Meeting, Seoul, October 7-10, 2002.

Neutronic studies in support to A.D.S. – The Muse experiments in the Masurca facility
R. Soule

The Muse-4 experiment – Prompt reactivity and neutron spectrum measurements
A. Billebaud, R. Brissot, D. Heuer, M. Kerveno, C. Lebrun, E. Liatard, J.M. Loiseaux, O. Méplan, E. Merle, F. Perdu, J. Vollaire

Measurement and calculation of control rod worths in Masurca
J.L. Kloosterman, Y. Rugama, M. Szieberth, C. Destouches

First MUSE-4 experimental results based on time series analysis
C. Jammes, G. Perret, G. Imel

First CIEMAT. measurements of the MUSE-4 kinetic response
D. Villamarin, E. Gonzalez-Romero

Steady state calculations in support of the MUSE 4 experimental programme
G. M. Thomas, R. Soule, W. Assal, P. Chaussonnet, C. Destouches, C. Jammes, J.M. Laurens, M. Plaschy

Theory and analysis of the Feynman-alpha method for deterministically and randomly pulsed neutron sources
I. Pázsit, M. Ceder

Foil activation studies of spectral variations in the MUSE 4 critical configuration
M. Plaschy , R. Chawla, C. Destouches, C. Domergue, H. Servière, P. Chaussonnet, J.M. Laurens, R. Soule, G. Rimpault

Transport effects for source-oscillated problems in subcritical systems
S. Dulla, P. Ravetto, M.M. Rostagno

Application of the multipoint method to the kinetics of accelerator-driven systems
P. Ravetto, M.M. Rostagno, G. Bianchini, M. Carta, A. D'Angelo

Measurements of production and distribution of radionuclides in the spallation target
W. Pohorecki, J. Janczyszyn, S. Taczanowski, A. Polanski

Monte-carlo simulation of time dependent processes in external-driven subcritical systems
S. Taczanowski, M. Kopec

Fast reactor core-reflector interface effects revisited
J.F. Lebrat, R. Jacqmin, F. Gabrielli, M. Carta, V. Peluso, G. Buzzi, G. Bianchini, A. D'Angelo, G. Aliberti, G. Palmiotti,

OECD/NEA – 7th International Exchange Meeting on Actinide and Fission Product Partitioning and Transmutation – Jeju – Republic of Korea – 14/16 October 2002

Determination of reactivity by a revised rod-drop technique in the Muse-4 programme – Comparison with dynamic measurements
G. Perret, C. Jammes, G. Imel, C. Destouches, P. Chaussonnet, J.M. Laurens, R. Soule, G.M. Thomas, W. Assal, P. Fougeras, P. Blaise, J.P. Hudelot, H. Philibert, G. Bignan

First measurements of the kinetic response of the MUSE-4 fast A.D.S. mock-up to fast neutron pulse
D. Villamarin, G. Perret, E. Gonzalez, R. Soule, C. Jammes, G. Imel, C. Destouches, P. Chaussonnet, J.M. Laurens, G.M. Thomas, P. Fougeras, G. Bignan

MUSE-4 Benchmark calculations using MCNP-4C and different nuclear data libraries
N. Messaoudi & al

New methods for the Monte Carlo simulation of neutron noise experiments in A.D.S.
M. Szieberth, J.L. Kloosterman

Investigation of local spectra differences between critical and driven subcritical configurations in MUSE-4
M. Plaschy & al

ENC 2002 – Lille – France – 7/9 October 2002

Steady state calculations in support of the MUSE 4 experimental programme
G. M. Thomas, R. Soule, W. Assal, P. Chaussonnet, C. Destouches, C. Jammes, J.M. Laurens, M. Plaschy

M&C 2003, Nuclear Mathematical and Computational Sciences : A Century in Review, A Century Anew, Gatlinburg, Tennessee, April 6-11, 2003, on CD-ROM

Application of the Stochastic Theory to Reactivity Measurements in a Subcritical Assembly Driven by a Pulsed Source
Y. Rugama, J.L.Munoz-Cobo, J.L. Kloosterman

On some features of neutron space kinetics for multiplying systems
S. Dulla, P. Ravetto, M.M. Rostagno, G. Bianchini, M. Carta, A. D'Angelo

Kinetic approximations and noise theory in source-driven subcritical systems
I. Pázsit

New Methods for the Monte Carlo Simulation of Neutron Noise Experiments
M. Szieberth and J.L. Kloosterman

ICONE 11 – Tokyo – Japan – 20/23 April 2003

Measurement of kinetic parameters in the fast subcritical core MASURCA in the framework of European ADS project MUSE
P. Baeten, H. Ait Abderrahim

ADOPT – International Workshop on P&T and ADS'2003 – Mol - Belgium – 6/8 October 2003

Progress of the MUSE-4 experiments and first results from the measurements at subcriticality levels representative of an ADS
F. Mellier – On behalf the MUSE collaboration

Pulsed Neutron Source measurements of kinetic parameters in the source-driven fast subcritical core MASURCA
E. González-Romero, D. Villamarín, M. Embid, G. Aliberti, G. Imel, V. Kulik, G. Palmiotti, C. Destouches, F. Mellier, C. Jammes, G. Perret, A. Billebaud, R. Brissot, D. Heuer, C. Le Brun, E. Liatard, JM.Loiseaux, O. Méplan, E. Merle, F. Perdu, J. Vollaire, A. D'Angelo, M. Carta, V. Peluso, J.L. Kloosterman, Y. Rugama, P. Baeten, F. Gabrielli

Measurement of kinetic parameters in the source-driven fast subcritical core MASURCA with noise methods
P. Baeten, G. Imel, C. Destouches, C. Jammes, F. Mellier, G. Perret, E. Gonzalez-Romero, D. Villamarin, J.L. Kloosterman, Y.Rugama

On line measurement of parameters relevant for ADS monitoring – Experimental technique validation in MASURCA
A. Billebaud, J. Vollaire, R. Brissot, D.Heuer, C. Le Brun, E. Liatard, J.-M. Loiseaux, O. Meplan, E. Merle-Lucotte, F. Perdu, C. Destouches, P. Chaussonnet, J.-M. Laurens

ADS neutronics
R. Klein Meulekamp, A. Hogenbirk, A.J. Koning

Contribution to the design and experimental program of the SAD accelerator-driven system
S. Taczanowski, G. Domanska, M. Kopec, J. Janczyszyn

Spatial distributions of reaction rates inside and next the spallation source
W. Pohorecki, T. Horwacik, J. Janczyszyn, S. Taczanowski, I.V. Mirokhin, A.G. Molokanov, A. Polanski

Interpretation of foil activation and fission rate measurements in critical and subcritical MUSE4 configurations
M. Plaschy, R. Chawla, M. Thomas, C. Destouches, G. Rimpault, F. Mellier

GLOBAL 2003, Atoms for Prosperity: Updating Eisenhower's Global Vision for Nuclear Energy, New Orleans, Louisiana, November 16-20, 2003.

MUSE-4 Experiment Progress at Subcriticality Levels Representative of ADS Operating
F. Mellier, G. Perret, C. Jammes, C. Destouches, J.F. Lebrat

The MUSE-4 Experiment : Prompt Reactivity and Delayed Neutron Measurements
A. Billebaud, J. Vollaire, R. Brissot, D. Heuer, C. Le Brun, E. Liatard, J.-M. Loiseaux, O. Méplan, E. Merle-Lucotte and F. Perdu

Winter meeting of the ANS – Reno – USA – 16/20 November 2003

Reactivity measurements in accelerator driven systems applying noise analysis techniques
Y. Rugama, J.L. Kloosterman

Dynamic Analysis of Source Driven Fast Neutron Systems for Experimental Techniques of Subcritical Reactivity Measurement
G. Aliberti, G. Imel +, G. Palmiotti, M. Salvatores, C. Jammes, G. Perret

Proceedings of the Euradwaste-2004 Conference, Luxembourg, March 29-31, 2004, to be published

Investigations of Radionuclide Production in a Spallation Target carried out in the frame of MUSE and SAD projects
W. Pohorecki, J. Janczyszyn, S. Taczanowski, I.V. Mirokhin, A.G. Molokanov, T. Horwacik, A. Polanski

PHYSOR 2004, The Physics of Fuel Cycles and Advanced Nuclear Systems: Global Developments, Chicago, Illinois, April 25-29, 2004, on CD-ROM, American Nuclear Society, Lagrange Park, IL. (2004)

Some Experimental Results from the Last Phases of the MUSE Program
Y. Rugama, C. Destouches, G. Imel, C. Jammes, F. Mellier

Study of the Influence of Source Type in the Kinetics Measurements in a Subcritical System
Y. Rugama, G. Imel

Reactivity Measurements and Neutron Spectroscopy in the MUSE-4 experiment
A. Billebaud, J. Vollaire, R. Brissot, D. Heuer, C. Le Brun, E. Liatard, J.-M. Loiseaux, O. Méplan, E. Merle-Lucotte, A. Nuttin, F. Perdu, C. Destouches, P? Chaussonnet, J.-M. Laurens and Y. Rugama

Reactivity Assessment and Spatial Time-effects from the MUSE kinetics Experiments
M. Carta, A. D'Angelo, V. Peluso, G. Aliberti, G. Imel, V. Kulik, G. Palmiotti, J. F. Lebrat, Y. Rugama, C. Destouches, E. González-Romero, D. Villamarín, S. Dulla, F. Gabrielli, P. Ravetto

The MUSE4 Pulsed Neutron Source experiments
E. González-Romero, D. Villamarín, M. Embid, M. C. Vicente, C. Destouches, P. Chaussonnet, J. M. Laurens, F. Mellier

Variance Reduction Techniques for the Monte Carlo Simulation of Neutron Noise Measurements
M. Szieberth and J.L. Kloosterman

ICRS 10, 21st Century Challenges in Radiation Protection and Shielding, Madeira, 9-14 May 2004, to be published in Radiation Protection Dosimetry 2005

Spatial Distributions of Residuals Production Inside a Spallation Target
W. Pohorecki, T. Horwacik, J. Janczyszyn, S. Taczanowski,V. P. Bamblevski, S. A. Gustov,I. V. Mirokhin, A. G. Molokanov, A. Polanski

Design and Experimental Objectives Considerations of the SAD Accelerator Driven System
S. Taczanowski, M. Kopeæ, G. Domañska, J. Janczyszyn

OECD/NEA, 4th International Workshop on the Utilisation and Reliability of High Power Proton Accelerators, Daejon, Republic of Korea, 16/19 May 2004

Numerical comparisons between neutronic characteristics of MUSE4 configurations and XADS-type models
M. Plaschy, S. Pelloni, P. Coddington, R. Chawla, G. Rimpault, F. Mellier

Proccedings of the XI International Seminar on Interaction of Neutrons with Nuclei - ISINN 2003, Dubna, Russia, May 28-31, 2004, pp 220-227, ISBN 5-9530-0043-x

Spatial distributions of rection rates inside and next the spallation neutron source
W. Pohorecki, T. Horwacik, J. Janczyszyn, S. Taczanowski, I.V. Mirokhin, A.G. Molokanov, A. Polanski

Twelfth International Symposium on Reactor Dosimetry, Gatlinburg, USA, May 8-13, 2005,

C. Destouches, M. Plaschy, D. Beretz, F. Mellier, H. Servière, P. Chaussonnet, "Determination of Adjusted Neutron Spectra in Different MUSE Configuration by Unfolding Techniques", Accepted for oral presentation.

Annex 2: List of PhD Thesis

C. A. BOMPAS, "Contribution à la validation expérimentale du couplage entre un accélérateur et un massif sous-critique : Expériences MUSE III et MUSE IV", Thèse de Docteur de l'Université Joseph Fourier de Grenoble, Décembre 2000

G. ALIBERTI, "Caractérisation neutronique des systèmes hybrides en régime stationnaire et transitoire", Thèse de l'Université Louis Pasteur, Strasbourg, 2001

G. PERRET, "Amélioration et développement des méthodes de determination de réactivité – Maîtrise des incertitudes associées", Thèse de Doctorat de l'Université Joseph Fourier de Grenoble, 2003

F. PERDU, "Contributions aux études de sûreté pour des filières innovantes de réacteurs nucléaires", Thèse de Docteur de l'Université Joseph Fourier de Grenoble, 2003

P. SELTBORG, "External Source Effects and Neutronics in Accelerator-driven Systems", Department of Nuclear and Reactor Physics, Royal Institute of Technology, Stockholm, 2003

M. PLASCHY, "Etudes Numériques et Expérimentales de Caractéristiques d'un Système Rapide Sous-Critique Alimenté par une Source Externe", Thèse de Docteur es Sciences n°2953, Ecole Polytechnique Fédérale de Lausanne, 2004

J. VOLLAIRE, "L'expérience MUSE-4 : Mesure en ligne des paramètres dynamiques d'un système sous-critique", Thèse de Docteur de l'Institut National Polytechnique de Grenoble, Octobre 2004

D. VILLAMARIN-FERNANDEZ, "Análisis dinámico del reactor experimental de fisión nuclear MUSE-4", PhD Thesis, Universidad Complutense de Madrid, 2004

Annex 3: MUSE-4 experiment planning

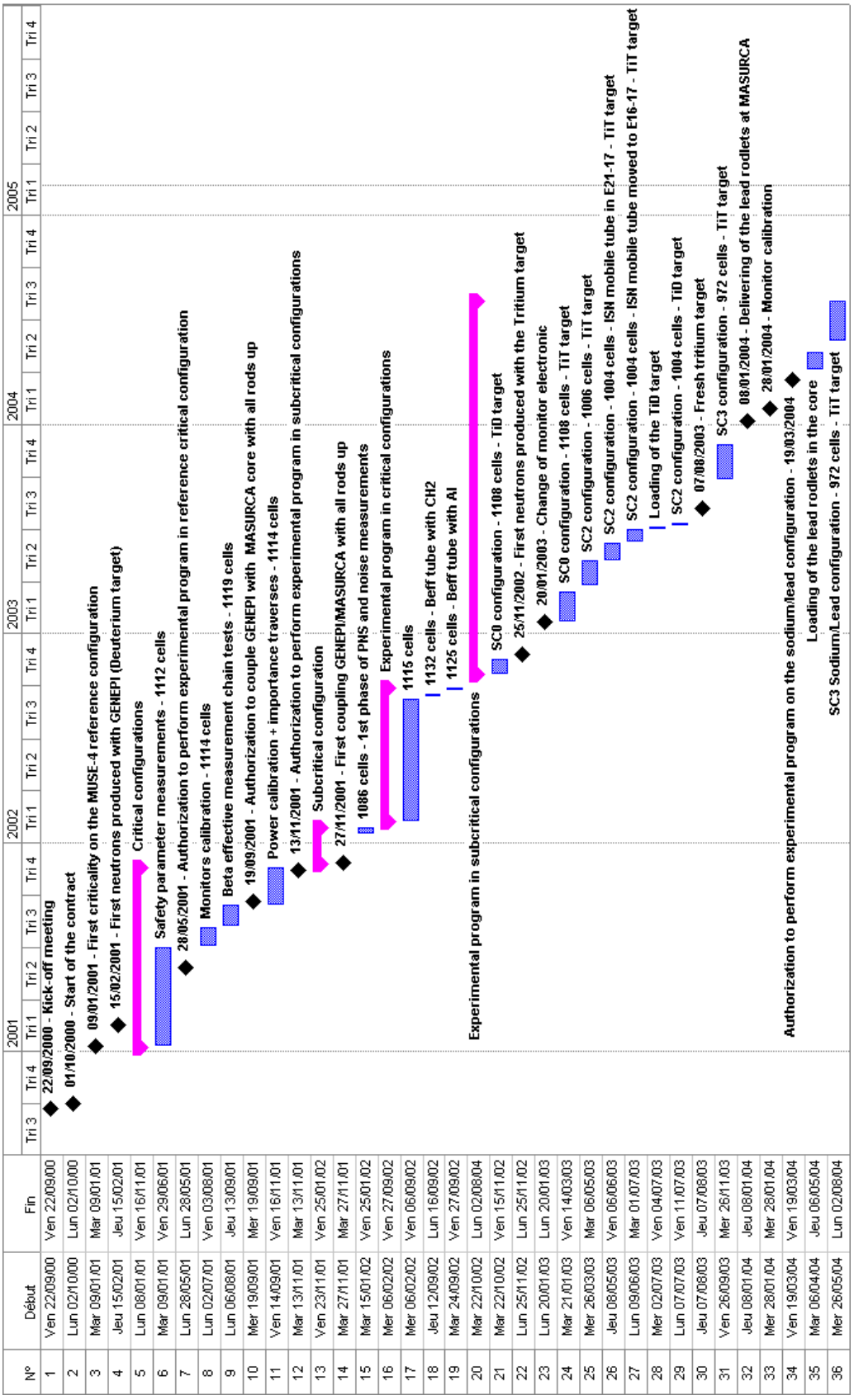

N°	Début	Fin
1	Ven 22/09/00	Ven 22/09/00
2	Lun 02/10/00	Lun 02/10/00
3	Mar 09/01/01	Mar 09/01/01
4	Jeu 15/02/01	Jeu 15/02/01
5	Lun 08/01/01	Ven 16/11/01
6	Mar 09/01/01	Ven 29/06/01
7	Lun 28/05/01	Lun 28/05/01
8	Lun 02/07/01	Ven 03/08/01
9	Lun 06/08/01	Jeu 13/09/01
10	Mer 19/09/01	Mer 19/09/01
11	Ven 14/09/01	Ven 16/11/01
12	Mar 13/11/01	Mar 13/11/01
13	Ven 23/11/01	Ven 25/01/02
14	Mar 27/11/01	Mar 27/11/01
15	Mar 15/01/02	Ven 25/01/02
16	Mer 06/02/02	Ven 27/09/02
17	Mer 06/02/02	Ven 06/09/02
18	Jeu 12/09/02	Lun 16/09/02
19	Mar 24/09/02	Ven 27/09/02
20	Mar 22/10/02	Lun 02/08/04
21	Mar 22/10/02	Ven 15/11/02
22	Lun 25/11/02	Lun 25/11/02
23	Lun 20/01/03	Lun 20/01/03
24	Mar 21/01/03	Ven 14/03/03
25	Mer 26/03/03	Mar 06/05/03
26	Jeu 08/05/03	Ven 06/06/03
27	Lun 09/06/03	Mar 01/07/03
28	Mer 02/07/03	Ven 04/07/03
29	Lun 07/07/03	Ven 11/07/03
30	Jeu 07/08/03	Jeu 07/08/03
31	Ven 26/09/03	Mer 26/11/03
32	Jeu 08/01/04	Jeu 08/01/04
33	Mer 28/01/04	Mer 28/01/04
34	Ven 19/03/04	Ven 19/03/04
35	Mar 06/04/04	Jeu 06/05/04
36	Mer 26/05/04	Lun 02/08/04

Annex 4: Time schedule of PRE-SAD measurements

1. June 2000 — Experiment 1 (JINR Dubna):
   - ♦ Measurements of neutron spectra around the lead target Ø 8.5 x 50 cm,
   - ♦ irradiation of samples around the target for the measurements of generated radioactivity.
2. July - December 2000 — Measurements of short-lived radioactivity (JINR Dubna).
3. January - December 2001 — Measurements of long-lived radioactivity (UMM Cracow). Elaboration of the results. Simulating calculations of the experiments.
   - ❑ Results: Activities generated in metallic elements compared with results of computer simulation. Cross sections for selected reactions of 650 MeV protons with natural Fe.
4. June 2001 — Experiment 2 (JINR Dubna), preparatory irradiation of samples inside the lead target Ø 8.0 x 30 cm for the measurement of axial distributions of target radioactivity.
5. November 2001 — Experiment 3 (JINR Dubna), irradiation of samples inside the lead target Ø 8.0 x 30.8 cm for the above measurement.
6. November - December 2001 — Measurements of short-lived radioactivity (JINR Dubna).
7. January - December 2002 — Elaboration of the results. Measurements of long-lived radioactivity (UMM Cracow). Simulating calculations of the experiments.
   - ❑ Results: Axial distributions of activities generated in Pb target compared with results of computer simulation.
8. March 2003 — Experiment 4 (JINR Dubna):
   - ♦ irradiation of Bi samples inside the lead target Ø 16.0 x 30 cm, for the measurement of radial distributions of target radioactivity,
   - ♦ irradiation of track detectors with heavy metal radiators behind the lead target, for the measurement of intensity of the high energy neutron induced fission.
9. March - June 2003 — Measurements of short-lived radioactivity (JINR Dubna). Etching the track detectors and measuring the track density.
10. July - December 2003 — Elaboration of the results. Measurements of long-lived radioactivity and fission fragment density (UMM Cracow). Simulating calculations of the experiments.
    - ❑ Results: Radial distributions of activities generated in Bi target (represented by Bi samples in Pb target) compared with results of computer simulation.
    - ❑ Results: Distributions of intensity of heavy metal fissions behind the target compared with results of computer simulation.
11. January - September 2004 — As above, plus preparation of equipment for microdosimetric measurements.

12.	September 2004	Experiment 5 (JINR Dubna): ♦ irradiation of Pb samples inside the lead target with higher proton beam intensity, for the measurement of axial distributions of target radioactivity, ♦ measurements of microdosimetric spectra in radiation fields generated by 660 MeV protons around a heavy metal target.
October 2004		Elaboration of the results. Simulating calculations of the microdosimetric spectra.